ABSTRACT

YAO, YINGFANG. Investigation of Fiber-induced Hybrid Proton Exchange Membranes. (Under the direction of Professors Xiangwu Zhang and Hechmi Hamouda).

In response to the energy needs of modern society and emerging ecological concerns, the pursuit of novel, low-cost, and environmentally friendly energy conversion and storage systems has raised significant interest. Among these systems, proton exchange membrane fuel cells (PEMFCs), have gained much attentions for their high efficiency, high power density, with low greenhouse gas emission. In conventional PEMFCs, Nafion® is used as the electrolyte, which however brings many drawbacks such as high production cost, environmental incompatibility, and low operation temperature (< 80 ℃). These bottlenecks hindered the development and commercialization of PEMFCs. Alternative types of PEMs thereby were adopted, such as hydrocarbon polymers and hybrid membranes. In the case of hybrid PEMs, many different types of fillers have been adopted into the polymer matrix to fabricate hybrid membranes with different methods. The composite method has proved to be an effective route to improve the practical properties of PEMs and offer the opportunity to operate PEMFCs at higher temperatures. However, severe problems still exist to limit their practical use in PEMFCs. Firstly, a vast majority of fillers with little protogenic groups were used as the additives of PEMs. The adoption of these fillers greatly decreased the ionic sites for proton transport and thus the conductivity. Furthermore, the natural conflict between high content of fillers and particle agglomeration makes it difficult to select a proper concentration for fillers that can not only be well dispersed in PEMs, but also construct inorganic pathways for improved proton conductivity. These shortcomings would greatly limit the implementation of hybrid PEMs. New strategies to form uniformly dispersed filler materials that can form

continuous proton pathway are appreciated.

In this dissertation, the fabrication of novel hybrid PEMs, in which fibers with surface sulfonic acid groups were incorporated, is demonstrated. Electrospinning and post-electrospinning treatments, such as sulfonation, calcinations, et al., were applied to fabricate the filler materials. Chemical or physical methods were applied to prepare the hybrid PEMs with ionomer matrices. In the novel hybrid PEMs, sulfonic acid groups surrounding the interconnected fibers help build a network of long-range ionic pathways on the interfaces of fibers and ionic polymer matrix for fast proton transport. Compared with conventional composite PEMs as well as Nafion, the novel hybrid PEMs possess much higher proton conductivity. Furthermore, the newly developed hybrid PEMs are easy to fabricate, highly controllable, and can be used in practical fuel cell systems. Therefore, this new technology offers a potential strategy on the rational design of advanced PEMs, and opens up new opportunities for high-perfomance PEMFCs, which are one of the promising power sources for consumer devices and electric vehicles, and will play a critical role in solving the worldwide critical energy issue.

Investigation of Fiber-induced Hybrid Proton Exchange Membranes

by
Yingfang Yao

A dissertation submitted to the Graduate Faculty of
North Carolina State University
in partial fulfillment of the
requirements for the degree of
Doctor of Philosophy

Fiber and Polymer Science

Raleigh, North Carolina

2011

APPROVED BY:

_____	_____
Prof. Xiangwu Zhang Committee Chair	Prof. Hechmi Hamouda Committee Co-Chair
_____	_____
Prof. Anatoli Melechko	Prof. Ahmed Mohamed El-Shafei

DEDICATION

To

my respected parents,

Purong Yao and Zhumei Sun,

who made all of this possible,

for warmhearted feeding, teaching, and supporting me.

Thank you for the love from my family,

I really appreciate all that you have done.

BIOGRAPHY

Yingfang Yao was born in Yizheng, Jiangsu, P. R. China. He completed his high school education in the No. 2 middle school attached to Nanjing Normal University, and then attended the Southeast University in September 1999, and graduated with a bachelor's degree in Electronical Engineering in July 2003. After graduation, he obtained a software engineer position in Linkage Technology Co.,Ltd., where he did one year of work on the maintenance of BOSS system.

In Sept. 2004, he went back to the Southeast University as a graduate student majoring in Biomedical Engineering and obtained his Master Degree in July 2007. During that time, He investigated the alignment of electrospun fibers and the application of aligned fibers in scattering polarizers.

In Aug. 2008, Yingfang Yao came to the U.S. and started working toward his Ph.D. degree majoring in Fiber and Polymer Science in the Department of Textile Engineering, Chemistry and Science at North Carolina State University. His research activities ranged from the preparation and characterization of protogenic organic/inorganic electrospun fibers and their application in energy conversion and storage systems, to the fabrication and functionlization of polymer or polymer composite materials for specific utilization.

ACKNOWLEDGMENTS

The author would like to offer his sincerest appreciation to respected advisors: Professors Xiangwu Zhang and Hechmi Hamouda, for supervising, supporting, and helping him grow during his Ph.D. studies; to his other committee members: Professors Yuntian Zhu and Ahmed Mohamed El-Shafei, for their wise counsel, advice, and support.

The author also acknowledges funding supports from the National Science Foundation.

Moreover, the author would like to thank Dr. Liwen Ji, Dr. Quan Shi, Dr. Bingkun Guo, Dr. Zhan Lin, Mr. Ozan Toprakci, Mr. Narendiran Vitchuli, Mr. Guanjie Xu, Mr. Mataz Alcoutlabi, Ms. Kyung-Hye Jung, Ms. Bohyung Kim, Ms. Shuli Li, Ms. Yinzheng Liang, Ms. Shu Zhang, Ms. Ying Li, Mr. Yao Lu, and Mr. Yang Liu at North Carolina State University for their earnest cooperation and warmhearted help during his Ph.D. study.

The author also deeply appreciates Mr. Chuck Mooney and Mr. Roberto Garcia in the Analytical Instrumentation Facility, Mr. Dzung Nguyen and Ms. Birgit Andersen in the College of Textiles at North Carolina State University, and Dr. Mark D. Walters in

the Shared Materials Instrumentation Facility at Duke University for their help in sample characterization.

TABLE OF CONTENTS

LIST OF TABLES

LIST OF FIGURES

ABBREVIATIONS

3D	Three dimension
AFC	Alkaline fuel cell
AFM	Atomic force microscopy
AIBN	Azobisisobutyronitrile
Al_2O_3	Alumina
AMPS	2-acrylamido-2-meathylpropane-sulfonic acid
CA	Cyanoacrylate
CO	Carbon monoxide
CO_2	Carbon dioxide
Co_3O_4	Cobalt(II,III) oxide
C-PAMPS	Crosslinked poly(2-acrylamido-2-meathylpropane-sulfonic acid)
CS_2	Carbon disulfide
Cu	Copper
$Cu(NO_3)_2$	Copper(II) nitrate
CuO	Copper(II) oxide
CVD	Chemical vapor deposition
DC	Direct current
DMF	N,N-dimethylformamide
DMFC	Direct methanol fuel cell
DMSO	Dimethyl sulfoxide

EGD	Ethylene glycol diacrylate
FT-IR	Fourier transform infrared spectra
GDE	Gas diffusion electrodes
H_2	Hydrogen
H_2S	Hydrogen sulfide
H_2SO_4	sulfuric acid
HPC	Hydroxypropylcellulose
IEC	Ion Exchange Capacity
kW	Kilowatt
MCFC	Molten carbonate fuel cell
MEA	Membrane electrode assembly
$MgTiO_3$	magnesium(II) titanate
Mo	Molybdenum
MoO_3	Molybdenum(VI) oxide
NaCl	Sodium Chloride
NaOH	Sodium hydroxide
Nb_2O_5	Niobium pentoxide
NH_3	Ammonia
$(NH_4)_2SO_4$	Ammonium sulfate
NiO	Nickel(II) oxide
O_2	Oxygen

PA	Polyamide
PAA	Poly(acrylic acid)
PAFC	Phosphoric acid fuel cell
PAN	Polyacrylonitrile
PBI	Polybenzimidazole
PC	Polycarbonate
PCL	Polycaprolactone
PE	Polyethylene
PEEK	Poly(oxy-1,4-phenyleneoxy-1,4-phenylenecarbonyl-1,4-pheneylene)
PEMFC	Proton Exchange Membrane Fuel Cell
PEO	Polyethylene oxide
PET	Poly(ethylene terephthalate)
PEV	Poly[ethylene-co-(vinyl acetate)]
PI	Polyimide
PLA	Polylactic acid
PMMA	Poly(methyl methacrylate)
PP	Polypropylene
PS	polystyrene
psi	Pounds per square inch
Pt	Platinum
PTFE	Polytetrafluoroethylene

PTT	Polytrimethylene terephthalate
PU	Polyurethane
PVB	Poly(vinyl butyral)
PVC	Poly(vinyl chloride)
PVDF	Poly(vinylidene fluoride)
PVP	Polyvinylpyrrolidone
RH	Relative humidity
rpm	Revolutions per minute
Ru	Ruthenium
S	Siemens
SEM	Scanning Electron Microscopy
SHE	Standard hydrogen electrode
SiO_2	Silica
SO_2	Sulfur dioxide
SO_2Cl_2	Sulfuryl chloride
$-SO_3H$	Sulfonic acid Group
SOFC	Solid oxide fuel cell
S-PS	Sulfonated polystyrene
$S-ZrO_2$	Sulfated Zirconia
TEM	Transimission Electron Microscopy
TGA	Thermogravimetric analysis

THF	Tetrahydrofuran
TiO_2	Titania
V_2O_5	Vanadium(V) oxide
W	Tungsten
XRD	X-ray Diffraction
ZnO	Zinc oxide
$Zr(NO_3)_4$	Zirconium(IV) nitrate
$Zr(OPr)_4$, $Zr(OC_3H_7)_4$	Zirconium propoxide
$ZrCl_4$	Zirconium(IV) chloride
$ZrO(NO_3)_2$	Zirconium(IV) oxynitrate
ZrO_2	Zirconia
$ZrOCl_2$	Zirconyl Chloride

CHAPTER 1. INTRODUCTION

1.1 Overview of Electrospinning

1.1.1 Introduction to Electrospinning

Although intensive research have been focused onto one-dimensional nanomaterials, and a large number of synthesis and fabrication methods have been demonstrated for generating one-dimensional nanostructures such as fibers, rods, wires, tubes, and so forth, [1, 2] electrospinning is probably the most studied technology for mass production of continuous fibers with diameters ranging from tens of microns down to several nanometers. [3 - 14] The advantages of electrospun fibers, including small diameter, high surface-to-volume ratio, large porosity, superior mechanical property, good flexibility and ductibility, and diversified architecture, and composition, lead them to being widely recognized and useful in many potential applications for applications many fields, as seen in Figure 1.1.

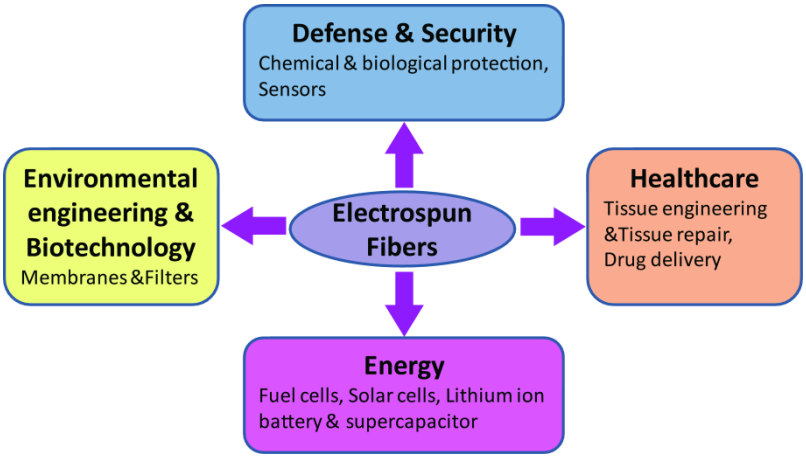

Figure 1.1. Potential applications of electrospun fibers.

1.1.2 The History of Electrospinning

The invention of electrospinning is the result of fluidic electrostatic dynamics. The observation of motions of liquid under electrostatic force started from 18th century. At the end of 19th century, Larmor etc. [15] used electrostatic dynamics to explain the stimulation of electrical field to insulate liquids. These discoveries greatly promoted the invention and development of the technology of electrospinning. In 1902, electrospinning was invented by Cooley [16] and Morton [17]. Early researchers of electrsopinning focused their major energies on the design of electrospinning process. For example, Cooley had used a secondary electrode to control liquid jetting onto a rolling collector.

In 1930's, Formhals made a series of innovative reformation on electrospinning apparatus. [18-21] Actually, many of present researches and reformations can find their roots from those research activities of half a century ago, such as multi-nozzle spinning, parallel electrodes to control the alignment of electrospun fibers, etc. American patents related to electrospinning before the year of 1976 are listed in Table 1.1.

Table 1.1. American patents related to electrospinning before 1976

Patent time	**Innovator**	**Patent Number**
02-04-1902	J. F. Cooley	692631
07-29-1902	W. J. Morton	705691
01-22-1929	K. Hagiwara	1699615
10-02-1934	A. Formhals	1975504
07-21-1936	C. L. Norton	2048651
04-13-1937	A. Formhals	2077373
02-22-1938	A. Formhals	2109333
05-10-1938	A. Formhals	2116942
07-19-1938	A. Formhals	2123992
05-16-1939	A. Formhals	2158415
05-16-1939	A. Formhals	2158416
06-06-1939	A. Formhals	2160962
08-01-1939	E. K. Gladding	2168027
01-16-1940	A. Formhals	2187306
06-29-1943	A. Formhals	2323025
12-14-1943	F. W. Manning	2336745
05-30-1944	A. Formhals	2349950
10-18-1966	H. L. Simons	3280229

One of the key challenges of electrospinning is to achieve high productivity of fibers.

Compared with most other industrial spinning technologies, the productivity of electrospun fibers is low. For example, the fiber productivity of industrial dry spinning can be as high as 200 – 1500 m/min, [22] while that of electrospinning is typically not higher than 30 m/min. [23] As a result, before 1990's, electrospinning did not gain much attention, [24] and only a few researchers used electrospinning to investigate the movement of micro-droplets under electrical field, [25-28] or only choose polymer melts as the electrospinning materials. [29-31] With the development of nanotechnology from 1990's, electrospinning was rediscovered and increasingly attracted attention as one of the most important approach of fabricating nanofibers. Because of the low productivity and low accuracy of control of the jetting process, research activities on electrospinning mainly focused on the control of the morphologies, secondary structures, and materials. In present, there are over 200 universities and institutions researching on electrospinning and electrospun fibers. Electrospinning related patents are increasing year by year. Many electrospun products have been developed and put in commercial applications.

1.1.3 Working Principal of Electrospinning

The formation of electrospun fibers is based on the uniaxial stretch of viscoelastic solutions. A typical electrospinning setup is shown in Figure 1.2. It includes a high power supply, a container for solution storage, a jetting setup, and a collector. Generally, a DC power supply is used to generate high voltage electrostatic field. A syringe or a vessel is used to store pre-spinning solution or melt, which is connected to the power

supply with a metal electrode to charge the solution/melt. The jetting setup is generally a capillary or a needle with inner diameter from 0.15 to 2 millimeters. The jetting setup is placed vertically or horizontally, and keeps at a certain angle with the collector. The feeding rate is generally controlled by a syringe pump, which extrudes the solution out of the needle at a preprogrammed rate. The collector could be a metal plate, a grid, or a roller, depending on the alignment of fibers needed.

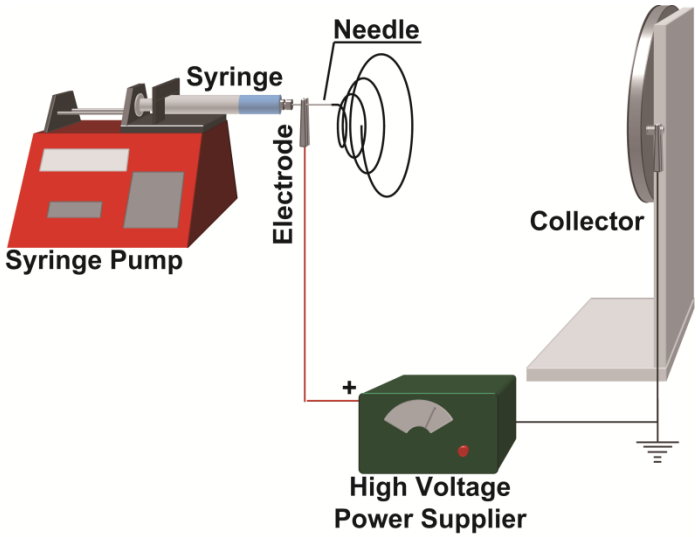

Figure 1.2. Schematic diagram of a typical electrospinning setup and working principle of electrospinning.

In a typical electrospinning process, a high electric field is applied to the droplet of a viscous polymer fluid coming out from the tip of a nozzle. The interactions of the electrical charges in the polymer fluid with the external electric field causes the pendant droplet to deform into a conical structure called Taylor cone. When electric charges in the fluid surpass the critical value at which repulsive electrostatic forces overcome the

surface tension, a fine charged jet is ejected from the tip of Taylor cone. The charged jets undergo a whipping motion and are elongated continuously by the electrostatic repulsion, until they are deposited onto a grounded collector, resulting in the formation of fine fibers. (Figure 1.2)

In the fabrication of electrospun fibers, several factors can affect the morphology of electrospun fibers. These factors can be classified as solution properties, such as viscosity, elasticity, conductivity, and surface tension; control variables, such as electrostatic potential in the capillary, voltage at the top of the capillary, distance between the capillary and the collector; environmental parameters, such as solution temperature, environment humidity and temperature, and airflow, etc. [5, 32] The major factors are listed as follow:

1. Viscosity of solution.

With increasing concentration of the solute, generally a polymer, the viscosity of the solution increases, leading to a stronger surface tension. At the same time, the stretching effect on the jet becomes weaker because of the enhanced surface tension, which causes a higher fiber diameter.

2. Strength of the electrical field.

With enhanced electrical field, the density of surface charge of the jet increases, leading to higher electrostatic repulsion on the polymer chains. Meanwhile, stronger electrical

field provides the jet with higher acceleration. Both factors lead to higher stretch force on the jet, and as a result, finer fibers can be electrospun.

3. Capillary - collector distance.

After the droplets jet from the top of the capillary, the solvent evaporates in the process of flying to the collector. The polymer condenses or solidifies and turns into fibers before collected by the collector. With the increase of the capillary - collector distance, the flying pathway and time also increase, leading to finer diameter of the fibers.

4. Feeding rate.

With a fixed inner diameter of the spinneret, the average feeding rate is proportional to the fiber diameter.

1.1.4 Theoretical Background

Closer inspection makes it much clearer that the electrospinning process is complex. For instance, the jet only follows a direct path towards the counter electrode for a very short distance, and then changes its jetting route significantly. The jet is moved laterally and forms a series of coils, the envelope of which has the form of a cone opening towards the counter electrode (Figure 1.3). [33, 34]

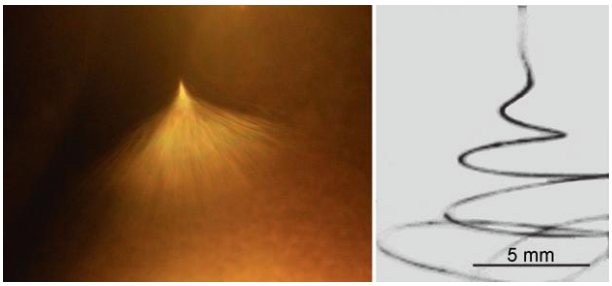

Figure 1.3. Photograph of a jet of PEO solution during electrospinning, and high-speed photograph of jet instabilities. [33]

The actual electrospinning process can be described as the interaction of several physical instability processes, [33-36] majorly including Rayleigh instability, axisymmetrical instability, and bending (or whipping) instability. According to Rayleigh instability, [37-40] a liquid strand undergoes complex structure-forming processes even in absence of an electric field, and the final state is a periodic pearl-necklace arrangement of drops of a given radius.

During electrospinning, the so-called axisymmetrical instability, and bending (or whipping) instability are induced by the coupling of the liquid strand with the electric field through the field-induced transport of charges into the liquid strand. In the case of the charge-driven axisymmetrical instability, a statistical variance of the jet's radius causes a modulation of the surface charge density. This modulation, in turn, generates tangential forces, which couple to the radius modulation and amplify it. The end result of such a coupling loop is the formation of beads, which are aligned along the fiber. By varying the spinning parameters, bead formation can be prevented.

In the actual fiber formation, bending instabilities also occur at high charge densities and fields, and they can typically be enhanced by increasing the electrical conductivity of the polymer solution. A straight section of the jet turns sideways and forms loops in the horizontal plane. The loop diameters increase with time during the motion towards the counter elctrode. During the process, the jet is highly stretched and reduced. Along these reduced fibers, bending occurs again and is followed by the formation of a new set of coils. This procedure is repeated until the fibers solidify or become resistant towards these instabilities, owing to their extreme thinness. [33 - 37]

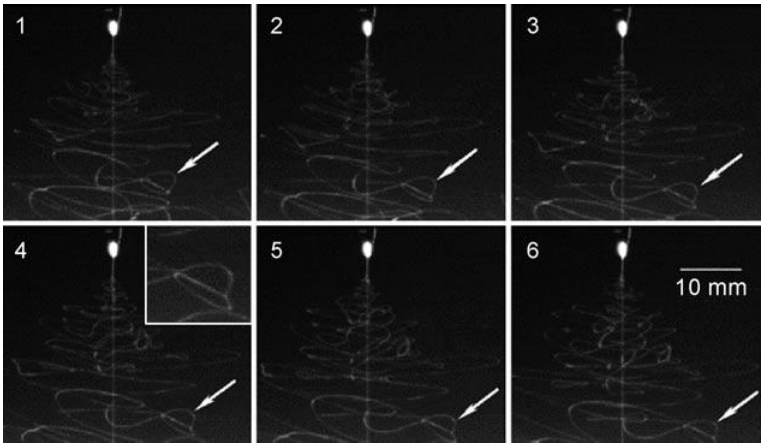

Figure 1.4. High-speed optical images of the formation of instability loops during electrospinning. The arrows indicate a double loop. Inset in frame 4: enlargement. [41]

Because of these instabilities, nanofibers with diameters down to a few nanometers can be generated stably and without decomposition of the jet into droplets. During electrospinning, typical stretching ratios are in the range of 10^5 and stretching rates are up to 10^5 s^{-1}. Such values are not accessible with other methods, such as fiber extrusion followed by mechanical stretching. [42]

1.1.5 Morphologies and Architectures of Electrospun Fibers

Besides electrospinning, several other methods have been developed that can be used to fabricate nanofibers, such as melting spinning, [43] airflow spinning, [44, 45] as well as nanoetching [46, 47] and self-assembly [48 - 51]. However, due to limitations in material type, controllability, cost, productivity, and so forth, these methods have practical difficulties for being widely used. On the contrary, electrospinning has been highly recognized as one of the major methods of producing nanofibers. Much attention has been drawn to meliorate the setups, including the composition of pre-spinning solution, the jetting setup, the collector, and the electrospinning environment. And the consequent electrospun fibers varied in morphology, and architecture, and acquired many superior properties, such as high flux, large surface-to-volume ratio, anisotropical properties, and so forth.

1.1.5.1 Formation of Beads in Electrospinning Process

On occasions, beads are formed during electrospinning. Fibers with beads like pearls on a string can also be formed. In some cases, the fibers are not round, but are flat ribbons. The shapes of the fibers formed depend on a large set of parameters, for example, the properties of the polymer itself, such as molecular weight, molecular-weight distribution, glass-transition temperature, and solubility, as well the properties of the polymer solution, such as viscosity, viscoelasticity, concentration, surface tension, and electrical conductivity. The vapor pressure of the solvent and the relative humidity (RH) of the surroundings can also have a significant impact. Furthermore, the properties of

the substrate, the feeding rate, and the field strength and geometry of the electrodes, and therefore, the form of the electric field, play a major role in fiber formation.

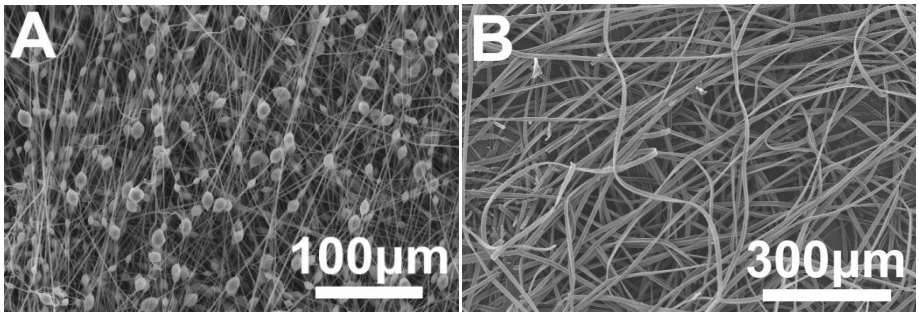

Figure 1.5. SEM images of A) irregularly shaped fibers of polystyrene (PS), and B) ribbon-like fibers of polymethyl methacrylate (PMMA)

1.1.5.1.1 The formation of Core–Shell Nanofibers by Coaxial Electrospinning

In many cases, the conventional electrospinning cannot meet the requirements of some applications where specific functional agents are needed. An important challenge is how to protect/keep the functionalizing agents, for example, enzymes, proteins, drugs, viruses, and bacteria, in a fluid environment to maintain their functionality. Another challenge may be the obstacle of electrospinning materials with low concentrations or molecular weights that are unable to be electrospun directly. To resolve these problems, core-shell nanofibers are developed.

A polymer shell can be deposited via chemical vapor deposition, CVD, [52, 53] whereas metal shells can be either deposited by electroless plating [54, 55] or sputtering [56].

However, coaxial electrospinning can provide a single step formation of core-shell fibers. Followed with post-electrospinning, such as heat treatment or chemical withdrawal, hollow tubes can be obtained. [57 – 68]

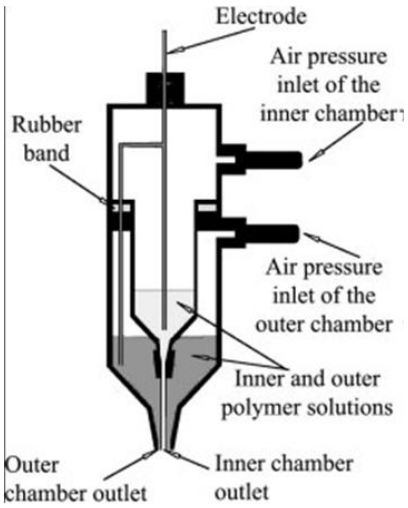

Figure 1.6. Scheme of the setup of a double-compartment plastic syringe for co-electrospinning.

In co-electrospinning, a syringe with two compartments containing different polymer solutions or a polymer solution (shell) and a non-polymeric liquid or powder (core) is used to initiate a core–shell jet (Figure 1.6). At the exit of the core–shell needle attached to the two-compartment syringe appears a core–shell droplet. Being subjected to a sufficiently strong electric field, it issues a compound jet, which undergoes the electrically-driven bending instability characteristic of the ordinary electrospinning process. With the assistance of this specifically designed syringe and needle, electrospun nanofibers with core-shell or hollow structure can be obtain (Figure 1.7).

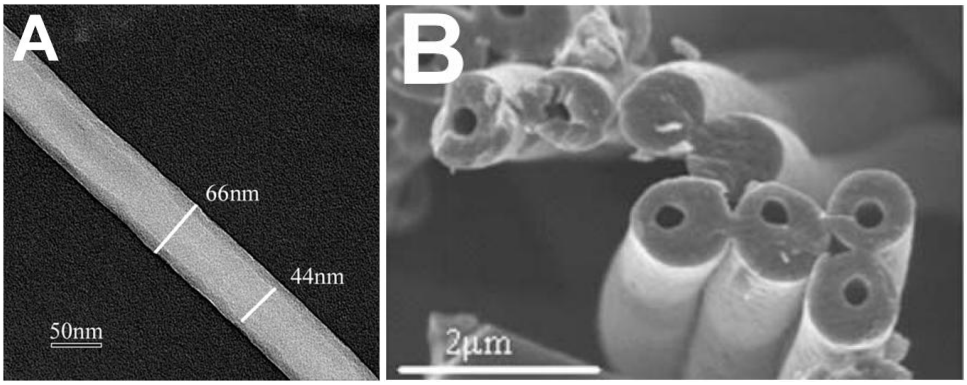

Figure 1.7. A) TEM micrograph of a core–shell nanofiber. The core and shell solutions are PSU and PEO, respectively. B) Turbostratic carbon nanotubes made via co-electrospinning followed by heat treatment.

1.1.5.2 Formation of Electrospun Nanofibers with Porous Structure

Electrospinning typically produce smooth fibers with a circular cross section; however in exceptional cases, other cross sectional structures can be formed. For a variety of applications, for example, tissue engineering, filtration, catalysis, drug delivery, and nanofiber reinforcement, it could be advantageous if the fiber surfaces were not smooth or were porous. In fact, it is now possible to generate different fiber topologies during the electrospinning process by choosing particular solvents or solvent mixtures, by varying the humidity, or by using polymer mixtures. In order to fabricate porous fibers, there are generally three methods:

1. By using volatile solvents and increasing environmental humidity.

During the electrospinning process, water vapor takes over the spots of volatile solvents

that have quickly evaporated. Because of the insolubility of the solute in water, nanopores can be formed on the surface of the fibers. [69]

2. By blending two different polymers.

Electrospun fibers with porous structure can also be obtained by blending two different polymers. After electrospinning, one of the polymers is dissolved and removed, while the other remains. As a result, porous fibers can be acquired. [70]

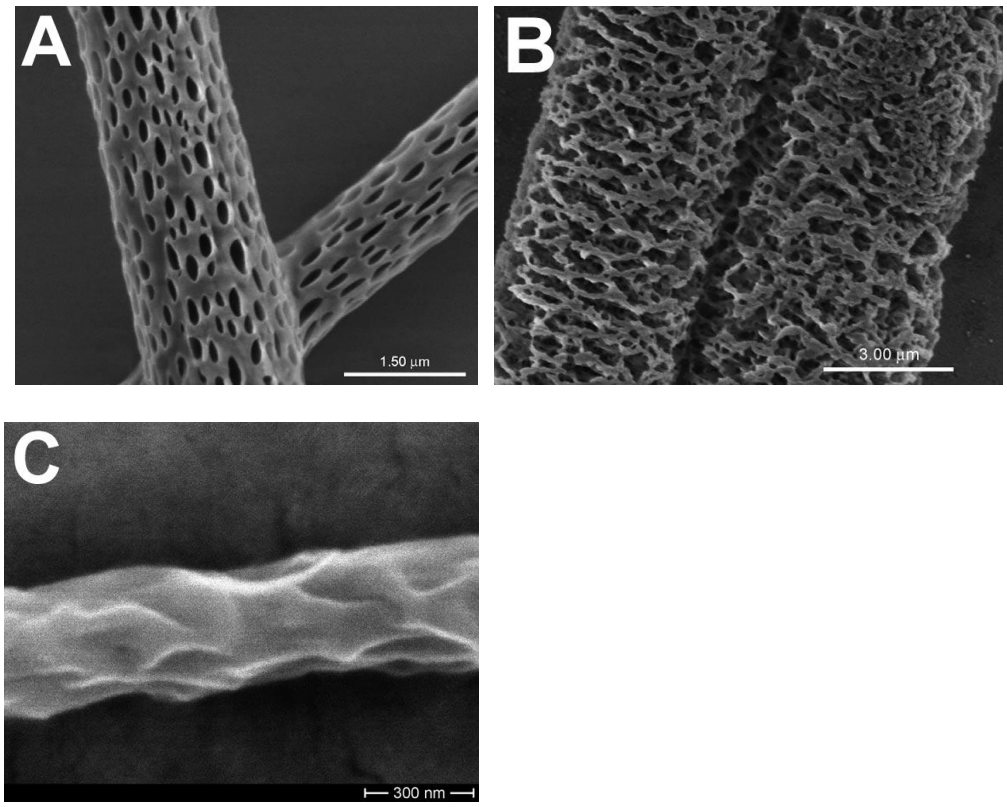

Figure 1.8. A) SEM image of electrospun porous PLA fibers. B) SEM image of electrospun fibers of a PLA/PEO blend after removal of the swelling agent, water. C) SEM image of electrospun fibers of a PLA/polyvinylpyrrolidone (PVP) blend after the selective extraction of PVP.

3. By blending polymers and inorganic components.

Similar to the second method, fibers with porous structure can also be obtained by dissolve or disperse inorganic salts into the pre-spinning polymer solutions. After electrospinning, the inorganic component is washed away by using acids or water. And remaining polymer forms porous fibers. (Figure 1.8) [71, 72]

1.1.5.3 Formation of Aligned Nanofibers with Specific Collector

Electrospinning is not limited to the production of nonwovens with a random planar fiber orientation. Nanofibers with a preferred arrangement (Figure 1.9) are of interest for structural reinforcement with nanofibers or for tissue engineering to give the cells a preferred growth direction.

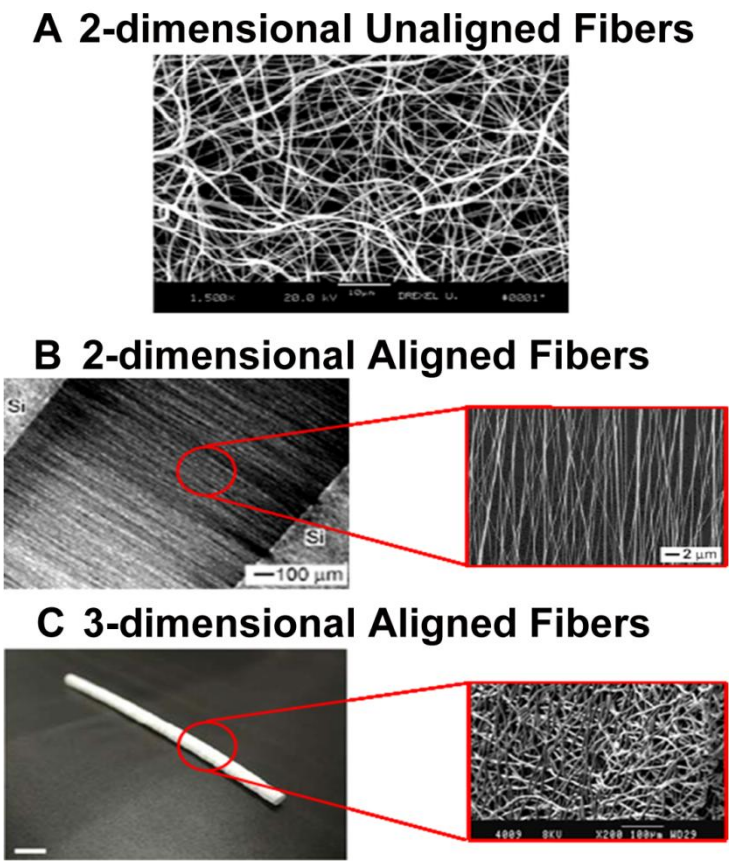

Figure 1.9. sub-structures: A) 2-dimensional unaligned, B) 2-dimensional aligned and C) 3-dimentional aligned structures of electrospun fibers.

Because of the randomness of the jetting and flying orbit of the electrospun fibers, the traditional flat collector can only obtain randomly organized nonwoven fiber mats. For the purpose of controlling the alignment of electrospun fibers, well-designed collectors and/or processes are required. So far, several methods have been reported to control the arrangement of electrospun fibers. The alignment on 2 or 3 dimensional electrospun fiber mats have been obtained. [73 - 83] These methods mostly used specially controlled electrical field between the spinneret and the collector, and/or kinetic setups, such as roller. For example, Xia's group [77] imposed a pair of parallel conductor as the collector.

With the electrical field between the parallel collectors and the repulsion between positively charged fibers, electrospun fibers preferentially aligned vertically to the collector and quasi-parallelly with each other. (Figure 1.10)

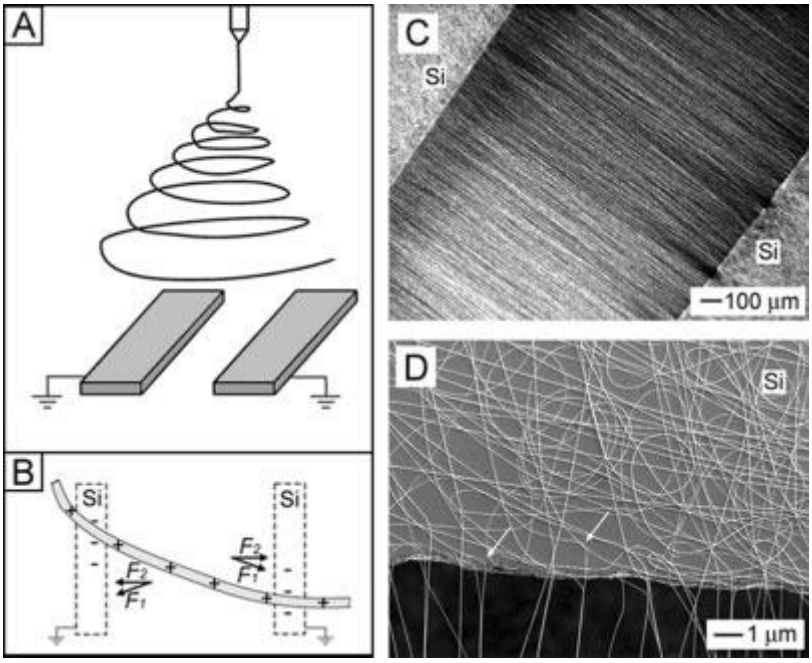

Figure 1.10. A) Schematic illustration of the setup used for electrospinning nanofibers as uniaxially aligned arrays. The collector was constructed from two conductive substrates separated by a void gap. B) The electrostatic force analysis of a charged nanofiber spanning across the gap. C) Dark-field optical micrograph of PVP nanofibers collected across the void gap between two parallel electrodes. D) SEM image of aligned fibers taken from the region close to the edge of a void gap. [77]

Besides the method of parallel counter electrodes to fabricate well-aligned electrospun fibers, many other methods were also reported, mainly based on the high-speed rotating drum as the collector. Some of them are listed in Table 1.2.

Table 1.2. Schematic diagram of various electrospinning set-ups to obtain aligned fibrous assemblies.

Diagram & Instruction	Advantages	Disadvantages	Reference
Rotating wire drum collector with low speed (~ 1 rpm) 	1. Simple setup. 2. Highly aligned fibres are possible.	1. Thicker layer of aligned fibres are not possible. 2. Fibres may not be aligned throughout the whole assembly.	Katta et al [84], 2004
Drum collector with wires that is perpendicular to the rotating direction wound on it 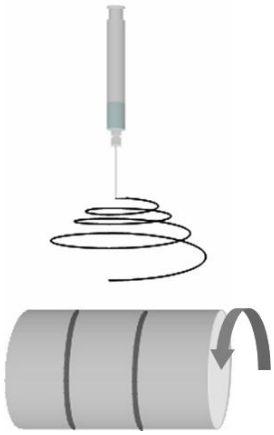	1. Simple setup. 2. Highly aligned fibres are possible 3. Area of aligned fibres on the wire is adjustable by varying wire thickness.	Aligned fibres are concentrated on the wire instead of the whole drum.	Bhattarai et al [85], 2005
Rotating tube collector with knife-edge electrodes below on which negative high voltage are applied 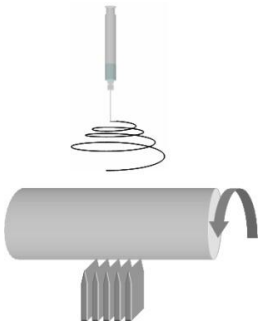	1. Highly aligned fibres possible 2. Aligned fibres covered the whole tube 3. Thicker layer of aligned fibre deposition is possible	1. Setup requires a negative electrode to be effective 2. Only possible for small diameter tube	Teo et al [86], 2005

Table 1.2 Continued

Controlling electrospun -ning Advantage jet using knife-edge electrodes 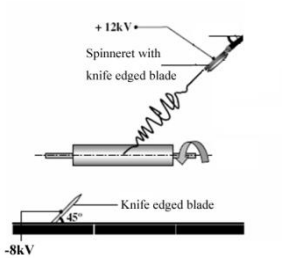	1. Highly aligned fibres possible 2. Able to control the direction of 3. Thicker layer of aligned fibre deposition is possible	1. Setup requires a negative electrode to be effective 2. Only possible for small diameter tube	Teo et al [87], 2005
Disc collector 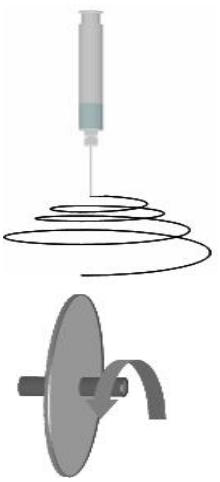	1. Simple setup 2. Highly aligned fibres are possible 3. Able to fabricate arrayed fibres by attaching a rotatable table on the edge of the disc	1. Unable to retain high fibre alignment at the same rotating 2. Speed when the deposited fibres are thicker 3. Small area of fibre alignment	Theron et al [88], 2001 Inai et al [89], 2005 Xu et al [90], 2004
Rotating drum with sharp pin inside 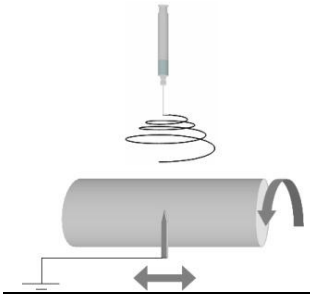	Large area of arrayed fibres can be fabricated	1. Setup is complicated 2. Thicker area of arrayed fibre assembly may not be possible	Sundaray et al [91], 2004
	1.	1.	

Table 1.2 Continued

Blade placed in line 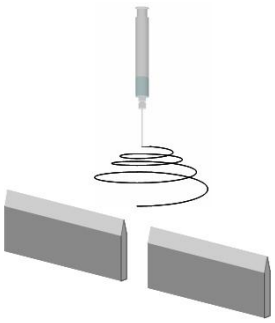	2. Simple setup 3. Yarn can be easily removed from the collector 4. Collected yarn is highly aligned	2. Fabricated yarn is of limited length 3. Deposited fibres have to be dipped in water first before yarn is formed	Dalton et al [92], 2005

In some applications, such as blood vessel engineering, 3D structure of electrospun fiber tubes is needed. As shown in Figure 1.9C, Boland et al. [93] used a rotating drum at a speed of 1000 rpm to collect aligned fibers. To fabricate a tubular scaffold, electrospun fibers can be deposited on a rotating tube and the deposited fiber layer subsequently extracted from the tube.

1.1.6 Materials of Electrospun Fibers

Early work on electrospinning mainly dealt with conventional organic polymers that could be synthesized with sufficiently high molecular weights and could be dissolved in appropriate solvents. In an effort to greatly expand the functionality and thus the scope of applications associated with fibrous structures, a variety of methods have recently been developed to increase the diversity of materials that can be adapted for use with electrospinning. Theoretically, nearly all soluble or fusible polymers can be processed into fibers by electrospinning, provided that the molecular parameters, such as solubility, glass-transition temperature, melting point, crystallization velocity,

molecular weight, molecular weight distribution, entanglement density, solvent vapor pressure, and pH value, and process parameters, such as concentration, electrical conductivity, surface tension, feeding rate, electrode separation and geometry, temperature, RH and so forth, are appropriately adjusted. As a result, various materials can be electrospun and fabricated to nanofibrous structure, including solvent-base polymers, polymer melts, polymer blends, inorganic materials, such as ceramics, metals, and so forth.

1.1.6.1 Electrospinning of Water Soluble Polymers

Water-soluble polymers like PEO, PVA, PVP, poly(acrylic acid) (PAA), olyacrylamide, polyelectrolytes, and hydroxypropylcellulose (HPC) offer a variety of advantages for electrospinning. The solubility properties of water can be adjusted by the pH value, the temperature, or the addition of surfactants or other solvents like alcohols. Electrospun fibers of water-soluble polymers decompose rapidly on contact with water. While this property may be useful for biomedical applications, additional stabilization of these fibers by cross-linking is necessary for other technical applications. Typical water-soluble polymers for electrospinning is shown in Table 1.3.

Table 1.3. Electrospun water soluble polymers

Polymer System	**Chemical Fomula**	**Reference**
PEO	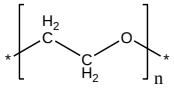	94 - 112
PVA	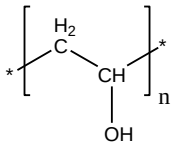	113 - 124
PAA	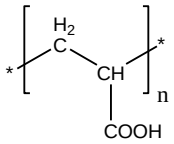	125 - 127
PVA/PAA		128 - 133
PVP	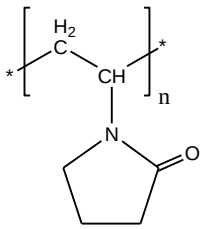	134, 135
PVP composite		136 - 160
PVP, coaxial		161 -163

1.1.6.2 Electrospinning of Organosoluble Polymers

there are many organosoluble polymers (Table 1.4), including PS, PAN, PMMA, polycarbonate (PC), aliphatic and aromatic PA, polyimides (PI), polybenzimidazole (PBI), poly(ethylene terephthalate) (PET), PU, poly[thylene-co-(vinyl acetate)] (PEV), poly(vinyl chloride) (PVC), poly(vinyl butyral) (PVB), and poly(vinylidene fluoride) (PVDF). Apart from of the large number of appropriate polymer systems, the main advantage of electrospinning from organic solvents is the availability of a broad range of solvent properties, for example, polarity and vapor pressure. However, the properties of the organic solvents, such as flammability, toxicity, and corrosiveness,

and so forth, can often be disadvantageous. These disadvantages are not a big issue in laboratory systems, but may play a major role in industrial production facilities, as the solutions used for electrospinning generally contain 85–95% solvent.

Table 1.4. Electrospun organosoluble polymers

Polymer System	Chemical Fomula	Reference
PS	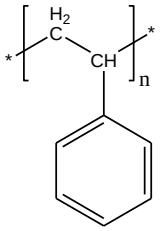	164 - 173
PAN	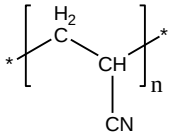	174 - 187
PC	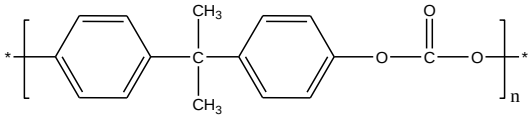	188, 189
PI	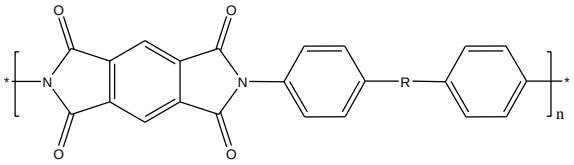	190 - 192
PBI	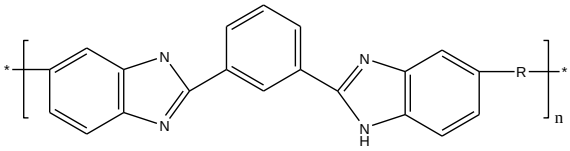	193, 194
PET	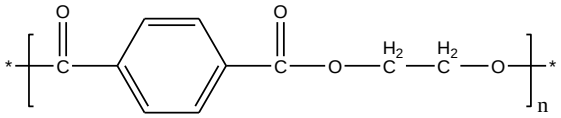	195 - 198
PTT	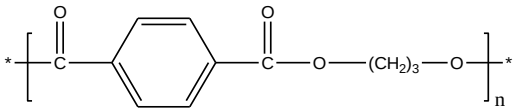	199
PU	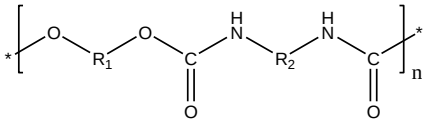	200 - 212
PVC	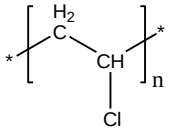	213, 214
PMMA	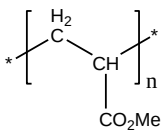	215 - 217

Table 1.4 Continued

PVB	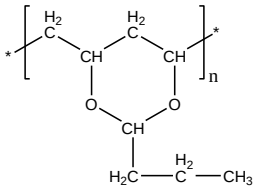	218
PVDF	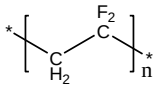	219

1.1.6.3 Melt-Eletrospun Polymers

The electrospinning of polymers from the melt avoids the use of solvents and is, therefore, attractive from the perspective of productivity and environmental considerations. However, the methods are limited by the fact that nanofibers with diameters of less than 400 nm and with a narrow diameter distribution cannot yet be fabricated. To date, polyethylene (PE), polypropylene (PP), polyamide 12 (PA 12), PET, PCL, and PU have been processed by melt electrospinning (Table 1.5). Fiber diameters of less than 300 nm could only be obtained from the low-melting PCL. [220] In this case, PCL was electrospun directly onto the tissue of living cells, without any visible harm to the cells. However, PCL is virtually unfeasible for most technical applications, because of its low melting range.

Table 1.5. Melt-electrospun polymers.

Polymer System	Chemical Fomula	Reference
PE	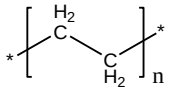	221, 222
PP	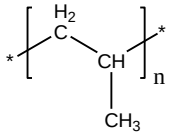	223 - 225
PA 12	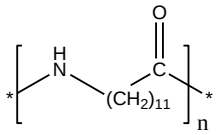	226
PET	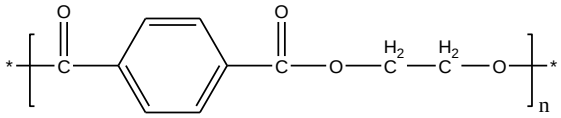	227
PCL	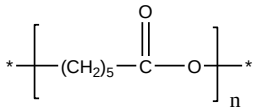	220
PU	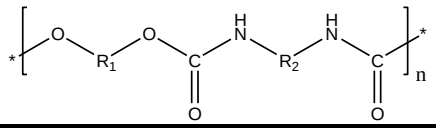	211

1.1.6.4 Electrospun Inorganic Materials

A large number of reports describe the electrospinning of inorganic materials. Inorganic salts, inorganic particles of different forms and dimensions, carbon nanotubes, and similar materials can be immobilized in high concentrations in polymer fibers by electrospinning form ternary solutions. By changing the solute and corresponding solvent, by combining electrospinning and sol-gel processes, a series of nano- to submicron fibers of different materials have been electrospun, such as, ceramics, including TiO_2, [228] SiO_2, [229] SiO_2/ZrO_2, [230] and Al_2O_3, [231] and metals,

such as Cu, [232] and composites. Xia group [228] added tetrabutyl titanate into the solution of PVP in isopropanel, and then electrospun. After that the as-spun fiber mats were placed in air at 500 ℃ for 3 hours to get the TiO_2 nanofibers. (Figure 1.11 A and B) In recent years, Bogintzki group[232] from Germany electrospun the PVB solution with $Cu(NO_3)_2$, and the resultant fiber mats were first calcinated in air to remove extra polymers and make CuO fibers. After that, the CuO fiber mats were annealed in H_2 to get the final product, Cu fibers with diameter of around 270 nm. (Figure 1.11 C and D) The use of various materials offers electrospun fibers a promising opportunity to be used in photocatalysis, [228] conductor, [232] photo-electronic devices, etc.

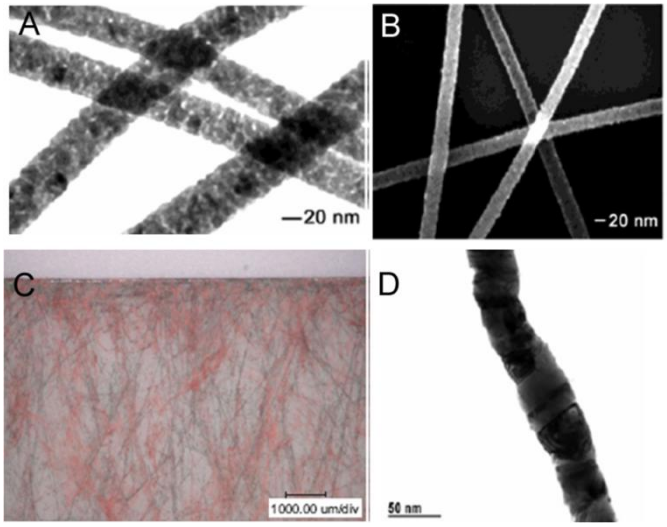

Figure 1.11. A) TEM and B) SEM images of TiO_2 nanofibers, [228] and C) photograph and D) TEM image of Cu nanofibers. [232]

1.2 Overview of PEMFCs

1.2.1 Introduction to Fuel Cells

The concept of fuel cell has existed for more than a hundred years and has attacted increasing attention in recent decades due to the high energy demands, fossil fuel depletions, and environmental pollution throughout the world. The first fuel cell was reported in 1838 by William R. Grove, who discovered that when arranging two platinum electrodes with one end of each immersed in a container of sulfuric acid and the other ends separately sealed in containers of oxygen and hydrogen, a constant current would flow between the electrodes. He combined several of these cells in a series circuit and called it a "gas battery". [233] In 1880's, designs for workable gas batteries began to emerge from laboratories in Europe and the USA. In 1889, Mond and Carl Langer described their experiments with a fuel cell using coal-derived "Mond-gas" and attained 6.45 mA cm^{-2} at 0.73 V *vs.* SHE. [234] However, the poisoning caused by the impurities of hydrogen and the high cost of Platinum (Pt) catalyst made the fuel cell impractical. It should be noted that these challenges are still faced by the present fuel cell industry. Despite these challenges, there were still many researchers working on the possibility of converting coal or coal gas directly into electricity by use of "gas battery". Till 1933, direct coal fuel cells were principally abandoned in favor of alkali electrolyte fuel cells, also named as "Bacon Cell". In 1939, Bacon built a cell that used nickel gauze electrodes and operated it under pressure as high as 3000 psi. In 1958 he also demonstrated an alkali fuel cell in a

stack of 10-inch diameter electrodes using alkali electrolytes, which was settled on potassium hydroxide instead of acid electrolytes. [235, 236] Though expensive, Bacon's fuel cell proved to be reliable enough to the U.S. space program of National Aeronautics and Space Administration (NASA) in 1960's. The space program gave fuel cells a kick-off development and successfully used them in supplying energy for space vehicles. Currently, researchers, who are developing various fuel cells for automobiles, buses, and cell phone towers etc, are expecting to see that fuel cells could play a practical and realistic role in the generators of power for all manner of electrical devices in a clean, quiet and petroleum-free way. [237, 238]

1.2.2 Types of Fuel Cells

Fuel cells can be classified according to the operating temperatures, which include low-temperature and high-temperature fuel cells. Low-temperature fuel cells includes alkaline fuel cell (AFC), proton exchange membrane fuel cell (PEMFC), direct methanol fuel cell (DMFC), and phosphoric acid fuel cell (PAFC). The high-temperature fuel cells are operated at temperatures 600-1000 ℃ and two different types of high-temperature fuel cells have been developed, including molten carbonate fuel cell (MCFC) and solid oxide fuel cell (SOFC). An overview of different fuel cell types is given in Table 1.6 in the sequence of operating temperature.[239]

Table 1.6. Different Fuel Cells realized and currently in use and development [239]

Type of fuel cells	**AFC** (Alkaline Fuel Cell)	**PEMFC** (Proton Exchange Membrane Fuel Cell)	**DMFC** (Direct Methanol Fuel Cell)	**PAFC** (Phosphoric Acid Fuel Cell)	**MCFC** (Molten Carbonate Fuel Cell)	**SOFC** (Solid Oxide Fuel Cell)
Operating temp. (℃)	<100	60 - 120	60 - 120	160 - 220	600 - 800	800 - 1000 low temperature (500 - 600) possible
Anode reaction	$H_2 + 2OH^- \rightarrow 2H_2O + 2e^-$	$H_2 \rightarrow 2H^+ + 2e^-$	$CH3OH + H_2O \rightarrow CO_2 + 6H^+ + 6e^-$	$H_2 \rightarrow 2H^+ + 2e^-$	$H_2 + CO_3^{2-} \rightarrow H_2O + CO_2 + 2e^-$	$H_2 + O^{2-} \rightarrow H_2O + 2e^-$
Cathode reaction	$\frac{1}{2}O_2 + H_2O + 2e^- \rightarrow 2OH^-$	$\frac{1}{2}O_2 + 2H^+ + 2e^- \rightarrow H_2O$	$\frac{2}{3}O_2 + 6H^+ + 6e^- \rightarrow 3H_2O$	$\frac{1}{2}O_2 + 2H^+ + 2e^- \rightarrow H_2O$	$\frac{1}{2}O_2 + CO_2 + 2e \rightarrow CO_3^{2-}$	$\frac{1}{2}O_2 + 2e^- \rightarrow O^{2-}$
Application	1. Transportation 2. Space 3. Military 4. Energy storage systems	Combined heat and power for decentralised stationary power systems	Combined heat and power for stationary decentralised systems and for transportation			
Realised Power	Small plants 5 - 150kW modular	Small plants 5 - 250 kW modular	Small plants 5 kW	Small - medium sized plants 50 kW – 11 MW	Small power plants 100 kW- 2 MW	Small power plants 100 – 250 kW
Charge Carrier in the Electrolyte	OH^-	H^+	H^+	H^+	CO_3^{2-}	O^{2-}

1.2.3 Applications of Fuel Cells

1.2.3.1 Stationary Power

The most important attributes of fuel cells for stationary power generation are the high efficiencies and the possibility for distributed power generation. In principle, both low-temperature and high-temperature fuel cells could be used for stationary applications. The low-temperature fuel cells have the advantage that usually a faster start-up time can be achieved. The needed operating time for the stationary applications is 40,000 hours, which could be a challenge for fuel cell systems. The high-temperature systems such as SOFC and MCFC generate high-grade heat, which can directly be used in a heat cycle or indirectly used by incorporating the fuel cell system into a combined cycle. SOFCs and MCFCs also have the advantage that they can operate directly on available fuels without the need for external reforming.

For a small distributed power system, for example, single-home or multiple-home power generation, a PEM, SOFC, or PAFC combined with a heat cycle could be used to provide all the needs for a household.

Small power plants in the range above 250 kW can be operated by high-temperature fuel cell systems. The high grade heat obtained from these systems can be used for direct heat or further electricity generation by steam engines. However, the start-up time of these systems are longer than for low-temperature systems.

1.2.3.2 Transportation

For the vehicular application of fuel cell systems, the available space in vehicles is critical and fast response times and start-up times are also required. As a result, low-temperature fuel cell systems are generally considered to be appropriate.

Prototype fuel cell powered vehicles have recently been demonstrated in Europe, Japan and North America by several car manufactures, as seen in Figure 1.12. All the DEMO vehicles are based on a basic conceptual design combining the PEMFCs with an electric drive. The PEMFCs is regarded as ideally suited for transportation applications due to its high power density, high energy conversion efficiency, compactness, light weight, and low-operating temperature. The recent PEMFC-driven electric vehicles have demonstrated the technical feasibility of the concept. However, among all applications, the transportation application involves the most stringent requirements regarding volumetric and gravimetric power density, reliability, and costs.

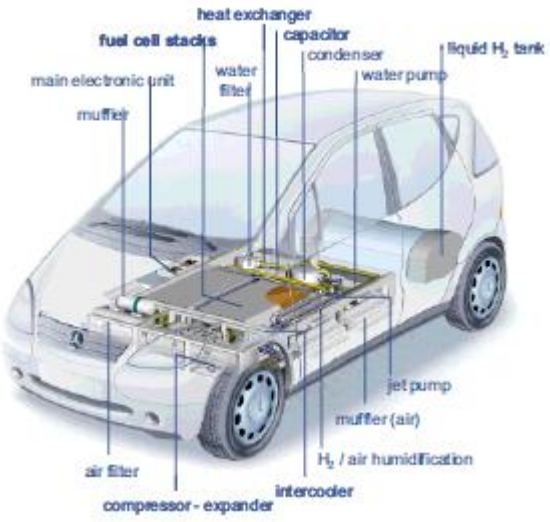

Figure 1.12. NECAR 4, components of a fuel cell vehicle with a PEM system operated with liquid H_2. [240]

1.2.3.3 Portable Applications

For small power applications like laptops, camcorders, and mobile phones, the requirements of the fuel cell systems are even more specific than for vehicle applications. Low temperatures are necessary and therefore PEMFCs and DMFCs are chosen. Possibilities for fuel cell systems are the combination of PEM with hydrogen storage by hydrides or gas cartridges or DMFCs. Other fuel cells are not suitable for this kind of applications.

1.2.4 Basic Principles of Fuel Cells

Fuel cells are galvanic cells, in which the free energy of a chemical reaction is convered into electrical energy with an outer electrical current. The Gibbs free energy change of a chemical reaction is related to the cell voltage via:

$$\Delta G = -nF\Delta U_0 \qquad (1.1)$$

where n is the number of electrons involved in the reaction, F the Faraday constant, and ΔU_0 the voltage of the cell for thermodynamic equilibrium in the absence of a current flow. The anode reaction in fuel cells is either the direct oxidation of hydrogen, or the oxidation of methanol. The cathode reaction in fuel cells is oxygen reduction, in most cases from air.

For the case of a hydrogen/oxygen fuel cell, the overall reaction is:

$$H_2 + 1/2\, O_2 \rightarrow H_2O \quad \text{with} \quad \Delta G = -237 kJ/mol \qquad (1.2)$$

with an equilibrium cell ΔU_0 voltage for standard condictions at 25 ℃ of:

$$\Delta U_0 = -\frac{\Delta G}{nF} = 1.23V \qquad (1.3)$$

A fuel cell is an electrochemical cell whereby each electrochemical reaction is characterized by the thermodynamic equilibrium potential described by the Nernst equation. Even under no-current conditions, the voltage of a fuel cell can be lower than the thermodynamic value due to mixed potential formation and other parasitic processes. [239] Thus the open circuit voltage can be lower than the Nernstian value. When the current flows, a deviation from the open circuit voltage occurs corresponding to the electrical work performed by the cell. The deviation from the equilibrium value is called the overpotential and has been given the symbol η. One of the reasons for the deviation of the potential from the equilibrium value is the finite rate of the reaction at the electrodes.

For a redox reaction at one electrode, the current density (*j*) is given by the Butler-Volmer equation:

$$j = j_0\{\exp(\alpha_A F\eta/RT) - \exp(-\alpha_C F\eta/RT)\} \qquad (1.4)$$

where j_0 is the exchange current density, α_A and α_C the transfer coefficients for the anodic and cathodic reaction, respectively, and η the overpotential to drive the reaction. This equation holds when the charge transfer dominates the reaction at small values of *j* and η.

The anode overpotential (η_A) and cathode overpotential (η_C) are:

$$\eta_A = U_A(j) - U_{0,A}, \text{ with } \eta_A > 0 \text{ (oxidation of fuel)} \qquad (1.5)$$

$$\eta_C = U_C(j) - U_{0,C}, \text{ with } \eta_C < 0 \text{ (reduction of oxygen)} \qquad (1.6)$$

where $U_A(j)$ and $U_C(j)$ are the exchange potentials of the anode and cathode, and $U_{0,A}$ and $U_{0,C}$ the thermodynamic equilibrium potentials of the anode and cathode, respectively. [239]

1.2.5 Introduction to PEMFCs

PEMFCs, also known as polymer electrolyte membrane fuel cells, are a type of fuel cell that successfully converses chemical energy into electrical power at low temperature. [241-245] PEMFCs have gained much attention because of superior performance of high efficiency, high power density, and low greenhouse gas emission. They are proved to be promising for transport applications as well as for stationary and portable fuel cell applications.

1.2.5.1 History of PEMFCs

Before the invention of PEMFCs, most existing fuel cell types, such as solid-oxide fuel cells, required very expensive materials and could only been applied in extreme conditions, e.g. at high temperatures. Such fuel cells were so large in size that they could only be used for stationary applications. These issues were addressed by the PEMFCs. The first PEMFC was invented in the 1963 by Willard Thomas Grubb and Leonard Niedrach of General Electric (GE). [246] GE announced this initial success in mid-1960 when the company developed a small fuel cell that was fueled with hydrogen generated by mixing water and lithium hydride for a program with the U.S. Navy's Bureau of Ships (Electronics Division) and the U.S. Army Signal Corps.

PEMFC technology served as part of NASA's Project Gemini in the early days of the U.S. piloted space program. However, because of several technical difficulties associated with early PEMFCs, including internal cell contamination and leakage of oxygen through the membrane, GE's PEMFCs were not accepted by Project Apollo. The first mission to utilize PEMFCs was Gemini V, served adequately for the remaining Gemini flights. Project Apollo mission planners, however, chose to use alkali fuel cells for both the command and lunar modules, based on Bacon's design, developed by Pratt and Whitney Aircraft, as did designers of the Space Shuttle a decade later.

GE researchers continued working on PEMFCs, and in the mid-1970s developed PEM

water electrolysis technology for undersea life support, leading to the US Navy Oxygen Generating Plant. The British Royal Navy adopted this technology in early 1980s for their submarine fleet. Other groups also began looking at PEMFCs.

Initially, PEMFCs were only successful in space programs and other special applications. It was not until the late 1980s and early 1990s that PEMFCs became a real option for wider application base. Several pivotal innovations, such as low Pt catalyst loading and thin film electrodes, drove the cost of fuel cells down, making the development of practical PEMFC systems more realistic. However, until now significant debate still exists as to whether PEMFCs will be a realistic technology for use in automobiles.

1.2.5.2 Working Principal of PEMFCs

A PEMFC transforms the chemical energy liberated during the electrochemical reaction of hydrogen and oxygen to electrical energy, as opposed to the direct combustion of hydrogen and oxygen gases to produce thermal energy.

A steam of hydrogen is delivered to the anode side of the membrane electrode assembly (MEA). At the anode, it is catalyzed by Pt, and split into protons and electrons. This oxidation half-cell reaction is represented as follow:

$$H_2 \rightarrow 2H^+ + 2e^- \qquad E^0 = 0V_{SHE} \qquad (1.7)$$

The formed protons permeate through the PEM. However, the electrons travel along an

external load circuit to the cathode side of the MEA, and provide electric power along the way. At the cathode, a stream of oxygen is meanwhile delivered, and the oxygen molecules react with the protons permeating through the PEM and the electrons arriving through the external circuit to form water molecules. The reduction half-cell reaction is represented as follow:

$$1/2O_2 + 2H^+ + 2e^- \rightarrow H_2O \qquad E^0 = 1.229V_{SHE} \tag{1.8}$$

The full-cell reaction is:

$$H_2 + 1/2O_2 \rightarrow H_2O \qquad E^0 = 1.229V_{SHE} \tag{1.9}$$

The scheme of a PEMFC can be see in Figure 1.13:

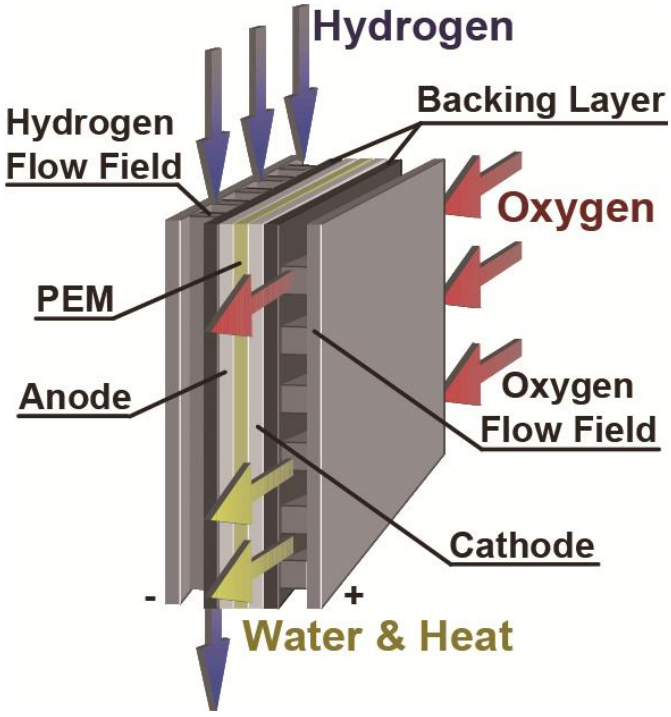

Figure 1.13. The schematic diagram of a PEMFC.

1.2.5.3 Components of PEMFCs

1.2.5.3.1 Electrodes

PEMFCs generally use porous gas diffusion electrodes to ensure the supply of the reactant gases to the active zones where the noble metal catalyst is in contact with the ionic and electronic conductor. The fabrication of gas diffusion electrodes (GDE) is an intricate procedure in which all details of the structure and preparation are important. The reason for this is that the function of the electrodes is far more than just catalyzing a reaction.

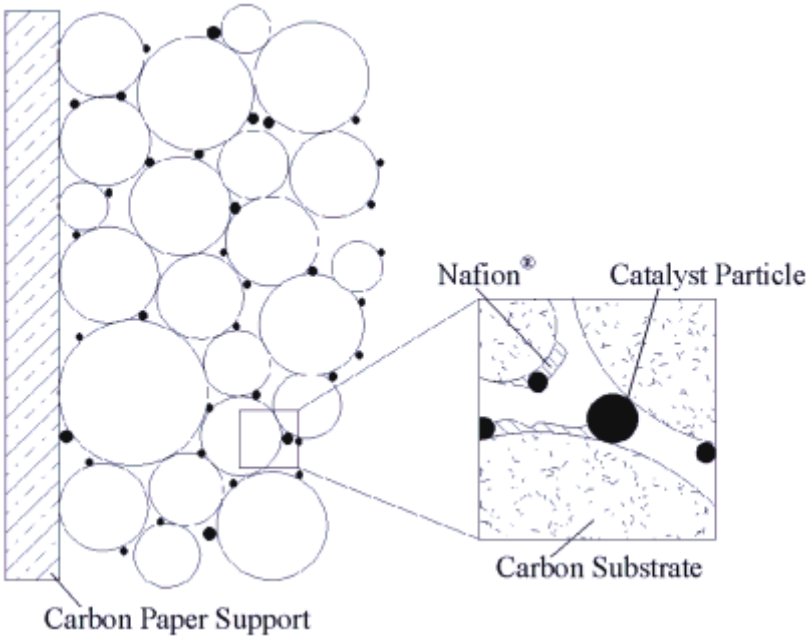

Figure 1.14. The three phase boundary formed by the catalyst particles, the ionomer and the gas phase in a porous structure, ensuring both electronic and ionic contact as well as gas transport. [247]

The main requirement of a good electrode is not only on the three-phase boundary between the gas supply, and but also on the catalyst particle and the ionic conductor. The particles must be in direct contact with an electronic conductor to ensure the electrons are supplied to or taken away from the reaction sites. Electronic conductivity is usually provided by a carbon support onto which the catalyst particles are supported. The three-phase boundary is made by impregnating the catalyst/support powder with some ionomer binder, which usually is Nafion solution, before pressing the electrode onto the membrane. This ensures good contact of most catalyst particles with ionomer material that has ionic contact with the membrane.

Gas diffusion occurs through the backing layer and the carbon support to the catalyst particles. When using humidified gases, the catalyst layer must be sufficiently hydrophobic to prevent the pores from flooding. This hydrophobicity can be provided by introducing polytetrafluoroethylene (PTFE) as a binder, in combination with Nafion that is hydrophilic. Usually the catalyst is made into an ink with water and isopropanol and mixed with the binder material (the optimum binder quantity depends on the type of catalyst) after which the ink can be cast straight onto the membrane. The effect of the binder content on the performance of the electrodes was studied both for the PTFE binder as for the Nafion binder. [248 - 250]

1. Cathodes

Although a huge variety of catalysts have been investigated, so far Pt based catalysts

are the superior material for the oxygen reduction reaction. Pt dispersed on carbon or other small Pt particles (such as colloids) exhibit a good performance. Due to the low temperature in PEMFCs, the loadings for the oxygen catalysts are significant to compensate for the slow reaction kinetics. [251] Because pure oxygen is seldom available, fuel cells typically use air for the cathode gas supply. The lower oxygen partial pressure in air leads to a decrease in activity compared to pure oxygen. Under operating conditions for longer times, a "ripening" of the Pt particles has been reported which manifests itself in a decrease of active surface area due to the formation of larger particles. [252]

2. Anodes

If pure hydrogen is used as fuel, the performance of the anode is excellent with pure Pt catalyzing the oxidation of hydrogen. Unfortunately in most practical systems, the fuel stream contains certain traces of elements or compounds, such as CO, S, and NH_3. All of these substances can lead to a greater or lesser extent poisoning on the anode catalysts.

CO is one of the major poisons in low temperature fuel cells. [253 - 255] In PEMFCs and PAFCs, CO poisoning occurs due to the adsorption of the species to the active sites of the Pt catalysts, so that little sites are available for reaction with H_2. To reactivate the surface, CO can be oxidized to CO_2.

To avoid CO contamination in the cell, a gas clean-up can be built in the fuel cell system. However, this method adds complexity to the system. Other methods to remove CO from the fuel cell are the mixing of the fuel feed with small amounts of air or oxygen. [253 - 255] This stimulates the oxidation of CO over the catalyst. This method requires an extensive control system, since the air content has to be closely monitored. The addition of hydrogen peroxide to the fuel stream has also been investigated as a method to minimize CO contamination. [256, 257] A recent method of operating PEMFCs with reformed hydrogen with reduced requirements for gas cleaning is the operation applying pulses to the cell. The electrical pulses increase the anode potential to values at which CO is oxidized to CO_2. In this way, the catalyst surface is continuously cleaned and the loss of cell voltage is minimized. [258]

CO-tolerant catalysts are still being investigated by numerous research groups in order to reduce the influenceof the problem. CO-tolerant anodes usually contain a Pt-Ru alloy as the state-of-the-art catalyst. The mechanisms of CO oxidation and CO tolerance of Pt-Ru catalysts with well-defined surfaces have been investigated and clarified by several groups. [259 - 263] For example, catalysts prepared via a DC-magnetron sputtering technique producing thin layers on standard fuel cell electrode substrates have been investigated. [264] Pt-Ru-W and Pt-Ru-Mo showed an improved CO tolerance over Pt and Pt-Ru catalysts.

1.2.5.3.2 Membranes

Nafion is probably the most studied and operated electrolyte for PEMFCs. However, other perfluorocarbon sulfonic acid membranes form Dow, Gore and Asahi Chemical are also used and investigated (Figure 1.15). [265] Most membranes usually have a small operating temperature range in which they are stable. The upper temperature limit is dictated by the need of humidification of the membranes.

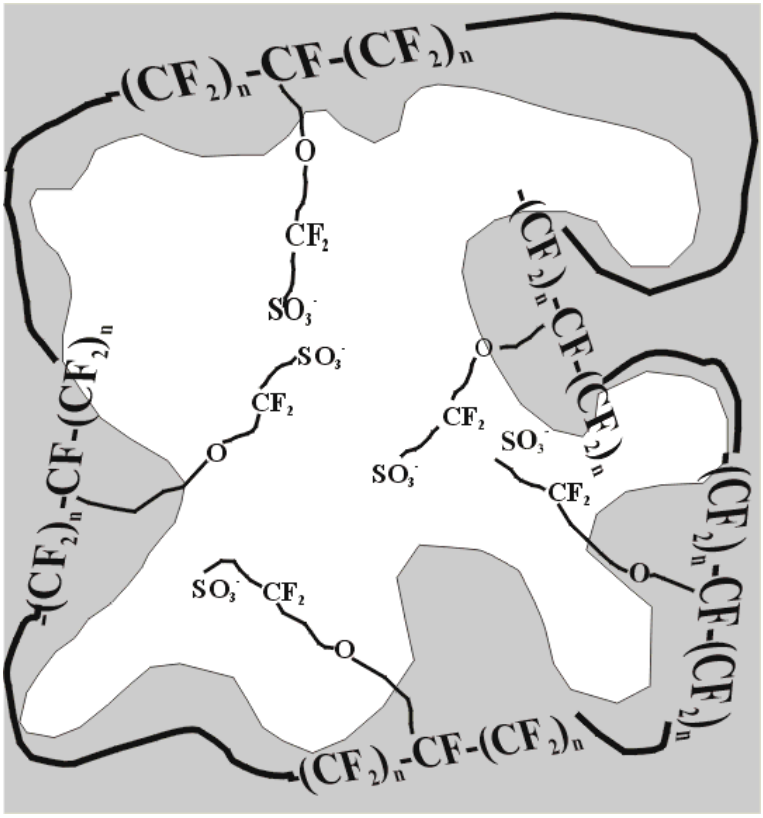

Figure 1.15. The structure of Nafion showing the three different regions: the hydrophobic PTFE backbone, the hydrophilic ionic zone, and the intermediate region. [266]

Improvements in membrane structure and conductivity and made by producing

composite membranes. This can be done in several ways, which will be discussed in section 1.2.6.

1.2.5.4 Water management in PEMFCs

Membranes in PEMFCs are generally filled with water to achieve high conductivity (Figure 1.16). A dried membrane possesses a lower conductivity as proton transport through a wet membrane is similar to that of an aqueous solution. Water management in the membrane is one of the major issues in PEMFC technology. Factors influencing the water content in the membrane are water drag through the cell, since for every proton a shell of H_2O is also transported through the membrane, and back diffusion from product water from the cathode into the membrane.

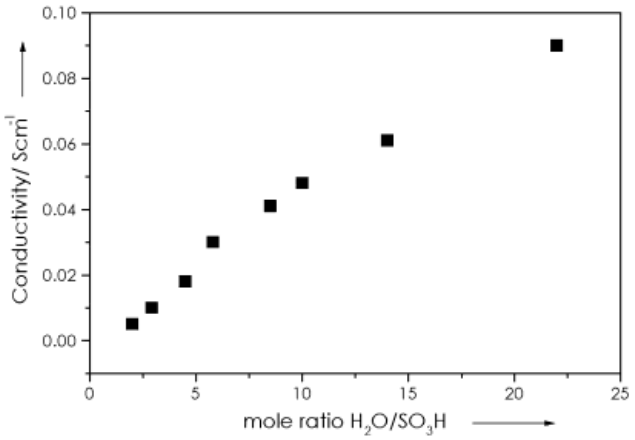

Figure 1.16. The influence of the water content on the conductivity of a Nafion membrane. [267 - 269]

One way for effective water management is to humidify the gases coming into the fuel cell. Another form of water management can be found in the direct hydration of

the membrane by mounting porous fiber wicks. [270 - 272] Twisted threads of porous polyester fibers are placed between the membrane and a cast thin film of Nafion ionomer and is hot pressed at 150 ℃. This encures a direct water supply form either the humidifiers or from product water at the cathode to the membrane by using a pressure difference.

1.2.6 Fabrication Technologies of PEMs

In general, PEMs are usually based on polymer electrolytes, which have negatively charged groups on the polymer backbone. These polymer electrolytes tend to be rather rigid and are poor proton conductors unless water is absorbed. The proton conductivity of hydrated PEMs dramatically increases with water content and could reaches values of $10^{-2} – 10^{-1}$ S/cm.

1.2.6.1 Polymeric PEMs

Table 1.7 gives the classification of the polymeric membranes materials used for PEMFCs. Polymer electrolytes used for PEMFCs generally fall into different membrane systems:

1. perfluorinated ionomers,
2. partially fluorinated polymers,
3. non-fluorinated membranes with aromatic backbone,
4. non-fluorinated hydrocarbons,
5. acid–base blends.

In Table 1.7, the structure and physical properties of the different polymer membranes and their performance are also compared.

Table 1.7. Structure–property relationships and performance of polymers

Category	Structure	Physical properties	performance
Perfluorinated membranes	● Fluorinated PTFE-like backbone ● Fluorocarbon side chain ● Ionic clusters consisting of sulfonic acid ions attached to the side chains	● Membranes are strong and stable in both oxidative and reductive environments	● Membrane is durable upto 60,000 h ● Proton conductivities in well humidified membranes are 0.1 S/cm at PEMFC operating temperatures ● Cell resistance of 0.05 Ω cm^2 for 100 μm thick membrane with voltage loss of 50mV at 1 A/cm^2
Partially fluorinated membrane	● Fluorocarbon base ● Hydrocarbon or aromatic side chain grafted onto the backbone	● Membranes are relatively strong, but degrage fast	● Less durable ● Low performance ● On suitable modification, yield membranes with comparable proton conductivity
Non-fluorinated hydrocarbon membrane	● Hydrocarbon base, typically modified with polar groups	● Membranes possess good mechanical strength ● Poor chemical and thermal stability	● Poor proton conductivity ● Exhibit low durability on account of swelling obtained by incorporation of polar groups

Table 1.7 Continued

Non-fluorinated aromatic membranes	● Aromatic base, typically modified with polar/sulfonic acid groups	● Good mechanical strength ● Chemically and thermally stable even at elevated temperatures	● Good water absorption ● Relatively high proton conductivity
Acid-base blend membranes	● Incorporation of acid component, into an alkaline polymer base	● Stable in oxidizing, reducing and acidic environments ● High thermal stability	● Good dimensional stability ● Proton conductivity comparable to Nafion ● Durability of the membranes is not good

1.2.6.1.1 Perfluorinated PEMs

The performance and lifetime of PEMFCs have been significantly improved since Nafion® was developed in 1968. Lifetimes of over 50,000 hours have been achieved with commercial Nafion® 120. Figure 1.17 shows the chemical structures of Nafion® and other perfluorinated PEMs.

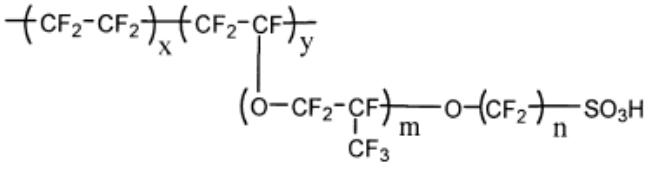

Nafion®117	m≧1, n=2, x=5-13.5, y=1000
Flemion®	m=0, 1; n=1-5
Aciplex®	m=0, 3; n=2-5, x=1.5-14
Dow membrane	m=0, n=2, x=3.6-10

Figure 1.17. Chemical structures of perfluorinated polymer electrolyte membranes.

Perfluorinated PEMs have also been developed by other corporations, such as Dow membranes by Dow chemical, which has an equivalent weight of approximately 800 and a thickness of 125 mm in the wet state. [273] In addition, Flemion® R, S, T, which have equivalent repeat unit molecular weights of 1000 and dry state thicknesses of 50, 80, 120 μm, respectively, have been developed by Asahi Glass Company. [274] Asahi Chemical Industry manufactured a series of Aciplex®-S membranes, which have equivalent repeat unit molecular weights of 1000 - 1200 and dry state thicknesses of 25 - 100 mm. These perfluorinated PEMs were developed from chlor-alkali electrolysis. The water uptake and proton transport properties of these membranes have significant effect on the performance of PEMFCs. These membranes have water uptakes of above 15 H_2O/-SO_3H, which highly improve the proton conductivity. In general, the proton conductivities can reach values of 10^{-2} - 10^{-1} S/cm. Because of their perfluorinated polymer backbones, all of these membranes possess good thermal, chemical, and mechanical properties.

Factors limiting the use of perfluorinated PEMs to large scale commercial application include poor proton conductivities at low humidities and elevated temperatures, easiness of chemical degradation at high temperatures, and high cost. These factors can adversely affect fuel cell performance and tend to limit the conditions under which a fuel cell can be operated. For example, the conductivity of Nafion® reaches

up to 10^{-1} S/cm in its fully hydrated state but dramatically decreases with temperature above the boiling point of water because of the loss of absorbed water in the membranes.

The major disadvantages of these Perfluorinated PEMs are:

1. The high cost of membrane amounting to US$ 700 per square meter,
2. Lack of safety during its manufacture and use,
3. Requirement of supporting equipment,
4. Temperature related limitations.

The developments of new PEMs, which cost much less than perfluorinated PEMs and possess sufficient electrochemical properties, have become one of the most important areas for the research in PEMFCs.

In general, PEMs for high performance PEMFCs have to meet the following requirements:[275]

1. low cost;
2. high proton conductivities at high temperatures and low humidities;
3. good water uptakes;
4. working hour of 5000 hours for portable equipments and 50000 hours for stationary ones.

1.2.6.1.2 Hydrocarbon PEMs

Another promising route to high-performance PEMs is the use of hydrocarbon polymers for polymer backbones, although there is some sacrifice in material lifetime and mechanical properties. The use of hydrocarbon polymers as PEMs for the space programs was abandoned in the initial stage of fuel cell development due to the low thermal and chemical stabilities of these materials. However, relatively cheap hydrocarbon polymers can be used in PEMFCs for transportation application, since the lifetime of electrolytes required in fuel cell vehicles are shorter compared to the use in space vehicles. Also, catalysts and fuel cell assembly technologies have been improved and brought advantages to the lifetimes of PEMFCs and related materials. There are many advantages of hydrocarbon polymers that have made them particularly attractive:

1. Hydrocarbon polymers are cheaper than perfluorinated ionomers;
2. Hydrocarbon polymers containing polar groups have high water uptakes over a wide temperature range, and the absorbed water is restricted to the polar groups of polymer chains;
3. Decomposition of hydrocarbon polymers can be depressed to some extent by proper molecular design.
4. Hydrocarbon polymers are easily recycled by conventional methods.

Several hydrocarbon polymers were employed and investigated as PEMs, including

sulfonated poly(styrene), [276, 277] poly(oxy-1,4-phenyleneoxy-1,4-phenylenecarbonyl -1,4-pheneylene) (PEEK) [278-281], poly(1,4-phenylene) [282-285], poly(oxy-1,4-phenylene) [286], poly(phenylene sulfide) [287], PBI [298], PIs [289], and other polymers [290-292]. The sulfonation agents could be concentrated sulfuric acid [303], chlorosulfonic acid [294], pure or complexed sulfur trioxide [295, 296], acetylsulfate [297], and so forth, in which the protogenic groups are covalently bound either to the polymer backbone or via a spacer.

Although extensive research has been carried on the hydrocarbon PEMs, there are still several problems that prevent this type of PEMs from practical applications. Firstly, since the hydrocarbon backbones are less hydrophobic than those of perfluorinated PEMs, which causes weaker phase separation between the hydrophilic side groups and the hydrophobic backbones, the formation of water pathways would be highly restricted, and thus limited water absorption and proton conductivities. Secondly, besides acid-doped PBIs, few hydrocarbon PEMs can be operated at temperatures higher than 100 ℃. Although the operating temperature of acid-doped PBIs can be as high as 150 ℃, the proton conductivity can only reach ~10^{-2} S/cm. [298-302] Finally, although the cost of the monomers of the hydrocarbon PEMs are relatively low, in some case, several steps of polymerization are needed, which restricts the yield at a low ratio. As a result, the cost of those polymers with complex structures could be highly increased.

1.2.6.1.3 Transport Phenomena in Polymer Electrolyte Membranes

The hydration Level is a critical parameter in Nafion and other polymer electrolytes that has to be maintained in order to retain the membrane performance at temperatures above 100 ℃. In the presence of water, protons as well as the sulfonic acid groups are in the solvated form, and this greatly facilitates the "hopping mechanism" of protons.

To understand the transport of water in polymer electrolyte membranes, quantitative and qualitative modeling studies have been conducted for supporting the optimization of not only the composition of the membrane but also the operating conditions, thereby yielding higher efficiencies and power densities. In terms of microscopic models, there have been many models based on statistical mechanics, molecular dynamics, and macroscopic phenomena applied to the microscopic structure of the membrane. These models provide a fundamental understanding of processes like diffusion and conduction in the membrane, mainly Nafion, on a microscopic scale including the effect of small perturbations, such as non-homogeneity of pores, electric fields on transport, and the introduction of small-scale structural effects. The basis for all these models is the description of the microscopic structure of the polymer that was proposed in the early 1980's by Gierke and Hsu. [303] In their work, the authors correlated the experimental data through geometric and phenomenological relationships for the swelling of the polymer due to the uptake of water and its effect on the diffusion coefficient of water in the membrane pores. The correlation evolved

by analyzing the data taken under different operating conditions led to the formulation of a widely accepted description of the polymeric membranes in terms of an inverted micellar structure, in which the ion-exchange sites are separated from the fluorocarbon backbone, and thus forming spherical clusters (pores). These clusters are connected by short narrow channels. The model was hence termed as "cluster network" model. When the membrane is dry, an average cluster has a radius of about 1.8 nm and it contains about 26 SO_3^- groups distributed on the inner pore surface. In the swollen state, the diameter increases to about 4 nm and the number of fixed SO_3^- groups goes up to about 70. Under these condictions, each pore is filled with about 1000 water molecules and the connecting channels have a diameter and a length of about 1 nm. The authors also proposed the use of percolation theory for the correlation of electrical conductivity with the water content of the membrane. According to this theory, there is a critical amount of water available in the membrane, below which proton transport is extremely difficult due to the absence of extended pathways. Above or near the threshold, the conductivity (σ) follows the law:

$$\sigma = \sigma_0 (c - c_0)^n \qquad (1.10)$$

Where c is the volume fraction of the aqueous phase, c_0 the percolation threshold for the water content in the membrane, n a universal constant which depends on the dimensions of the system, and σ_0 a factor related to the molecular interactions that can only be computed from specific microscopic models. A comparison between experimental results and percolation theory showed a good agreement.

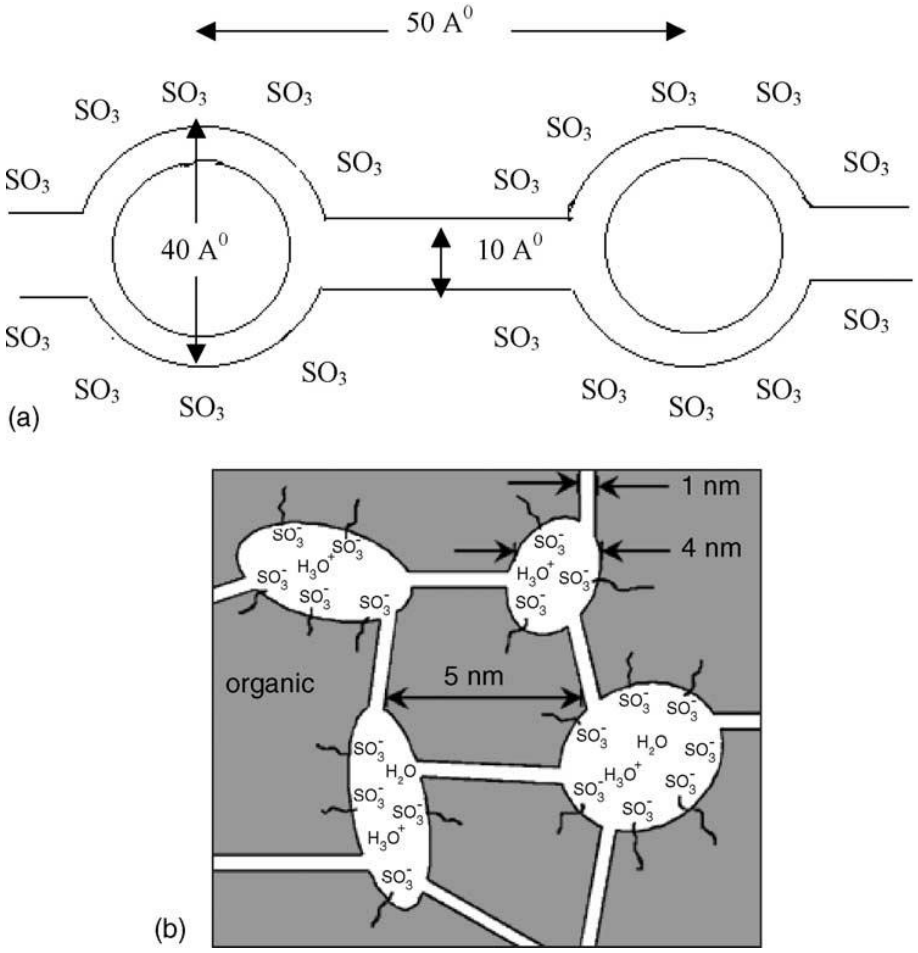

Figure 1.18. Schematic diagrams of (a) "cluster network model" and (b) "random cluster network" model.

Resent studies propose an interpretation of the percolation properties of proton conductivity as a function of water content by using a "random network model", [304] which is a modification of the "cluster network model". This model includes an intermediate region wherein the side chains ending with pendant sulfonic acid groups, which are ionically bonded to the perfluorinated backbones, tending to form cluster within the overall structure of the material resulting in the formation of hydrated regions. Unlike the "cluster network model", the hydrated regions in this model are

distributed randomly in the polymer matrix, which facilitates quicker transport of protons upon the rotation of these side chains. In this case, although the hydrated regions drift apart, the traverse motion of protons through the membranes is possible. A schematic of the cluster network and random network nodels is depicted in Figure 1.18. Haubold et al. verified through small angle X-ray scattering (SAXS) that the "random network model" could be applied to Nafion. [305] James et al. deployed the atomic force microscopy (AFM) technique and found the "random network model" to be generally acceptable on Nafion 117, which is a commonly available Nafion membrane, Typically used in the region of 9 – 34% RH. [306]

1.2.6.2 Hybrid PEMs

In the past 10 years, hybrid membranes have been realized as one of the most promising PEM materials that can potentially offer a superior performance in PEMFCs. With the addition of hygroscopic inorganic particles, working as a water reservoir, [307, 308] water content can be well managed to improve the performance of PEMs. Furthermore, series of functional groups, such as sulfonate acid, phosphonate acid groups, and so forth, can be introduced onto inorganic particles. As a result, the proton conductivities of PEMs can be improved at higher temperatures with high mechanical and oxidation stabilities.

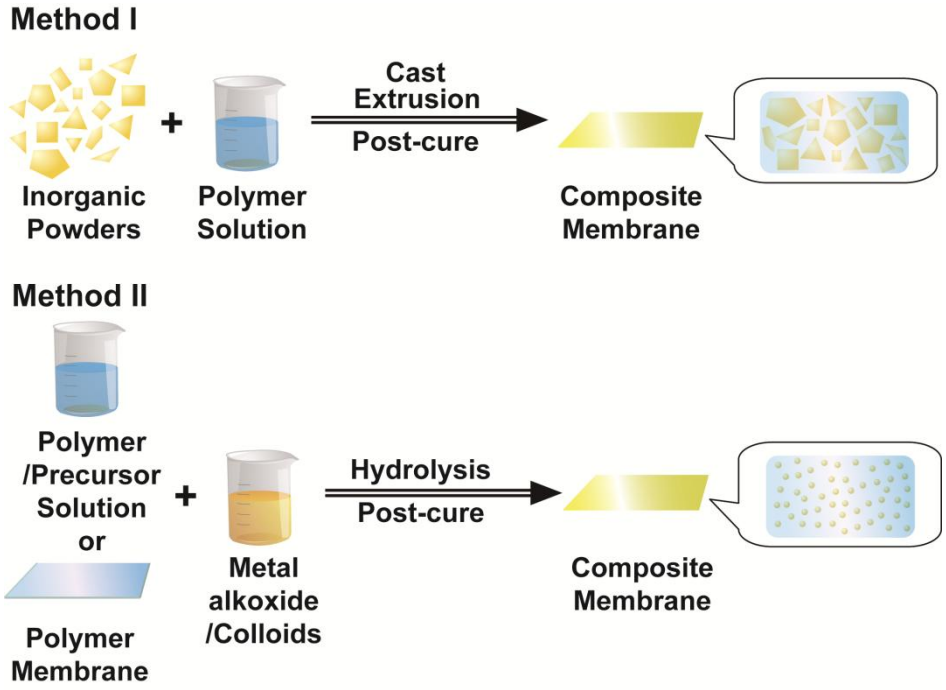

Figure 1.19. A scheme of the basic preparation methodology for ionic organic-inorganic composite membranes.

Basically, two types of approaches have been used to synthesize ionic organic-inorganic composite membrane materials as shown in figure 1.19. The first method deals with the formation of macro- or nano-composites in which the size of inorganic particles is in the micron or nanometer range. A simple way of synthesizing these types of membrane is the physical blending of two components in an appropriate solvent. During the preparation process, a major challenge is the undesired precipitation and agglomeration. In the second case, the hybrid structure is obtained at molecular level by copolymerization of inorganic precursor in the presence of polymer solutions or pre-polymer monomers in a proper solvent with or without catalyst. The general methodology used to prepare these membranes is a sol–gel

process. This process occurs at room temperature in liquid state with organometallic precursors by hydrolysis-condensation in presence of suitable catalysts. [309, 310] In some cases, ionomer membranes are swollen in a proper solvent, immersed into an organometallic precursor to allow the precursor permeate from one side or both sides of the membrane. With the hydrolysis-condensation reactions of impregnated alkoxides, the hybrid membranes with inlaid nanometric inorganic clusters can be fabricated. [312-314]

In the preparation of hybrid PEMs, a variety of inorganic components have been incorporated, such as functionalized and unfunctionalized silica materials, zirconium phosphate, heteropolyacids, metal oxides, solid acids, or the combination of mentioned materials. Table 1.8 gives brief information about the organic and inorganic components of the hybrid PEMs with highlighted properties.

Recently, with the accelerating progress in new materials research and the recognition of the mechanism of PEMs, inorganic and organic functionalized materials have been incorporated into hybrid PEMs in order to improve their performances. For example, with the addition of sulfonic acid functionalized single-walled carbon nanotubes (S-SWCNT), the proton conductivity of Nafion can increase to as high as 6×10^{-1} S/cm, and keep at a high level even at 120 °C. [359] In order to simulate the water pathways observed in polymer electrolytes, some hybrid PEMs based on inorganic frames were developed. Azzaroni group developed hybrid PEMs using macroporous

silica membranes with holes normally oriented to the plane of the membrane and functionalized polymer brushes grafted onto the surfaces of the holes. [360-362] This kind of PEMs can reach a stable proton conductivity of ~10^{-2} S/cm even at low humidity (RH = 30%); and the steady proton conductivity can last as long as 8 days with ignorable conductivity loss. Moghaddam group also developed a PEM based on nanoporous silicon membrane fabricated by etching method, assembled with monolayer of functional molecules. [363] To maintain high conductivity to be maintained at low humidities, an ultrathin conformal layer of silicon dioxide is deposited at the mouth of each of the larger silicon nanopores, creating small apertures. This PEM can obtain a proton conductivity of 8×10^{-2} S/cm at room temperature with wide range of humidity from 20% to 100%.

However, severe problems still exist on these PEMs. For the nano- or micro-particle incorporated PEMs, firstly, many currently used fillers, such as SiO_2 and sulfated or phosphate SiO_2, organic silanes, metal oxides, heteropolyacid, and so on, do not have or only have limited protogenic groups, which restrict the improvement of the proton transport and thus the conductivity of PEMs. Furthermore, the natural conflict between high content of fillers and particle agglomeration makes it difficult to select a proper concentration for fillers to form effective proton-transport pathways through the membrane. Nevertheless for those hybrid PEMs with inorganic frames, although stable performance was acquired, this kind of PEMs is still in the stage of laboratory investigation, since excessive inorganic and insulated component has to be added into

the PEMs. Therefore, the technological impact of developing new fillers that can form uniformly dispersed and continuous proton transport pathways would be significant and needs further exploration.

Table 1.8 Ionic organic-inorganic composite membranes with important physical and electrochemical properties

Polymer	**Inorganic material**	**Descriptions**	**References**
Nafion	Tetraethylorthosilicate	~20% increase in water uptake compare to Nafion	313, 314
	Cross-linked network of 4,4'-methy- lenedianiline and 3-glycidoxypropyl-trimethoxysilane	$\sim\sigma = 3.4 \times 10^{-1}$ S/cm	315
	Diphenyldichlorosilane and merca- ptopropyltrimethoxysilane	$\sim\sigma = 1.0 - 2.2 \times 10^{-1}$ S/cm, water content 16 – 21%	316 - 320
	Zirconia	20 – 25% higher water uptake, $\sigma = 2 \times 10^{-2}$ S/cm	312, 321
	Sulfated Zirconia	$\sim\sigma = 2.3 \times 10^{-1}$ S/cm, 105–135 ℃	322, 323
	Zirconium phosphate	$\sim\sigma = 1.6 - 2.7 \times 10^{-1}$ S/cm	324
	Heteropolyacids	Water content 60–95%, $\sim\sigma = 1.5 - 9.5 \times 10^{-2}$ S/cm	308, 325, 326
	SO_3H-heteropolyacid-SiO_2	Single cell performance at 80 – 200 ℃, 33 – 44 mW cm^2	327
	Poly(oxypropylene) backboned quarternary ammonium salt modified Montmorillonite	Water content ~28 – 32%, 4.2×10^{-2} S/cm	328
	-SO_3H modified clay	Water content ~70 – 87%, $\sim\sigma = 0.2 - 3.0 \times 10^{-2}$ S/cm	329
PVDF	ZrO_2 SO_4^{2-}	$\sigma = 1.2 - 5.2 \times 10^{-2}$ S/cm, single cell power 32 mW/cm^2.	330
PVDF-HFP copolymer	Heteropolyacids	Current density 1.6 A/cm^2	331

Table 1.8 Continued

SPEEK	SiO_2	$\sigma \geq 1.0 \times 10^{-2}$ S/cm	332, 333
	SiO2–N-(-3-triethoxysilylpropyl)-4,5-dihydroimidazole	40% reduction in water content	334
	Montmorillonite	~50% water content, $\sim\sigma = 1.2 \times 10^{-2}$ S/cm	335
	Laponite	~50% water content, $\sim\sigma = 0.3 \times 10^{-2}$ S/cm	336
	Heteropolyacids	$\sigma = \sim 1 \times 10^{-1}$ S/cm at 100 ℃	337 - 340
	TiO_2	~5% water content, $\sigma = \sim 0.2 \times 10^{-2}$ S/cm	341
	BPO_4	~35% water content, $\sigma = \sim 2 \times 10^{-2}$ S/cm	342
SPAEEKK	SiO_2	$\sigma = 2.0 - 9.7 \times 10^{-2}$ S/cm	343
PPEK	SO_3H–SiO_2	Water uptake 35%, 3.6 fold increase in σ	344
SPEK	SiO2–N-(-3-triethoxysilylpropyl)-4,5-dihydroimidazole	40% reduction in water content	345
Poly(ether sulfone)	SO_3H–SiO_2	Water uptake ~20% and $\sigma = \sim 1 \times 10^{-2}$ S/cm at 90% humidity	346
	PO_3H_2–SiO_2	Water uptake ~28%, $\sigma = \sim 6.3 \times 10^{-2}$ S/cm	347
	$Zr(HPO_4)_2$	$\sigma = \sim 1.9 \times 10^{-2}$ S/cm at 90 ℃ and 90% humidity	348
Poly(biphenyl ether sulfone)	Ag–SiO_2	Better oxidative stability and long term cell performance with low limiting current density	349
Poly(ether imide)	SO_3H–SiO_2	Water uptake ~20% and $\sigma = \sim 1 \times 10^{-2}$ S/cm at 90% humidity, good hydrolytic and oxidative stability	346
Poly(vinyl alcohol)	SiO_2	$\sigma = \sim 1 \times 10^{-2}$ to 10^{-1} S/cm	350, 351
	SO_3H–SiO_2	Water uptake ~32%, $\sigma = \sim 0.1 - 1.2 \times 10^{-3}$ S/cm	352
	PO_3H_2–SiO_2	Water uptake ~123%, $\sigma = \sim 5.5 \times 10^{-2}$ S/cm	353
PEG	SiO_2	$\sigma = \sim 1 \times 10^{-4}$ S/cm	354, 355
	Heteropolyacids	$\sigma \geq 1 \times 10^{-2}$ S/cm	356
	$Zr(HPO_4)_2$	$\sigma = \sim 1 \times 10^{-4}$ S/cm at 80 ℃	357
	Heteropolyacids, PDMS	$\sigma = \sim 7.7 \times 10^{-2}$ S/cm, high temperature stability	358

CHAPTER 2. OBJECTIVES

It has been demonstrated that the easy ionic pathways for fast proton transport are of vital essence for the proton conductivity of PEMs. [360–365] However in present PEMs, only short and randomly packed nanochannels are formed, [366] which restricts the content of absorbed water and especially continuous hopping routes for protons, [367] leading to unsatisfactory proton conductivity. In order to overcome this obstacle, PEMs comprised with continuous networks of proton-transport pathways are highly expected. Therefore, we proposed to design conductive fiber mat-based hybrid PEMs by taking advantage of long-range functionalized 1-D nanomaterials, such as electrospun fibers.

A novel approaches were proposed to fabricate hybrid PEMs. In this approach, solid superacid or sulfonated polymer electrospun fibers are used as the inorganic filler materials, and functional polymers as the matrix. Hydrophilic attractions between functional groups such as sulfonic acid groups on both the inorganic or polymeric fibrous filler and ionomer matrix attribute to the aggregation of sulfonic acid groups of polymer matrix onto the interfaces during the formation of hybrid PEMs. With the induce of 1-D nanomaterials, a network of long range ionic channels are formed by aggregated functional groups serving as proton transport pathways, which can significantly improve the proton conductivity of PEMs. (Figure 2.1)

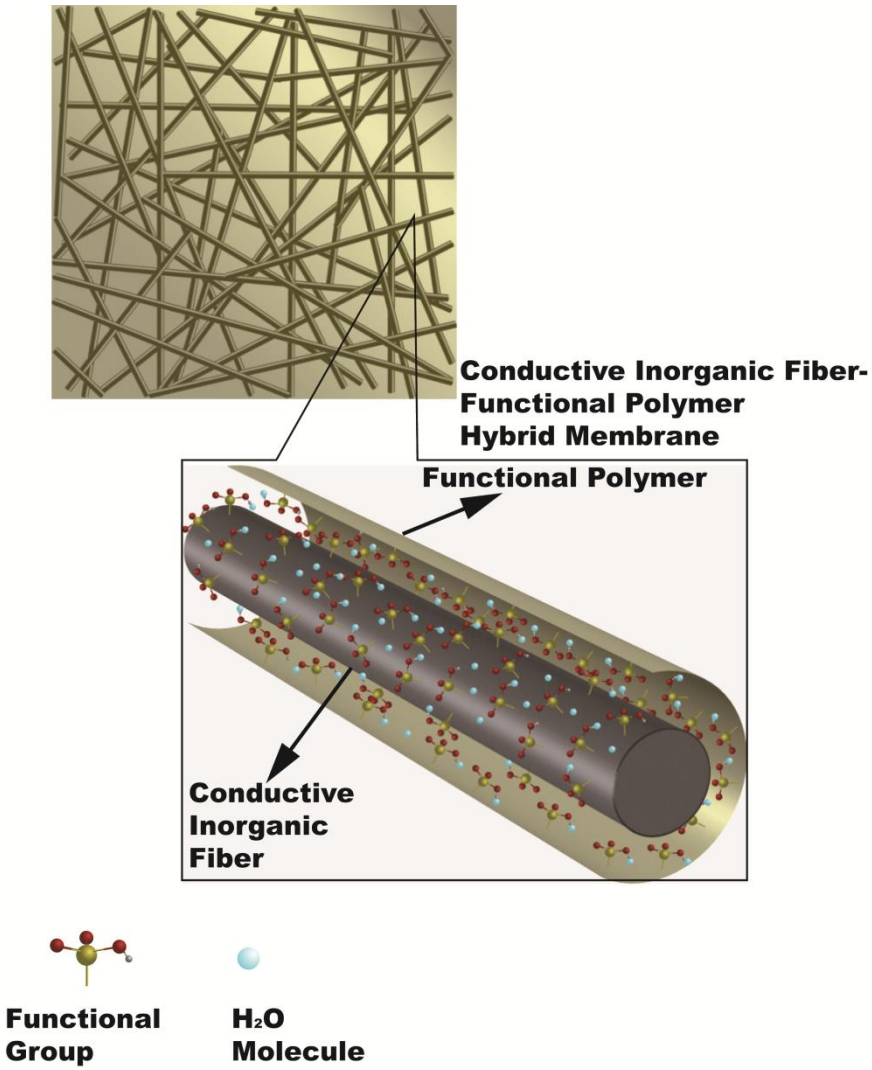

Figure 2.1. Conductive fiber/based hybrid membrane, and the network of long-range ionic pathways between the conductive fiber and functional polymer matrix.

In our work, we focused on the improvement of electrochemical properties, such as the proton conductivities, ion exchange capacities (IECs), and water uptake of hybrid membranes with the incorporation of solid superacid or sulfonated polymer fibers fabricated via electrospinning and post-electrospinning processes. The following are the objectives of the work:

1. Fabrication of electrospun fibers with attached sulfonic acid groups:

   i) Fabricated solid superacidic sulfated zirconia (S-ZrO_2) fibers via electrospinning and post-electrospinning methods;

   ii) Fabricated sulfonated polystyrene (S-PS) fibers via electrospinning and post-electrospinning methods;

2. Fabrication and characterization of hybrid hydrocarbon polymer electrolyte membranes incorporated with solid superacid fibers:

   i) Fabricate S-ZrO_2 fiber/Crosslinked poly(2-acrylamido-2-meathylpropane-sulfonic acid) (C-PAMPS) hybrid PEMs via *in-situ* radical polymerization.

   ii) Evaluated the electrochemical performance of S-ZrO_2 fiber/C-PAMPS hybrid PEMs, including proton conductivities, IECs, and water uptakes.

   iii) Obtained optimized S-ZrO_2 fiber/C-PAMPS hybrid PEMs by selectively adjusting crosslinking degree of polymer matrix, fiber diameters and fiber volume fractions.

3. Fabrication and characterization of perfluorosulfonic acid polymer electrolyte membranes incorporated with solid superacid fibers:

i) Fabricated S-ZrO_2 fiber/Nafion hybrid PEMs via the casting method.

ii) Evaluated the electrochemical performance of S-ZrO_2 fiber/Nafion hybrid PEMs, including proton conductivities, IECs, and water uptakes.

iii) Obtained optimized S-ZrO_2 fiber/Nafion hybrid PEMs by selectively adjusting fiber diameters and fiber volume fractions.

4. Fabrication and characterization of perfluorosulfonic acid polymer electrolyte membranes incorporated with sulfonated polymeric fibers:

i) Fabricated S-ZrO_2 fiber/Nafion hybrid PEMs via the casting method.

ii) Evaluated the electrochemical performance of S-ZrO_2 fiber/Nafion hybrid PEMs, including proton conductivities, IECs, and water uptakes.

iii) Obtained optimized S-ZrO_2 fiber/Nafion hybrid PEMs by selectively adjusting fiber diameters and fiber volume fractions.

CHAPTER 3. OVERALL EXPERIMENTAL

3.1 Electrospinning Device

The device for standard electrospinning can be seen in Figure 3.1. It consisted of two aluminum disks 15 cm in diameter at an adjustable distance up to 20 cm. A rigid plastic lab-stand supported the collecting disk as the collector of electrospun fibers. The parallel-disk arrangement provided a uniform external electric field that helped to direct uniform deposition of the fibers onto the collector. Placing a disk around the capillary also reduced the likelihood of corona discharge, which could cause explosion if the fluid is volatile and flammable.

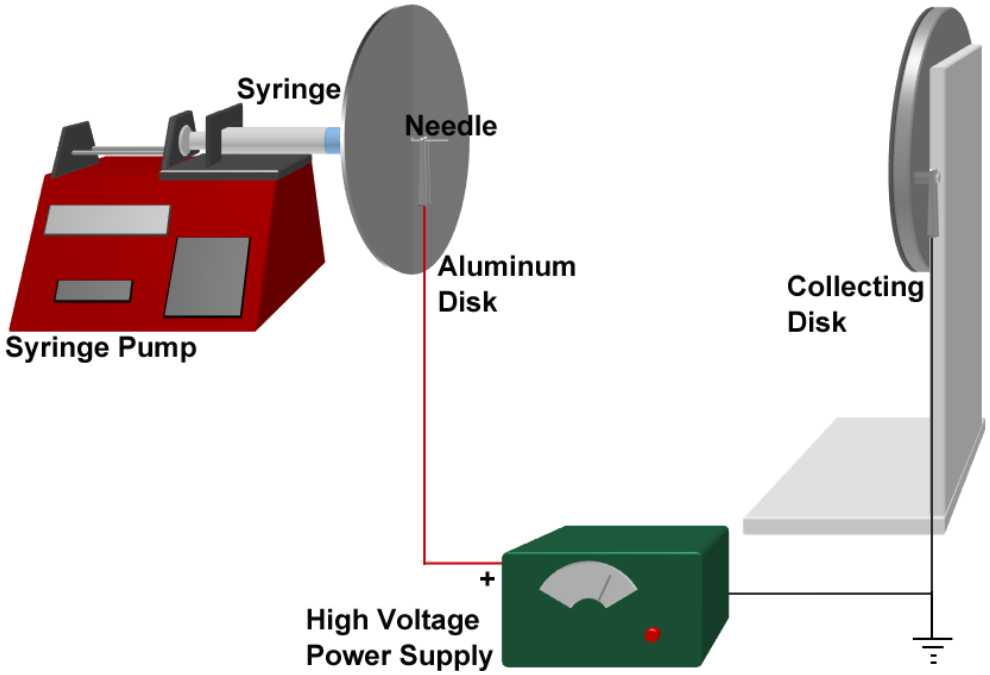

Figure 3.1. Schematic diagrams of the electrospinning device.

The aluminum disk at the pump side was connects to a Stainless Steel needle (Mcmaster-carr®, #75165A686) that protruded 2 cm out from the center hole of the disk. The needle was 1.5 inch (38.1 mm) in length with an inner diameter of 0.012 inch (0.30 mm) and an outer diameter of 0.020 inch (0.0050 mm). A syringe pump (New Era Pump Systems, Inc. # NE-1000) delivered the fluid from the syringe the needle. A power supply (Gamma High Voltage Research®) provided up to 40 KV of high voltage to the electrode. The strength of the electrical field was adjusted to obtain steady state jetting, such that the pulling rate was not too fast or too slow to cause interruption of the spinning, and the whipping instability persisted. The collecting disk was positioned at a sufficient distance (15 – 25 cm) from the disk at the electrode side during operation, such that the fiber dried out by the time it reached the collector. The collector was covered by an aluminum foil for collecting fibers (Novelis Foil®, # 1217-SE).

3.2 Chemicals

Poly polyvinylpyrrolidone (PVP, Mw = 1300000), polystyrene (PS, Mw = 230000, zirconium propoxide ($Zr(OPr)_4$), isopropanol, tetrahydrofuran (THF), N,N-dimethylformamide (DMF), sulfuric acid (H_2SO_4), 2-acrylamido-2-meathylpropane-sulfonic acid (AMPS), azobisisobutyronitrile (AIBN), ethylene glycol diacrylate (EGD), and dimethyl sulfoxide (DMSO) were purchased from Sigma-Aldrich®. Nafion solution (15%, EW = 1100 g) was purchased from Dupont®. All chemicals were used as received without further purification. All solutions were disposed after two weeks.

3.3 Procedure

3.3.1 Electrospinning

3.3.1.1 Electrospinning fibers with Zr Precursor

Electrospinning solutions were prepared by dissolving 3-5 wt% PVP and 2-8 wt% $Zr(OPr)_4$ in isopropanol. The solutions were electrospun at 15 kV for 2-8 hours with a feed rate of 2.5 ml/hr. Electrospun fiber mats were collected on the aluminum collector placed at a distance of 20 cm from the electrospinning needle.

3.3.1.2 Electrospinning polystyrene fibers

Electrospinning solutions were prepared by dissloving 20-30 wt% PS in a blend solvent of THF and DMF (weight ratio: 1:4). The solutions were then electrospun at 12 kV for 1-10 hr with a feed rate of ~1.0 ml/hr. Electrospun fiber mats were collected on the aluminum collector placed at a distance of 15 cm from the electrospinning needle.

3.3.2 Post-spinning Processes

3.3.2.1 Fabrication of S-ZrO_2 Fibers

The as-spun nanofibers were firstly cold pressed at the pressures of 760, 380, and 0 psi, respectively, to acquire fiber mats with different volume densities, and then treated in air at 280 ℃ for 6 hr. The treated nanofiber mats were soaked into excessive 1 M H_2SO_4 for 24 hr to anchor the sulfate groups. After that, the mats were dried in a vacuum oven at 60 ℃ for 4 hr, and then calcinated to form S-ZrO_2 nanofibers in air at 620 ℃ for 4 hr

with 2 ℃ /min ramping.

3.3.2.2 Fabrication of S-PS Fibers

The as-spun fibers were firstly cold pressed at the pressures of 380 psi to acquire fiber mats with higher volume density, and then soaked into excessive 10 M H_2SO_4 for 24 hours under the temperature of 100 ℃ for 4 hr to anchor the sulfate groups sufficiently. After that, the obtained S-PS fiber mats were rinsed in deionized water for 6 times, and dried in a vacuum oven at 60 ℃ for 8 hr.

3.3.3 Fabrication of hybrid membranes

3.3.3.1 Fabrication of S-ZrO_2 Fiber/C-PAMPS hybrid membranes

S-ZrO_2 fiber/C-PAMPS hybrid membranes were synthesized by free radical polymerization. Monomer AMPS (0.9 g), initiator AIBN (0.06 g), and crosslinker EGD (0.08-0.25 ml) were dissolved in DMSO (2.7 ml) under nitrogen (N_2). The solution was then added to S-ZrO_2 fiber mats, which were tightly clipped between two Teflon plates. After degassing, the solutions were heated at 60 ℃ for 8 hr and then post-cured at 120 ℃ for 1 hr under N_2 to form hybrid PEMs. For comparison, C-PAMPS membranes with different crosslinking degree were also prepared without the presence of fiber mats.

3.3.3.2 Fabrication of S-ZrO_2 Fiber/Nafion hybrid membranes

S-ZrO_2 nanofiber/Nafion hybrid membranes were fabricaited by the casting method. In

a typical fabrication process, 6 mL of 7.5% Nafion solution was added to S-ZrO_2 fiber mats. After degassing, the solutions were heated at 60 ℃ for 8 hr and then post-cured at 120 ℃ for 1 hr under N_2 to form hybrid membranes.

3.3.3.3 Fabrication of S-PS Fiber/Nafion hybrid membranes

S-PS fiber/Nafion hybrid membranes were fabricaited by casting method. During process, 7.5% Nafion solutions were added to S-PS fiber mats. After degassing, the solutions were heated at 60 ℃ for 8 hr and then post-cured at 100 ℃ for 2 hr under N_2 to form S-PS fiber/Nafion hybrid PEMs. For comparison, recast Nafion films were also prepared without the presence of fiber mats.

3.3.4 Membrane characterization

The X-ray Diffraction (XRD) data of S-ZrO_2 fiber mats were collected using a Philips XLF ATPS XRD 100 diffractometer applying CuKα radiation (λ = 1.5405 Å) over the range of 5 - 90 °. Fourier transform infrared spectra (FT-IR) of nanofiber mats were obtained using a Nicolet Nexus 470 spectrometer in the range of 4000 - 400 cm^{-1}. Thermogravimetric data of various membranes were recorded on a PerkinElmer Pyris 1 TGA with the temperature range of 50-700 ℃ and ramping at 10 °C /min .

The nanostructure of the hybrid membranes at each fabrication stage was determined using field emission scanning electron microscopy (FESEM, JEOL JSM-6400F). The distribution of ionic clusters in S-ZrO_2-Nafion and S-PS-Nafion hybrid membranes

was observed with a transmission electron microscopy (TEM, Hitachi HF-2000).

Before TEM imaging of S-ZrO_2-Nafion hybrid membranes, S-ZrO_2 fibers were removed by dipping the hybrid membrane in HF solution for 24 hr and then thoroughly rinsed in distilled water. After that, the membrane was stained with sodium for the clear observation of the ionic clusters by dipping into 1M NaOH solution for 24 hr and then thoroughly rinsed in distilled water.

3.3.5 Water uptake

All the electrolyte membranes were dried in vacuum for 4 h at 60 ℃ giving the weight of dry membranes.

The C-PAMPS films and S-ZrO_2-C-PAMPS hybrid membranes were exposed in a temperature/humidity chamber (Ransco RTH-600-S) with 100% RH at room temperature for 24 h giving the weight of hydrate membranes. The hydrated membranes were taken out and weighed immediately.

All the Nafion-based membranes, including recast Nafion films, S-ZrO_2-Nafion and S-PS-Nafion hybrid membranes immersed in deionized water at room temperature for 24 hr giving the weights of hydrated membranes.

The water uptake was calculated by the following equation:

$$Water\ uptake = \frac{W_w - W_d}{W_d} \quad (3.1)$$

where W_d and W_w are the weights of the dry and water-swollen samples, respectively.

3.3.6 Ion Exchange Capacity (IEC)

The IEC values of the membranes in acid form was measured by the classical titration technique. Membranes in the acidic form were immersed in 40 ml of 1.0 M NaCl solution for 24 h. Solutions were titrated with 1M NaOH solution until pH=7. The IEC was calculated according to the equation:

$$IEC(mequiv/g) = (V_{NaOH} \times C_{NaOH})/W_d \quad (3.2)$$

where V_{NaOH} and C_{NaOH} are the volume and molar concentration of NaOH solution, respectively.

3.3.7 Proton Conductivity

The resistance of the membranes was measured using the two-probe impedance method over the frequency range of 1 Hz-1 MHz on a potentiostat (Gamry Instruments Reference 600). The humidity and temperature were controlled in a temperature/humidity chamber (Ransco RTH-600-S). The proton conductivity was calculated according to the equation:

$$\sigma = L/RA \quad (3.3)$$

where σ is s was the proton conductivity, L was the distance between the two electrodes, R was resistance of the membrane, and A was the cross-sectional area of the membrane.

CHAPTER 4. Fabrication of Functionalized Electrospun Fibers

Abstract

A novel type of nano- to micro-sized S-ZrO_2 fibers were fabricated with electrospinning method and post-electrospinning process. The fiber diameters of the S-ZrO_2 fibers were controlled by changing the concentration of $Zr(OPr)_4$ and PVP in the pre-spinning solution. And cold pressing was conducted to the as-spun fiber mats to control the fiber volume fractions. The mophologies of the fiber mats at each stage were determined by SEM. XRD and FT-IR spectra were conducted to characterize the sulfation and the formation of S-ZrO_2 fibers. All the results verified the successful preparation of S-ZrO_2 fibers.

S-PS fiber mats were also fabricated with electrospinning method and post-electrospinning process. The fiber diameters of the S-PS fibers were controlled by changing the concentration of PS in the solution. Proper cold pressing was conducted to the fiber mats in order to increase the fiber volume fraction. The mophologies of the fiber mats were deternined by SEM. FT-IR spectra were conducted to charecterize the sulfation fo PS fibers. All the results verified the successful preparation of S-PS fiber mats.

4.1 Introduction

4.1.1 Review on Electrospinning Ceramic Fibers

Historically, electrospinning has been limited to the fabrication of nano- to submicron fibers from organic polymers due to the stringent requirements on the viscoelastic behavior of the pre-electrospinning solution. However, since the first decade of this century, it has been proved that conventional sol-gel precursor solutions could also be employed for producing composite and/or ceramic fibers via electrospinning and post-electrospinning processes, such as pyrolysis. For example, Larsen etc. demonstrated that viscous inorganic sols can be directly electrospun and fibers consisted of TiO_2/SiO_2 and Al_2O_3 can be successfully fabricated. [368] Similarly, $PbZr_xTi_{1-x}O_3$ (PZT), [369, 370] and SiO_2 fibers [371, 372] were also prepared via electrospinning sol-gel precursor solutions. The key strategy to the success of producing ceramic electrospun fibers was to control the hydrolysis rate of a sol-gel precursor by adjusting the pH value or aging conditions. It is important to form a solution with viscoelastic behavior similar to that of polymer solution.

However, fibers prepared via direct electrospinning of inorganic sols are usually hundreds of nanometers in diameter. Since it was very difficult to precisely control the viscoelastic behavior of a sol-gel system, further reducing the size of these fibers becomes a major challenge. Better approach was developed by Xia etc., in which the sol-gel reaction took place mainly in the spinning jet rather than in the stock

solution.[373-375] In a typical procedure, a sol-gel precursor such as a metal alkoxide was mixed with a PVP solution in alcohol. The function of PVP in the solution was to increase the viscosity and thus to control the viscoelastic behavior. After the solution was electrospun into a thin jet, the metal alkoxide immediately started to hydrolyze by reacting with the moisture in the environment to generate a gel network within the polymer matrix. As a result, nanofibers consisting of a composite of inorganic gel and polymer composite could be obtained. Ceramic nanofibers could be readily obtained by removing the organic part via pyrolysis of the composite fibers at elevated temperatures in air. The diameter of the ceramic fibers could be well controlled by changing the concentrations of PVP and sol-gel reaction precursor in the solvent, and the diameter could be from tens of nanometers to hundreds of nanometers with relatively narrow size distribution.

With the use of the simple electrospinning technique, many other ceramic fibers have been obtained, including SiO_2, SnO_2, indium tin oxide, GeO_2, $NiFe_2O_4$, $LiCoO_2$, and $BaTiO_3$, etc. The SEM and TEM analyses indicated that the ceramic nanofibers were polycrystalline in structure, with domain size on the scale of a few nanometers. It was also found that the nanocrystallites in these fibers were more uniform in dimension than those prepared using a conventional sol-gel process, because of the rapid and uniform hydrolysis during electrospinning. In addition to PVP, PVA, poly(vinyl acetate) (PVAc), and PEO have also been used as the polymer matrices to host inorganic precursors by several other groups. [376-386] A number of oxide fibers, including Al_2O_3, CuO, NiO,

TiO_2-SiO_2, V_2O_5, ZnO, Co_3O_4, Nb_2O_5, MoO_3 and $MgTiO_3$, have been fabricated by using these polymer matrices.

All the studies clearly demonstrate that electrospinning may provide a powerful route to inorganic nanofibers that can find use in many applications, such as components for structural reinforcement, active units in sensing, membranes for purification and separation, supports in catalyses and electrode materials in energy conversion or storage devices.

4.1.2 Review on S-ZrO_2

The invention of S-ZrO_2 started from 1962, in which Holm etc. [387] found that a platimun containing sulfat-treated zirconia gel exhibited superior catalytic performance compared to a commercial Pt/alumina catalyst. However, detailed studies of S-ZrO_2 did not appear until almost 20 years later. [388, 389] Early investigations of this material focused on the catalytic functions, because the use of solid superacids are more environmental friendly than that of liquid acids, and because of its high Hammett acidity function of -16.02 (Figure 4.1). [390,391] The potential use of S-ZrO_2 as the proton conductive material was recently noticed. Hara etc. [392] investigated the proton conductivity of S-ZrO_2, and illustrated that S-ZrO_2 exhibited a high conductivity of 5.0×10^{-2} S/cm at 60–150 ℃. Navarra etc. [393] found that the addition of S-ZrO_2 can improve the conductivity of Nafion membranes at the range of RH from 20% to 98%. All these results show that S-ZrO_2 can be a promising

candidate used as the inorganic component in hybrid PEMs.

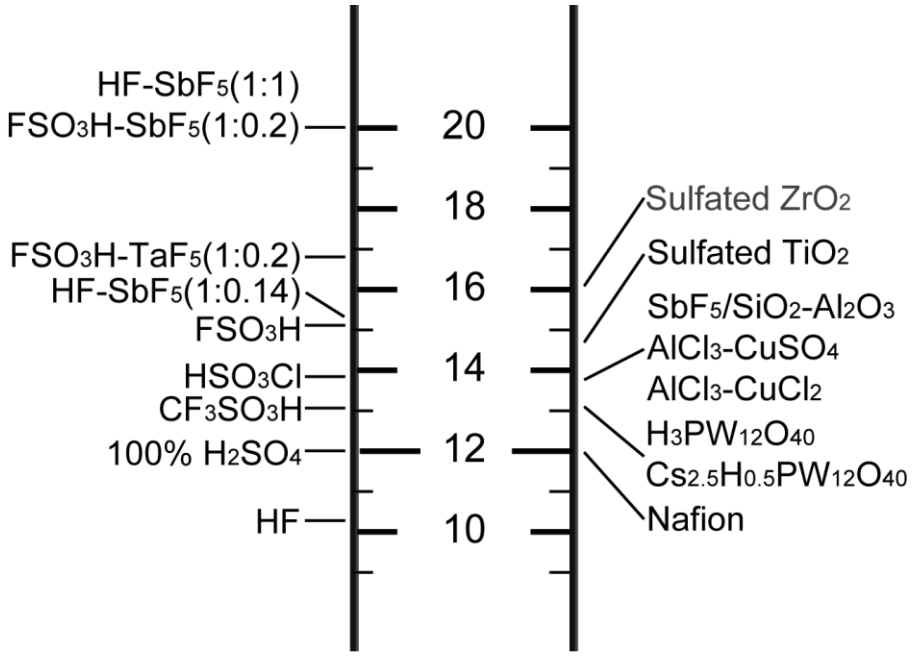

Figure 4.1. Acid strengths of liquid and solid superacids.

Many methods have been reported for the preparation of S-ZrO_2 particles. They may be classified into two categories: I) two-step approach and II) one-step approach.

1. Two-step Approach:

The two-step approach includes the preparation of zirconium hydroxide, followed by a second step of sulfating the zirconium hydroxide (Figure 4.2). The classical method based on the original method of Arata etc. [388, 389] is to prepare S-ZrO_2 powders by first hydrolyzing a zirconium salt, such as $ZrOCl_2$ or $ZrO(NO_3)_2$, with aqueous ammonia to produce zirconium hydroxide, and then to sulfate the zirconium

hydroxide with H_2SO_4 or $(NH_4)_2SO_4$ solution. The resultant sulfated zirconium hydroxide must be calcined in air at 550 – 650 ℃ to generate strong acidity.

In addition to $ZrOCl_2$ and $ZrO(NO_3)_2$, other zirconium salts such as $ZrCl_4$, $Zr(NO_3)_4$, and zirconium propoxide [$Zr(OC_3H_7)_4$], etc. were also used as the zirconium source. [394-400] SO_2, H_2S, CS_2, and SO_2Cl_2, etc. were used as the source of sulfur. [398, 399, 401, 402] Researchers also studied the process of preparing S-ZrO_2, and found that many parameters, including the sulfur content, sulfation procedure, and the calcinations temperature, etc. played an important role in the final acidity of S-ZrO_2.

In addition to the method mentioned above, zirconium hydroxide could also be obtained via the sol-gel technique. [403] In this method, a metal alkoxide undergoes hydrolysis and subsequent condensation in an alcohol solvent, forming a polymeric oxide network referred to as an alcogel. After the removal of extra solvent via air drying, followed with sulfation, S-ZrO_2 could also be obtained.

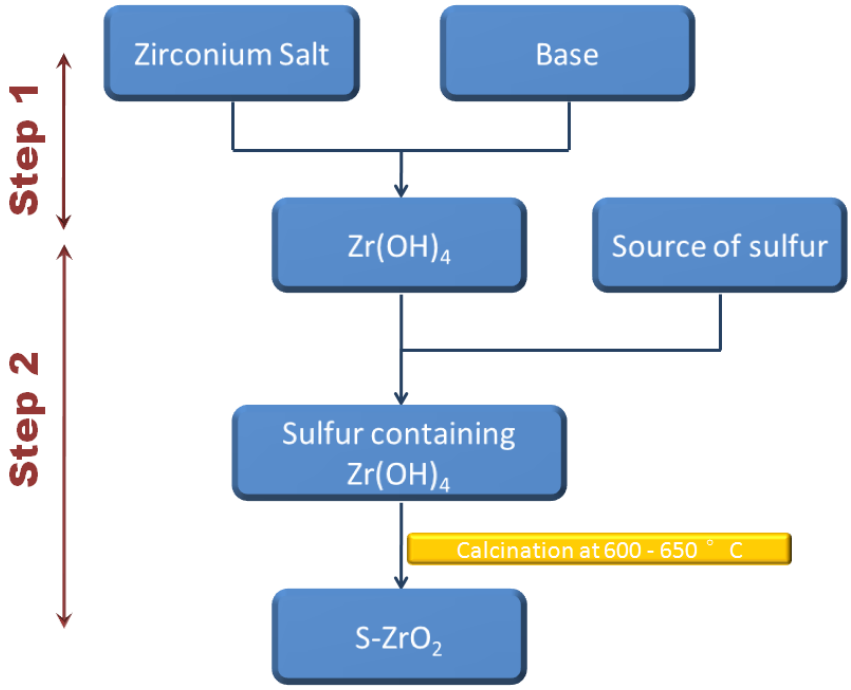

Figure 4.2. Schematic illustration of the two-step method for the preparation of S-ZrO_2.

2. One-step Approach:

In 1994, Ward etc. [404] reported on the preparation of S-ZrO_2 in a single step using a sol-gel method. In this method, $Zr(OPr)_4$ was mixed with n-propanol, nitric acid and sulfuric acid. This solution was then mixed with another solution containing n-propanol and water, and the mixture was vigorously stirred for gelation. The resultant alcogel was aged for 2 hours at room temperature. The solvent was then removed by supercritical drying with CO_2. The researchers found that sulfate ions were initially trapped in the bulk of the aerogel. During calcinations and crystallization of the zirconia, sulfate is expelled onto the surface and transformed into active species.

4.2 Results and Discussion

4.2.1 Preparation of S-ZrO_2 Fibers

In spite of the successful fabrication of oxide nanofibers via electrospinning and post-electrospinning processes, it is not easy to graft sulfonic acid groups onto zirconia. Preparing S-ZrO_2 fibers with the one-step approach is challenging since most polymers are not compatible with H_2SO_4 in solutions. The fiber integrity is often damaged while immersing the brittle fiber mats in H_2SO_4, hence the two-step approach is not suitable for fabricating S-ZrO_2 fibers. Accordingly, in our work a multi–step approach was used:

1. The sol-gel method was adoped to make Zr-containing fiber. A solution of PVP and $Zr(OPr)_4$ in n-propanol was electrospun into fiber mat.

2. A compressing step was applied on the fiber mat to increase the volume density of fibers, since the increase of fiber volume fraction caused by compaction could lead to higher proton conductivity. [405]

3. The compressed fiber mat was heat treated at 280 ℃ in air to form a carbon-like brown mat containing ZrO_2, since it was found that the carbon-like mats were more flexible and easier to operate than ZrO_2 fiber mats.

4. The mat was immersed into 1M H_2SO_4 to graft sulfonic acid groups onto ZrO_2.

5. The mat was dried in air and then calcinated at 620 ℃ in air to obtain an S-ZrO_2 fiber mat.

Detailed fiber preparation process can be seen in Sections 3.3.1.1 and 3.3.2.1

4.2.2 Characterization of S-ZrO_2 Fibers

In a typical process, randomly oriented PVP-$Zr(OC_3H_7)_4$ composite fibers were electrospun by using the solution of 5wt% PVP and 5wt% $Zr(OC_3H_7)_4$ in n-propanol. (Figure 4.3A and B) The as-spun mats were then compressed under the pressure of 191.0 psi. After pressing, the fiber fraction increased from 7.9 vol% to 23.5 vol% averagely, while fiber diameters kept at around 310 nm and no diameter change was observered. (Figure 4.3C and D) The pressed mats were then heated up to 280 ℃ in air. The diameter of fibers shrank to 275nm (Figure 4.3E and F). After heat treatment, the fiber mate was then dipped into H_2SO_4 for sulfation. (Figure 4.3G and H) And the final S-ZrO_2 nanofibers was obtained with the diameter of 155 nm after sulfation in H_2SO_4 and final calcination, as shown in figure 4.3I and J.

Figure 4.3. SEM images and fiber diameter distributions of (A, B) electrospun fiber with average diameter (AD) = 310 ± 150 nm, (C, D) fibers after compressing, AD = 311 ± 119 nm, (E, F) fibers after heat treatment of 280 ℃, AD = 275 ± 103 nm, (G, H) fibers after sulfation in H_2SO_4, AD = 273 ± 116 nm, (I, J) fiber after calcination at the temperature of 650 ℃, AD = 155 ± 93 nm.

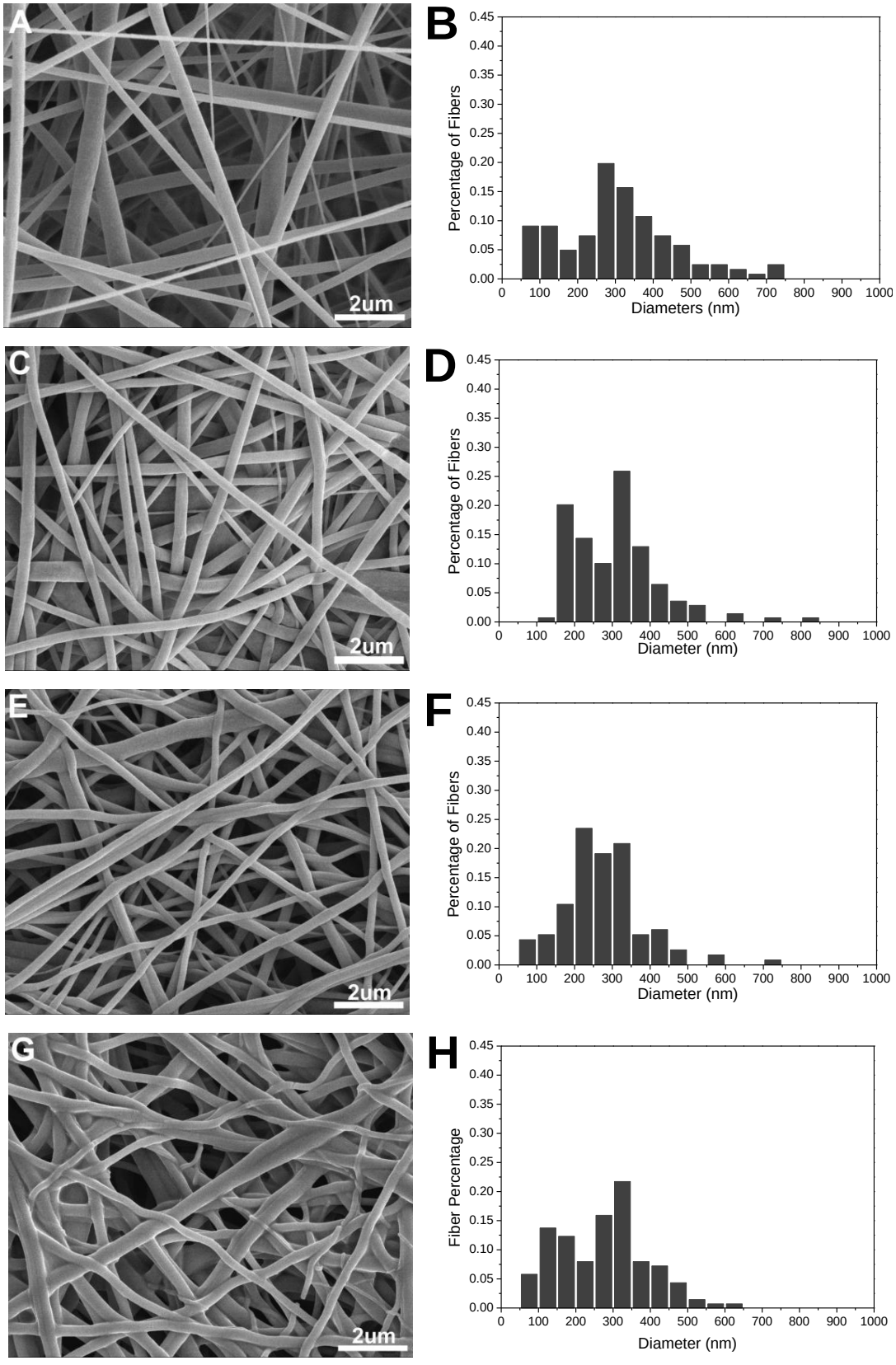
A
2um
B
Percentage of Fibers
Diameters (nm)
C
2um
D
Percentage of Fibers
Diameter (nm)
E
2um
F
Percentage of Fibers
Diameter (nm)
G
2um
H
Fiber Percentage
Diameter (nm)

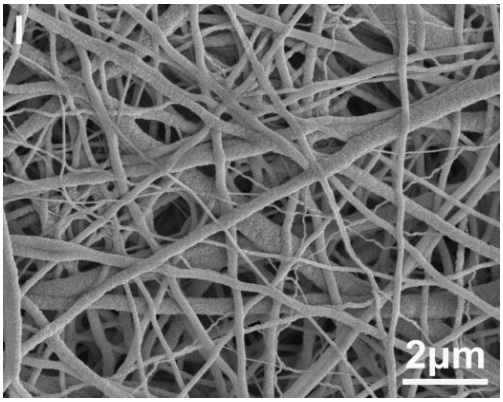
I
2μm

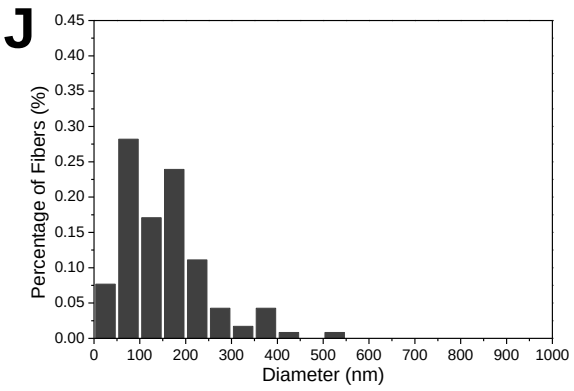
J
Percentage of Fibers (%)
0.45
0.40
0.35
0.30
0.25
0.20
0.15
0.10
0.05
0.00
0
100
200
300
400
500
600
700
800
900
1000
Diameter (nm)

In order to compare the electrochemical properties of PEMs with different fiber diameters, different pre-spinning solutions of 4wt% PVP with 2wt% $Zr(OC_3H_7)_4$, and 6wt% PVP with 8wt% $Zr(OC_3H_7)_4$ in n-propanol were used to prepare finer and coarser fibers, respectively. The final diameters of the fibers were 81 nm and 369 nm respectively, as shown in figure 4.4.

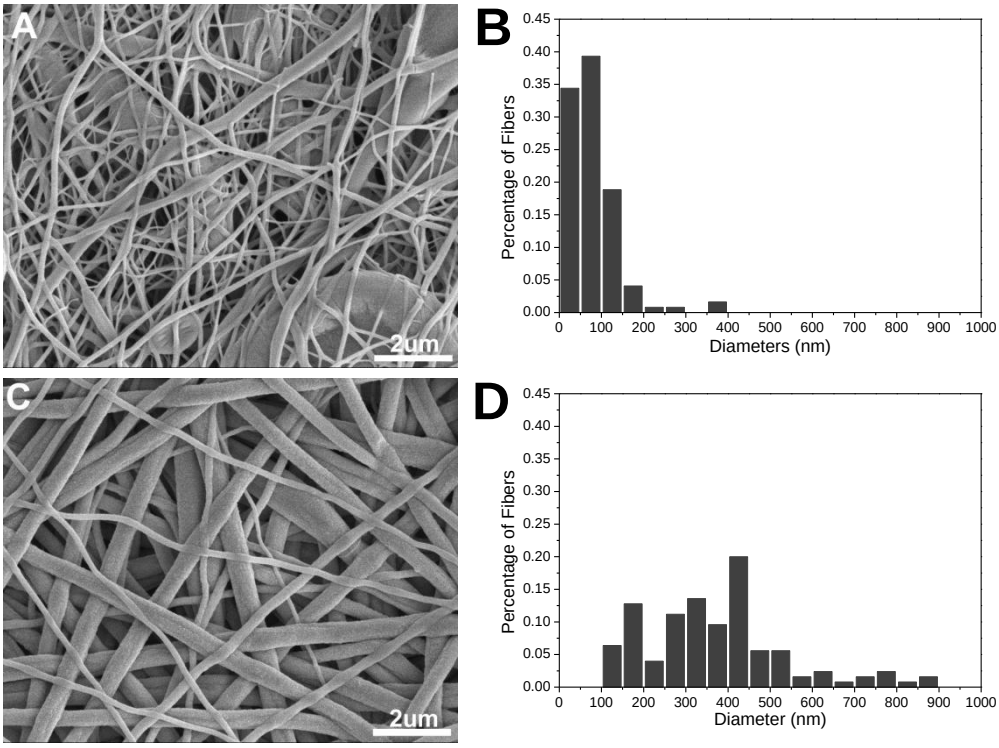

Figure 4.4. SEM images and fiber diameter distributions of S-ZrO_2 fibers with (A, B) AD = 81 81 ± 57 nm, and (C, D) AD = 369 ± 167 nm.

The phase composition and structure of the S-ZrO_2 nanofibers were examined by X-ray diffraction (XRD, Figure 4.5). Song etc. have monitored the crystallographic changes of both pure and sulfated zirconia, [406] and found that with sulfation, at a calcinations temperature of 550 - 700 °C, only the tetragonal phase of ZrO_2 existed.

However, pure ZrO_2 shows both the tetragonal and monoclinic phases at 550 °C, and only the monoclinic phase at temperatures higher than 650 ℃. In our final product, all of the strong reflection peaks of the XRD pattern could be readily indexed to tetragonal ZrO_2, and no other impurities could be indexed from the final mats, indicating the successful formation of S-ZrO_2 fibers.

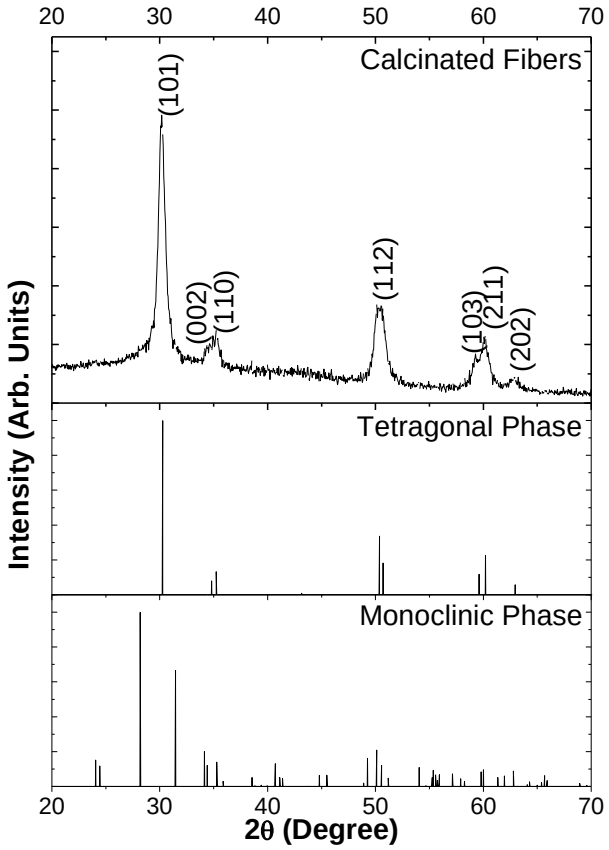

Figure 4.5. XRD pattern of calcinated S-ZrO_2 fibers compared with the standard XRD patterns of tetragonal and monocilinic phases of ZrO_2.

The structure of S-ZrO_2 fibers was also studied by the fourier transform infrared (FT-IR) spectroscopy (Figure 4.6). The spectrum shows a broad peak having shoulder

peaks at 1049, 1082 and 1144 cm^{-1}, which are typical of a chelating bidentate sulfate ion coordinated to metal cation, showing the successful preparation of S-ZrO_2.

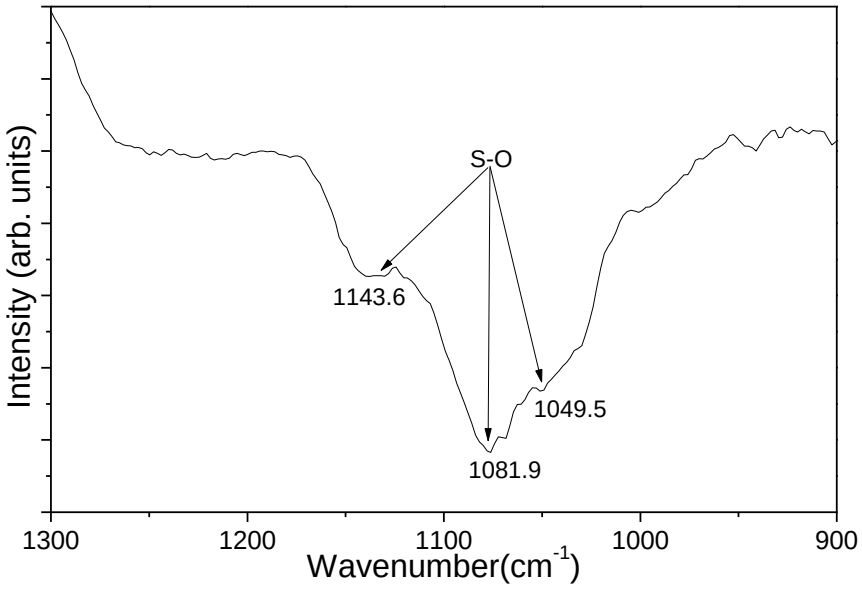

Figure 4.6. FTIR spectra for the S-ZrO_2 fiber mat.

4.2.3 Preparation and Characterization of S-PS Fibers

PS fibers were first prepared using the electrospinning method. The SEM images and diameter distribution of electrospun fiber mats are shown in figure 4.7. The fiber diameters were controlled by selectively adjusting the concentrations of PS in the pre-electrospinning solutions. It is seen that electrospun fibers with lower concentrations can obtain finer fiber diameters. When the concentration increases from 20%, 25% to 30%, the average fiber diameter increases from 1.23 to 2.65 and 4.51 μm, respectively. The detailed electrospinning process is shown in Section 3.3.1.2.

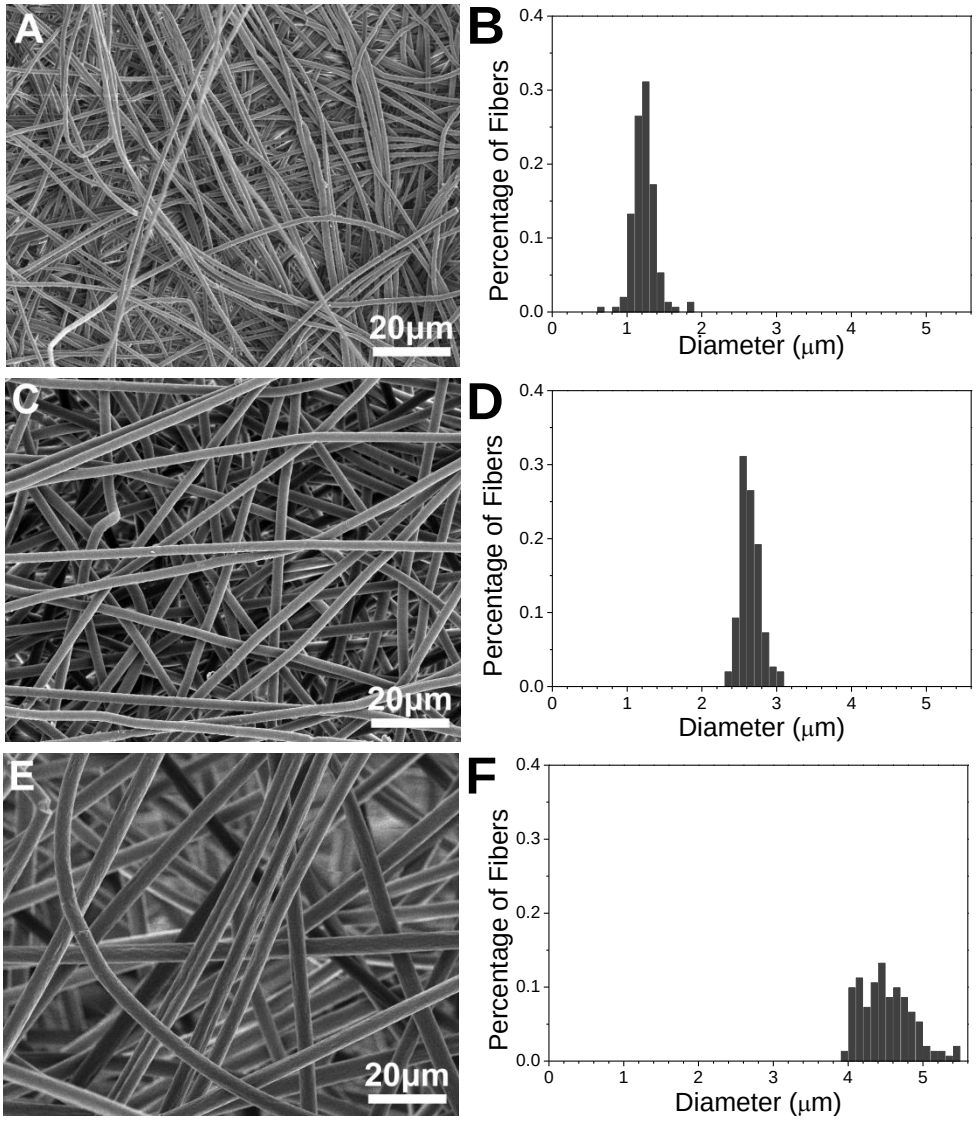

Figure 4.7. SEM images and histograms of fiber diameter distribution of PS electrospun fibers. The fiber diameters were controlled via changing the concentration of PS in pre-electrospinning solution. A, C, E) are the SEM images of PS fibers with diameters of A) 1.23 μm, B) 2.65 μm, and C) 4.51 μm, with the concentration of PS at 20%, 25%, 30%, respectively. B, D, F) are the histograms of the fiber diameter distribution of PS electrospun fibers. Each histogram was plotted with the measurement of more than 150 fibers.

After electrospinning, the fiber mats were compacted under pressure to increase the volume density of fibers. For fiber mats after electrospinning, the volume fraction of fibers was around 5%, and the fiber volume fractions increased to 10% when the

compression was completed. The compressed fiber mats were then sulfonated in 10 M H_2SO_4. To create interconnecting protonic pathways, a high temperature of 100 ℃ (higher than the glass transition temperature) was applied during sulfonation to bond the neighboring fibers. And the detailed post-electrospinning processes can be seen in Section 3.3.2.2. Figure 4.8 shows the SEM images and diameter distribution of electrospun fiber mats before sulfonation. It is seen that all samples still keep the fiber network structure, but the fiber diameters decrease to 0.98, 2.21, and 3.60 μm, respectively, after sulfonation for fibers with pre-electrospinning solution concentrations of 20%, 25%, and 30%. Probable possible explanation is that some of the polymer chains were fully sulfonated to polystyrene sulfonic acid and dissolved into the H_2SO_4 solution.

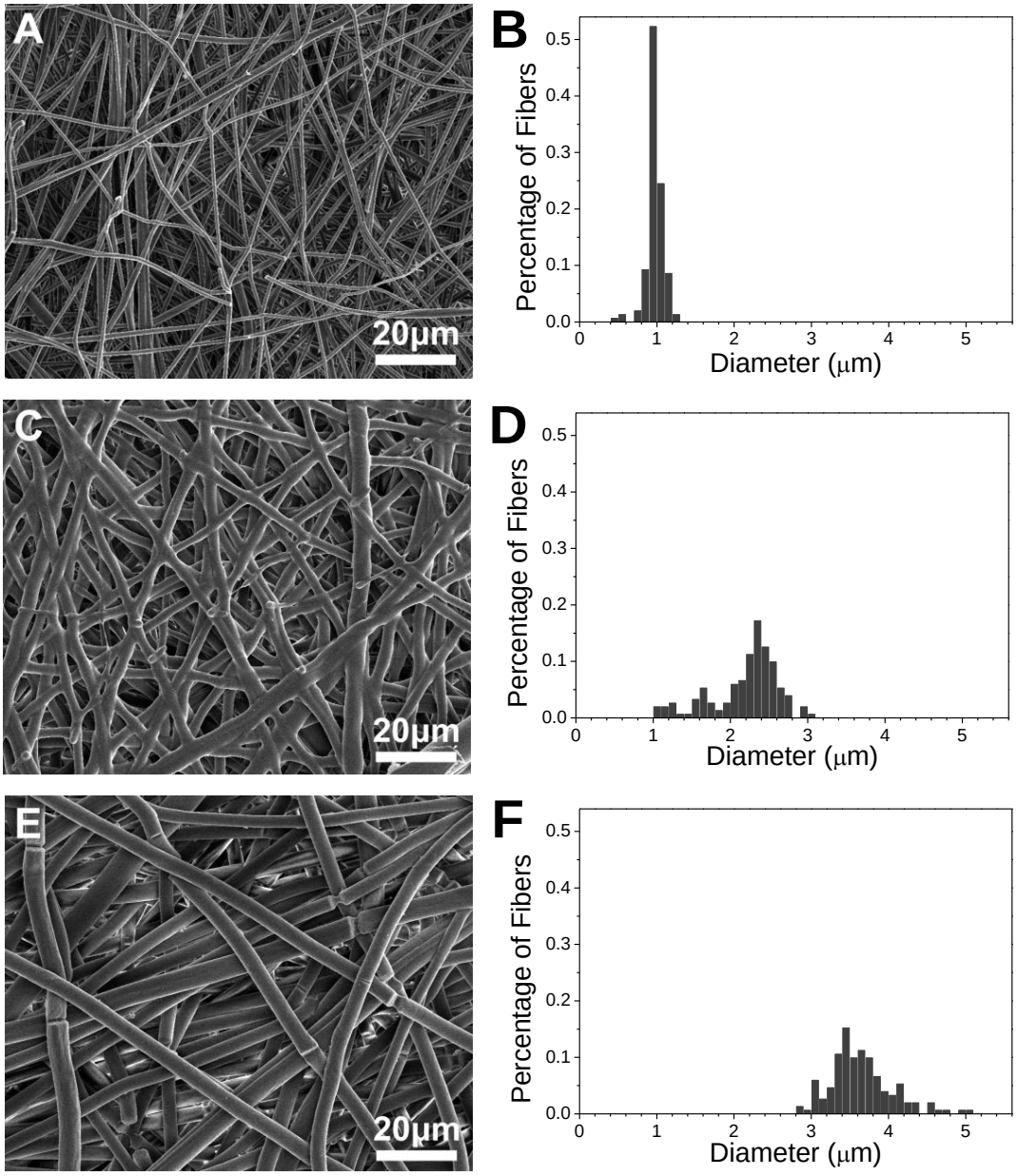

Figure 4.8. SEM images and histograms of fiber diameter distribution of S-PS fibers after sulfonation. A, C, E) are the SEM images of S-PS fibers with diameters of A) 0.98 μm, B) 2.21 μm, and C) 3.60 μm. B, D, F) are the histograms of the fiber diameter distribution of PS electrospun fibers. Each histogram was plotted with the measurement of more than 150 fibers.

The FT-IR spectra of both PS and S-PS are represented in figure 4.9. It is seen that S-PS fiber mats have sulfonic group bands at 1178, 1129 and 1035 cm^{-1}, [407] which are

absent from the un-sulfonated PS fibers. This indicates the successful formation of S-PS by the sulfonation process.

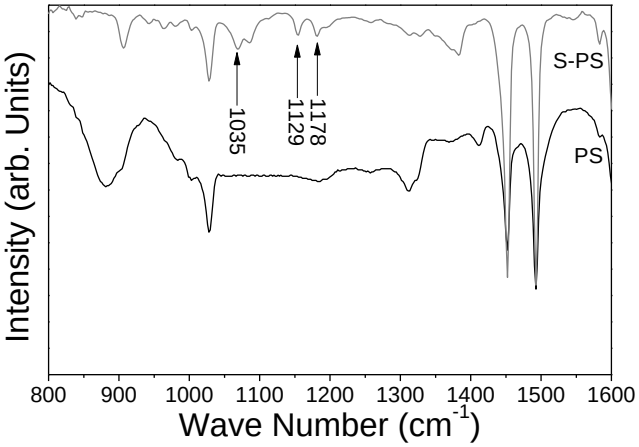

Figure 4.9. FT-IR spectra of PS and S-PS fiber mats.

4.3 Summary

The preparation and characterization of S-ZrO_2 and S-PS fiber mats by the combination of electrospinning and post-electrospinning process were studied. Because of the difficulties of preparing S-ZrO_2 fibers by conventional methods, proper ameliorations were made. The fiber diameters of the fiber mats were tuned by changing the concentration of pre-electrospinning solutions. And the fiber volume fractions were controlled by cold pressing. SEM images, XRD and FT-IR spectra were also obtained, and the results verified the successful preparation of both S-ZrO_2 and S-PS fibers.

CHAPTER 5. SULFATED ZIRCONIA FIBER/CROSSLINKED PAMPS HYBRID PROTON EXCHANGE MEMBRANES

Abstract

Novel proton-conductive superacidic fibers/polymer hybrid membranes were obtained by immersing S-ZrO_2 fiber mats into AMPS solutions followed with *in situ* polymerization and crosslinking process. Induced by electrospun inorganic fibers, long-range ionic channels were formed by agglomerating functional groups, which served as continuous hopping pathways for protons and significantly improved the proton conductivity of PEMs. These superacidic fiber/polymer hybrid PEMs can also avoid the aggregation of inorganic components, which often cause localized stress and poor mechanical properties.

5.1 Introduction

In recent decades, proton exchange membrane fuel cells (PEMFCs) have attracted much attention because of their high power density and high efficiency with low greenhouse gas emission. [408] These fuel cells are mainly based on Nafion®, a currently commercial PEM, which has good thermal, mechanical and chemical stabilities, and relatively high proton conductivity. [409] However, the drawbacks of Nafion®, such as high production cost, environmental incompatibility, and low operation temperature (<80 ℃), hinder the widespread commercialization of PEMFCs. [410]

To overcome these problems, great efforts have been dedicated to develop PEMs based on inorganic/organic hybrid membranes. [411] Many inorganic fillers, [412] in the form of micro- or nano-particles, have been incorporated into polymer matrix to prepare hybrid PEMs with several different methods, such as polymer blending, and sol-gel methods, etc. [411, 412] The resultant inorganic/organic hybrid membranes have been proved to be effective in improving PEMFC performance and offering the opportunity to operate PEMFCs at higher temperatures. However, problems still exist to limit their use in practical PEMFCs. For example, most currently used fillers, such as SiO_2, ZrO_2, metal oxides, and heteropolyacid, do not have or only have limited surface protogenic groups, which restricts the improvement of the proton transport and thus the conductivity of PEMs. Furthermore, the agglomeration of filler particles makes it difficult to increase the filler content to form effective proton-transport pathways through the entire

membrane. Therefore, new strategies to form uniformly dispersed inorganic fillers with continuous proton-transport pathways are appreciated. The technological impact of new fillers would be significant and needs further exploration.

In inorganic/organic hybrid membranes, ionic channels are formed by the ionic groups distributed at the interfaces, and these channels play a significant role in improving the membrane performance. It has been demonstrated that continuous ionic channels are important for water transport and proton conductivity of hybrid PEMs. [413] However in most present hybrid PEMs, only short channels have been formed, [412, 414] which restrict the content of absorbed water and the formation of continuous hopping routes for protons, leading to unsatisfactory proton conductivity. Therefore, we designed highly-conductive S-ZrO_2 fiber/filled C-PAMPS hybrid PEMs by taking advantage of the continuous inorganic fibers to form long-range conductive pathways, as shown in figure 2.1. During hybrid PEM formation, functional groups such as sulfonic acid groups from both the inorganic fibrous additives and polymer matrix are distributed on the interfaces to form long-range ionic channels, which serve as proton hopping pathways to significantly improve the proton conductivity of PEMs.

5.2 Synthesis of Hybrid Membranes

S-ZrO_2 fiber/C-PAMPS hybrid PEMs were constructed by immersing S-ZrO_2 fiber mats into AMPS monomer, followed by *in-situ* polymerization with AIBN as an initiator and crosslinking with EGD as a crosslinker. PAMPS was selected as the

polymer matrix due to its high conductivity accompanying with high water uptake. Diao etc. have investigated PAMPS membrane crosslinked with divinylbenzene (DVB), [198] and found that the conductivity could be as high as 5.89×10^{-2} S/cm, and the IEC was practically as high as 1.80 mmol/g. Detailed sample preparation process can be seen in Section 3.3.3.1.

5.3 Characterization of the Hybrid PEMs

5.3.1 SEM of the Hybrid PEMs

After the fabrication of the S-ZrO_2 fiber/C-PAMPS hybrid PEMs, SEM images of both the top view and the cross-sectional view were obtained. As seen in Figure 5.1A, from the top view of the hybrid PEMs, it is obvious that all the fibers in the membrane is encapsulated in polymer matrix, and no holes is observed, demonstrating good structural integrity of the hybrid PEMs. The cross-sectional view (Figure 5.1B) on the hybrid PEMs further proves that the pores between fibers have been filled with synthesized polymers, which verifies the successful synthesis of the hybrid PEMs.

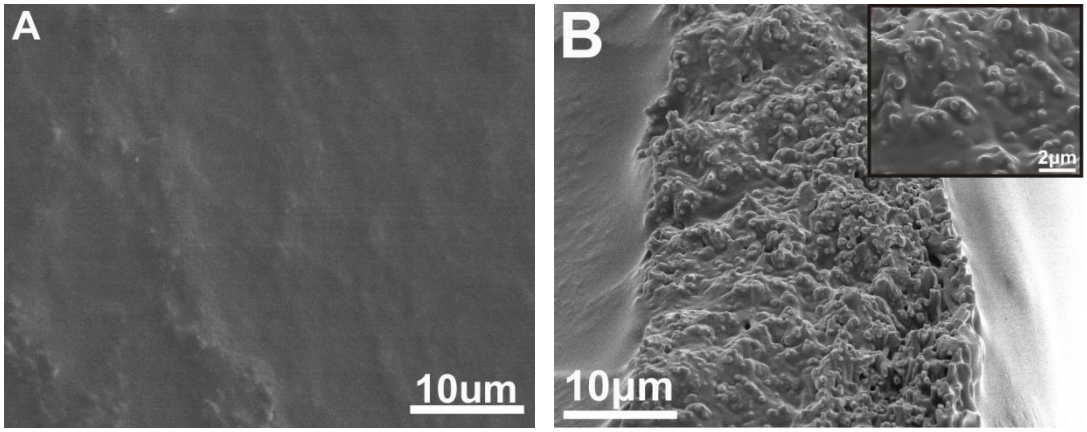

Figure 5.1. The SEM images of A) the top view and B) the cross-sectional view of the S-ZrO_2 fiber/C-PAMPS hybrid PEMs. And the inset of B) shows the images with higher magnification.

5.3.2 FT-IR spectroscopy of the Hybrid PEMs

Figure 5.2 shows the FT-IR spectra of both C-PAMPS membranes and S-ZrO_2 fiber/C-PAMPS hybrid PEMs. It is found that no apparent difference can be observed between the FT-IR spectra of pure C-PAMPS and the hybrid PEMs, indicating that the S-ZrO_2 fibers have been completely covered by the polymer matrix. The characteristic absorption band at 1645 cm^{-1} is ascribed to the stretching vibration of carbonyl groups (C=O), and the peak at 1553 cm^{-1} is assigned to the stretching vibration of imino groups (N-H). The absorption peaks at around 1037 and 1215 cm^{-1} were assigned to the symmetric and asymmetric stretching vibrations of sulfonate ($-SO_3^-$) groups, respectively. Obviously, the hybrid PEMs have been successfully prepared.

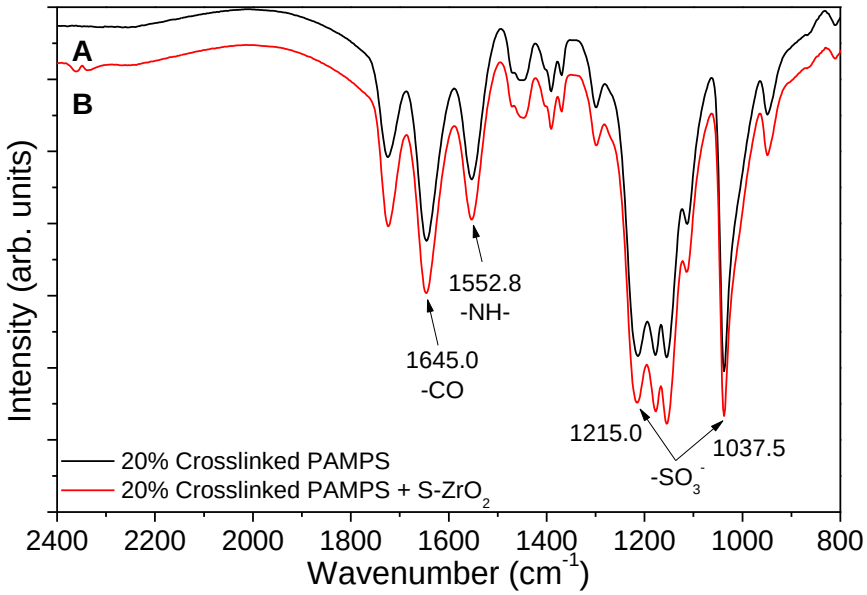

Figure 5.2. FT-IR spectra of A) pure C-PAMPS membrane and B) hybrid PEMs.

5.3.3 Thermal Analysis of Hybrid PEMs

The thermal degradation of both C-PAMPS membranes and S-ZrO_2 fiber/C-PAMPS hybrid PEMs were studied by TGA, as shown in Figure 5.3. Both types of membranes show three main decomposition stages. The first drop of mass at around 200 ℃ can be ascribed to the loss of structural water. The second decomposition temperature occurred at 300 ℃ can be assigned to the decomposition of sulfonate groups, propenyl groups, or cross-linking agent. The third thermal degradation that takes place at about 380 ℃ was ascribed to main-chain degradation of polymer. The incorporation of S-ZrO_2 fibers in the membrane did not affect thermal stability of the prepared polymer membranes. This type of membrane indeed confirms a sufficient thermal stability, far beyond the range of interest for application in PEMFCs within the medium operating temperature range

(<200 ℃).

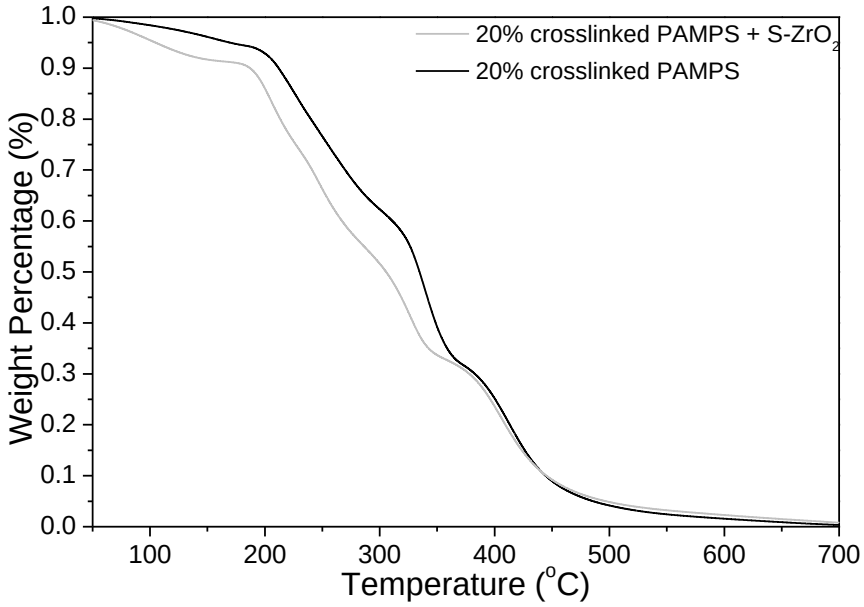

Figure 5.3. Thermogravimetric analysis of hybrid membrane and 20% C-PAMPS in nitrogen at a heating rate of 10 ℃/min.

5.3.4 Properties of the Hybrid PEMs

The in-plane proton conductivities of the hybrid PEMs were then measured at 80% RH. As shown in Figure 5.4, the proton conductivities of hybrid PEMs are higher than those corresponding C-PAMPS membranes. For example, at 100 °C, the conductivity of 20% C-PAMPS is 8.1×10^{-2} S/cm, which increased to 2.4×10^{-1} S/cm with the introduction of around 20wt% S-ZrO_2 fibers. In addition, the conductivities of hybrid membranes are also higher than those of Nafion 112.

The practical use of PEMs requires high conductivity at high temperatures, and the incorporation of S-ZrO_2 fibers improves the response of PEMs to high temperature.

The proton conductivity of 20% C-PAMPS decreases from 9.4×10^{-2} S/cm at 80 °C to 8.1×10^{-2} S/cm at 100 °C, while it rises from 0.22×10^{-1} S/cm at 80 °C to 2.4×10^{-1} S/cm at 100 °C with the impregnated S-ZrO_2 fibers. And the same trend is observed on the 10% and 30% C-PAMPS.

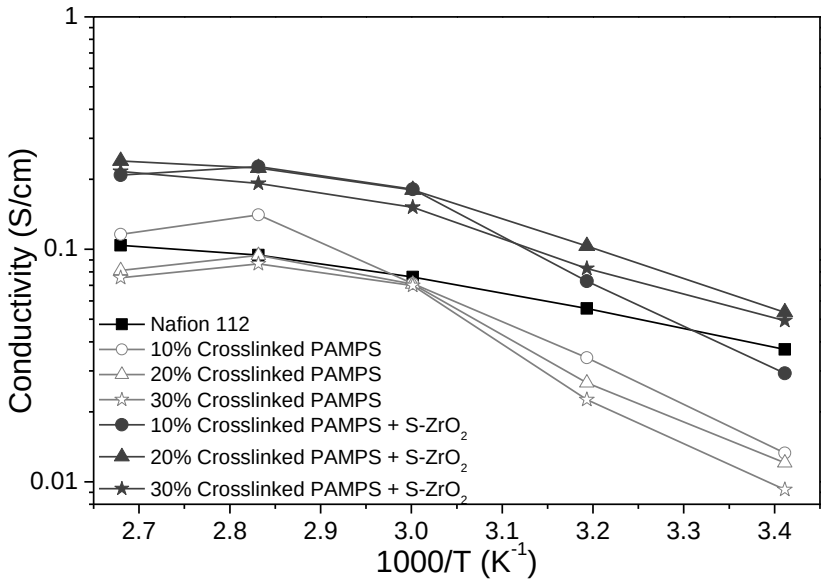

Figure 5.4. Temperature-dependent proton conductivity of hybrid PEMs (fiber diameter = 155nm, and fiber volume fraction = 20.4%) compared with pure C-PAMPS and Nafion 112.

The high conductivities of S-ZrO_2 fiber/C-PAMPS hybrid membranes can be ascribed to the fiber-induced long range water channels that are formed along the entire fiber length. Table 5.1 shows the IEC and water uptake values of both hybrid PEMs and C-PAMPS. It is found that the IEC of S-ZrO_2 is much lower than that of C-PAPMS, implying that in the process of sulfation, the sulfonic acid groups are mainly anchored on the surface of ZrO_2 fibers. During the polymerization process, the hydrophilic attractions between sulfonic acid groups of S-ZrO_2 and C-PAMPS lead to high

agglomeration of sulfonic acid groups of C-PAMPS onto the inorganic-organic interfaces. Long-range channels are hence formed along the S-ZrO_2 fibers, with sulfonic acid groups highly aggregated on the inner and outer surfaces of channels to provide easier hopping of protons, and anchor more water molecules (Figure 2.1). Although the existence of S-ZrO_2 and increasing crosslinking degree lower the IEC of hybrid PEMs (Table 5.1), the fiber-induced interconnected water channels work as the fast hopping pathways for protons and keep the proton conductivity and water content at a high level over the entire temperature range.

Table 5.1. IEC and water uptake values of S-ZrO_2 fibers, C-PAMPS, and hybrid PEMs.

Samples	**S-ZrO_2 Percentage (%)**	**IEC (mequiv/g)**	**Water Uptake (%)**
S-ZrO_2	-	0.69 ±0.01	2.9 ±1.3%
10% C-PAMPS	0	2.97 ±0.16	64.6 ±3.8%
20% C-PAMPS	0	2.62 ±0.11	55.7 ±12.3%
30% C-PAMPS	0	2.36 ±0.06	51.1 ±2.7%
10% C-PAMPS + S-ZrO_2 (155nm)	21.8	2.67 ±0.11	106.8 ±7.0%
20% C-PAMPS + S-ZrO_2 (155nm)	20.4	2.31 ±0.07	64.8 ±8.5%
30% C-PAMPS + S-ZrO_2 (155nm)	19.6	2.04 ±0.04	56.0 ±4.1%
20% C-PAMPS + S-ZrO_2 (81nm)	21.4	2.34 ±0.13	72.1 ±1.7%
20% C-PAMPS + S-ZrO_2 (369nm)	19.7	2.27 ±0.04	62.2 ±1.9%
20% C-PAMPS + S-ZrO_2 (8%)	8.0	2.41 ±0.08	71.4 ±4.6%
20% C-PAMPS + S-ZrO_2 (30%)	30.2	2.21 ±0.13	47.1 ±4.7%

5.3.5 Fiber Parameters affecting the Electrochemical Properties of Hybrid PEMs

In order to further identify the major effect of the long-range water channels induced by S-ZrO_2 fibers and to clarify parameters affecting the performance of the water channels, the fiber diameter dependences of proton conductivities of hybrid PEMs were measured and are shown in Figure 5.5A. It is found that hybrid membranes with thinner fiber diameters have higher proton conductivity. With decrease in fiber diameter, the surface area and number density of S-ZrO_2 fibers increase, leading to the

formation of more water channels, which in turn increases IEC and water uptake (Table 5.1), and consequently the proton conductivity. As illustrated in Figure 5.5A, with the diameter decreasing to 85 nm, the proton conductivity increases to 3.2×10^{-1} S/cm at 100 °C, much higher than 1.2×10^{-1} S/cm for membranes with fiber diameter of 369 nm.

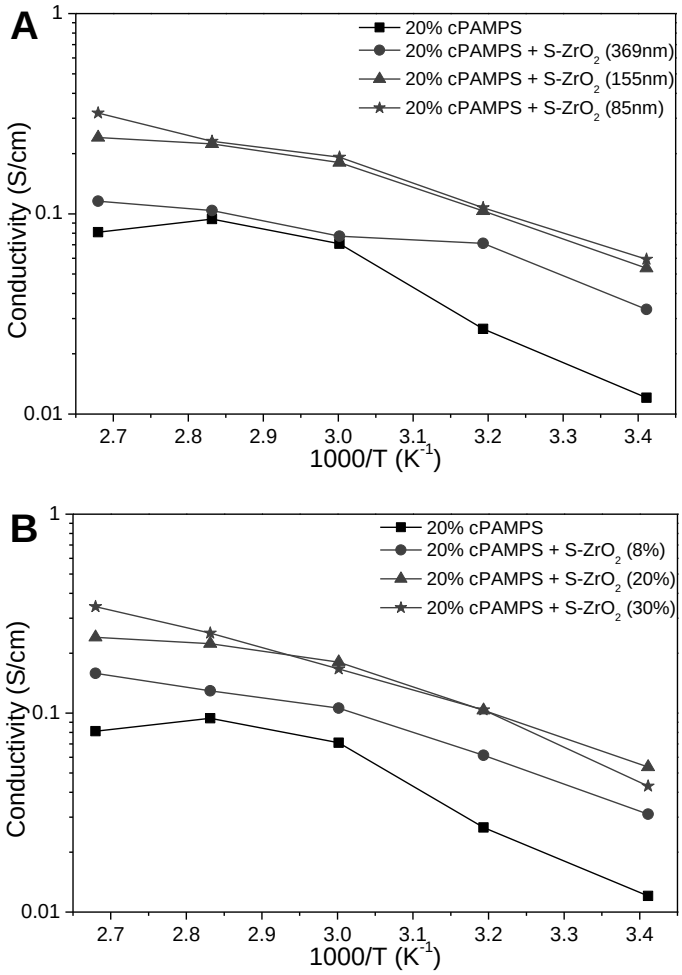

Figure 5.5. A) Proton conductivity of hybrid PEM with different fiber diameters and the comparison with C-PAMPS. B) Proton conductivity of hybrid PEM with different fiber content and the comparison with C-PAMPS.

The effect of fiber volume fraction, which relates to the changing number of water channels, on the conductivity of hybrid PEMs was also examined, and the results are shown in Figure 5.5B. With increase in fiber volume fraction, the proton conductivity of hybrid PEMs increases although both the IEC and water uptake drop significantly (Table 5.1). For example, with the fiber volume fraction increasing from 8% to 30%, the proton conductivity ascends from 1.6×10^{-1} S/cm to 3.4×10^{-1} S/cm at 100 °C, which should attribute to the increasing number of water channels. Eventually, when the fiber diameter and volume fraction are 155 nm and 30%, respectively, the highest conductivity, 3.4×10^{-1} S/cm at 100 °C, is obtained for S-ZrO_2 fiber/C-PAMPS hybrid PEMs. This conductivity value is much higher than either that of C-PAMPS films, [405] or that of S-ZrO_2 nanoparticle blended membranes, [415] indicating the premium performance of S-ZrO_2 fibers incorporated hybrid PEMs.

5.4 Summary

The fabrication and characterization of S-ZrO_2 fiber/C-PAMPS hybrid membranes was studied. SEM, FT-IR and TGA were operated on the hybrid PEMs, and the comparison with C-PAMPS membranes was also made to verify the successful fabrication and compact filling of hybrid PEMs. Electrochemical properties, including the proton conductivities, IEC, and water uptake, were measured and compared with PAMPS membranes. It was found that with the incorporation of S-ZrO_2 fibers, the proton conductivities of PEMs were highly improved, which verified the beneficial effect of S-ZrO_2 fiber-induced long range water channels on the electrochemical

properties. It was also found that the fiber diameters and fiber volume fractions are the major parameters that influence the formation of water channels and finally influence the proton conductivities of hybrid PEMs.

CHAPTER 6. SULFATED ZIRCONIA NANOFIBER/NAFION HYBRID PROTON EXCHANGE MEMBRANES

Abstract

A novel type of hybrid membrane was fabricated by incorporating superacidic S-ZrO_2 nanofibers into recast Nafion for the application in PEMFCs. With the introduction of electrospun superacidic nanofiber mats, large amount of sulfonic acid groups in recast Nafion aggregated onto the interfaces between S-ZrO_2 fibers and the ionomer matrix, forming continuous pathways for fast proton transport. The resultant hybrid membranes had high proton conductivities, which were controlled by selectively adjusting the fiber diameter and fiber volume fraction. Consequently, the superacidic S-ZrO_2 electrospun nanofibers are promising filler materials and hybrid membranes containing S-ZrO_2 nanofiber mats can be potentially used in high-performance fuel cells.

6.1 Introduction

Invented in the late 1960s by DuPont, Nafion, a perfluorosulfonic acid polymer, has been extensively studied as the PEMs in fuel cells. [409, 416, 417] Nafion has maximum proton conductivity at around 0.1 S/cm, with good thermal, chemical and mechanical stabilities. However, the drawbacks of Nafion, including low operation temperature (<80 ℃), environmental incompatibility, high production cost, and especially unsatisfactory proton conductivity, hinder the widespread commercialization of PEMFCs. [410, 418, 419]

Nafion consists of a polytetrafluoroethylene backbone and perfluorinated vinyl ether pendant side chains terminated with sulfonic acid groups. This amphiphilic composition leads to a nanophase separation between the hydrophobic matrix and hydrophilic ionic groups in hydrated Nafion. [420] The ionic groups in Nafion could form a network of clusters that leads to efficient water swelling and proton transport through the hydrophobic domains. [366, 421–424] Thus, the performance of Nafion can be enhanced either by increasing the content of protogenic groups to form more acid-water clusters [425] or by creating hybrid structures for constructing connective pathways for proton transport. [426]

Until now, various inorganic nanoparticles, including silica, [316, 420, 427, 428] zirconia, [312, 321] titania, [429, 430] etc., have been incorporated into Nafion to form hybrid membranes.

Although several properties of hybrid membranes were improved, such as mechanical strength, thermal stability, selective permeability, and so forth, most filler particles lack protogenic groups, which restrict the fast proton transport and thus the conductivity of the membranes. So far, there are only a handful of reports on the filler materials that can offer additional protogenic groups for acid-water clusters, such as sulfonic acid functionalized single-walled carbon nanotubes, [425] solid acids, [431] and so forth. However, the low content of dispersed filler particles makes it difficult to form effective proton-transport pathways in membranes. [309] Hence, the overall performance of these Nafion-based hybrid membranes still does not meet the requirement of practical fuel cell applications. [241] Therefore, new strategies that can introduce both additional ionic groups and effective ionic pathways are highly demanded, and the technological impact of new fillers would be significant and needs further exploration.

Recently, electrospinning, an approach that can be used to prepare nanofibers through an electrically-charged jet of a polymer solution/melt, has received much attention. [11, 13, 14, 432, 364, 373] Because of the unique properties of electrospun nanofibers, such as large specific surface areas, superior mechanical properties, diversified composition, etc., they have been increasingly applied in energy storage, filtration, medical and pharmacological products, and textiles. In recent years, electrospun polyelectrolyte nanofibers, such as Nafion, sulfonated polyimide, etc., were embedded into nonionic polymer matrix, and results showed that they could create effective proton transport

pathways on the axial direction of fibers. [405, 433] Herein we present a novel type of Nafion-based hybrid membranes incorporated with superacidic electrospun S-ZrO_2 nanofibers. The solid superacid nanofibers help gather a large amount of protogenic groups of Nafion to the interfaces to construct a network of continuous ionic pathways for effective proton transport in the membranes. The new S-ZrO_2 nanofiber/Nafion hybrid membranes offer the potential of setting up a new strategy for the rational design of PEMs.

6.2 Results and Discussion

6.2.1 Preparation and Structural Characterization of S-ZrO_2 Nanofiber/Nafion Hybrid Membranes

S-ZrO_2 nanofiber/Nafion hybrid membranes were fabricated using a casting method with S-ZrO_2 fiber mats immersed in Nafion solution. The detailed procedure of preparation is shown in Section 3.3.3.2. Figure 6.1 shows a photogragh of a S-ZrO_2 nanofiber/Nafion hybrid membrane, in which the fiber diameter is 85 nm. It is seen that the hybrid membrane is free standing and flexible. The macroscopic appearance does not change when the fiber diameter changes.

Figure 6.1. Photograph of a free-standing, flexible S-ZrO_2 nanofiber/Nafion hybrid membrane held with a tweezer.

Figure 6.2 shows both the top and cross-sectional view of an as-prepared S-ZrO_2 nanofiber/Nafion hybrid membrane. It is seen that after filling with Nafion, no obvious holes can be found on the surface of the membrane (figure 6.2A). Nanofibers are clearly seen from the cross-sectional view, with polymer filling the interfiber voids (figure 6.2B).

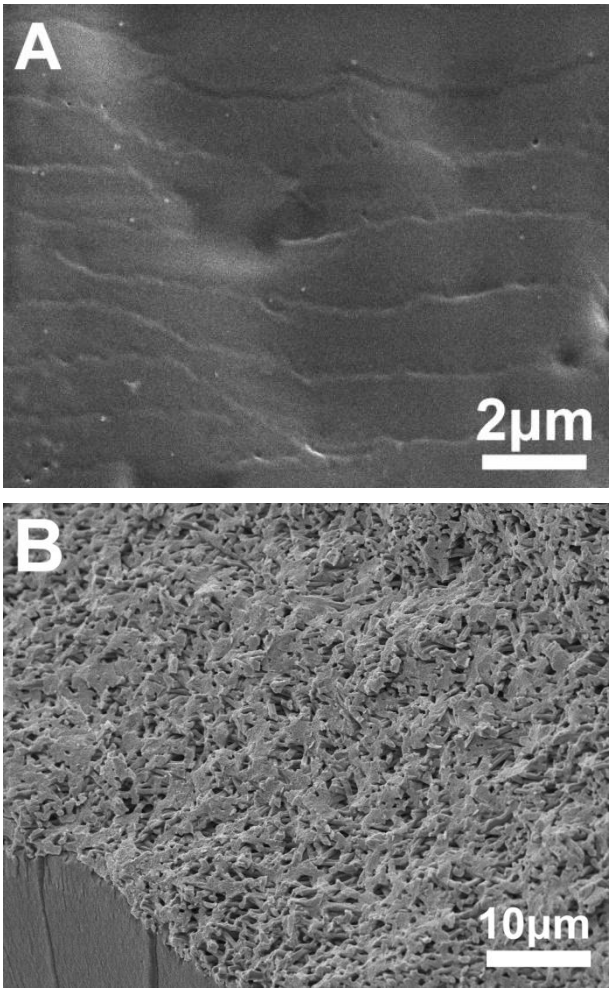

Figure 6.2. SEM images of (A) top view and (B) cross sectional view on a S-ZrO_2 nanofiber/Nafion hybrid membrane. (D = 369 nm, fiber volume fraction = 20%)

6.2.2 Proton Conductivities of S-ZrO_2 Nanofiber/Nafion Hybrid Membranes

Proton conductivity measurement was performed on S-ZrO_2 nanofiber/Nafion hybrid membranes with different volume fractions of superacidic nanofibers (figure 6.3A). The average fiber diameter for these membranes was 81 nm. For comparison, the conductivities of recast Nafion film were also meansured and shown in figure 6.3A. It is seen that S-ZrO_2 nanofiber/Nafion hybrid membranes have higher condutivities than

that of recast nafion at all temperatures. In addition, with increase in nanofiber volume fraction, the proton conductivities of S-ZrO_2 nanofiber/Nafion hybrid membranes increase. For example, at the temperature of 100 ℃ and relative humidity (RH) of 80%, the proton conductivity of recast Nafion is 9.2×10^{-2} S/cm. However, S-ZrO_2 fiber nanofiber/Nafion hybrid membranes with fiber volume fractions of 8, 12, and 20% are 1.9×10^{-1}, 2.3×10^{-1}, and 3.0×10^{-1} S cm^{-1}, respectively (figure 6.3B). Therefore, the addition of superacidic proton-conducting S-ZrO_2 nanofibers increases the proton conductivity of Nafion.

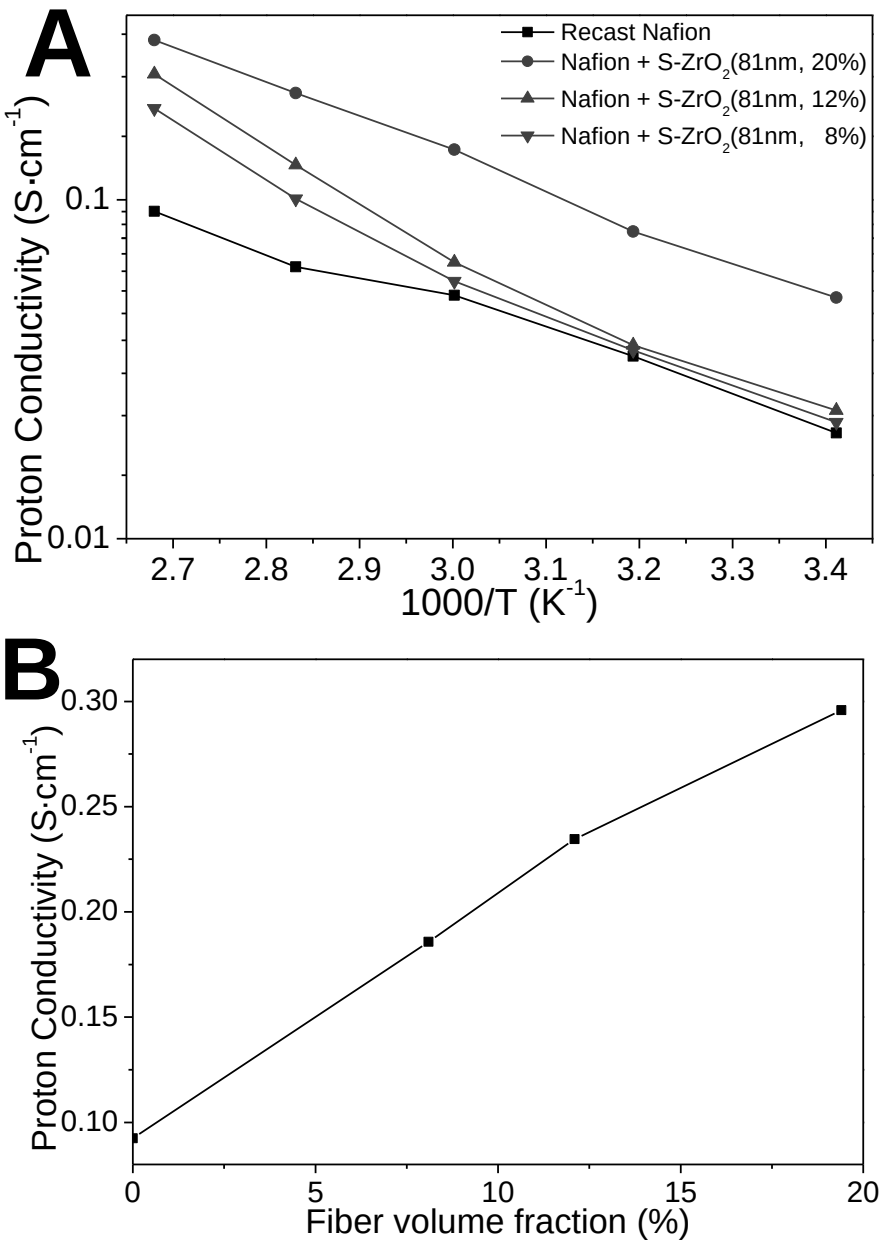

Figure 6.3. (A) Temperature-dependent proton conductivities of recast Nafion and S-ZrO_2 nanofiber/Nafion hybrid membranes (D = 81 nm) with different fiber volume fractions at 80% RH. (B) Proton conductivity vs. fiber volume fraction at 100 ℃ and 80% RH.

In most reported polymer electrolyte membranes, proton conductivity is strongly related to the amount of sulfonic acid groups or the water content, and membranes with high ion exchange capacities (IEC) or high water uptakes typically have high

proton conductivities. [434, 435] Table 6.1 shows the IECs and water uptakes of S-ZrO_2, recast Nafion, and S-ZrO_2 nanofiber/Nafion hybrid membranes. It is seen that when the fiber volume fractions increase, which are 0 (pure recast Nafion), 8, 12, 20%, the water uptake values of the membranes only increases slightly, which are 14.2, 15.1, 16.4, 17.7%, respectively. And at the same time, the IEC value decreases slightly, with the decreased values of 0.84, 0.83, 0.82, 0.79 mequiv/g, respectively, probably because of the low IEC of induced S-ZrO_2 fibers. Although the IEC value decreases, the proton conductivity of the membranes improves, with the values of 9.2×10^{-2}, 1.9×10^{-1}, 2.3×10^{-1}, 3.0×10^{-1} S/cm respectively at 100 °C and 80% RH (figure 6.3B). This indicates that it is unlikely to attribute the remarkable improvement in membrane conductivity to the increase of IEC or water uptake values of the membranes. A probable explanation is that a significantly amount of protogenic groups has been distributed along the S-ZrO_2 fiber length, forming long-range ionic pathways which in turn improve the proton conductivity without enhancing the IEC, as discussed in the following section.

Table 6.1. IEC and water uptake values of S-ZrO_2, recast Nafion, and S-ZrO_2 fiber/Nafion hybrid membranes.

Samples	**IEC (mequiv/g)**	**Water Uptake (%)**
S-ZrO_2	0.69 ±0.01	2.9 ±1.3
Recast Nafion	0.84 ±0.03	14.2 ±3.9
S-ZrO_2 (81nm[1], 8%[2]) + Nafion	0.83 ±0.04	15.1 ±5.5
S-ZrO_2 (81nm, 12%) + Nafion	0.82 ±0.13	16.4 ±5.3
S-ZrO_2 (81nm, 20%) + Nafion	0.79 ±0.08	17.7 ±1.4

[1] S-ZrO_2 fiber diameter.

[2] S-ZrO_2 fiber volume fraction.

6.2.3 TEM images of hybrid membranes

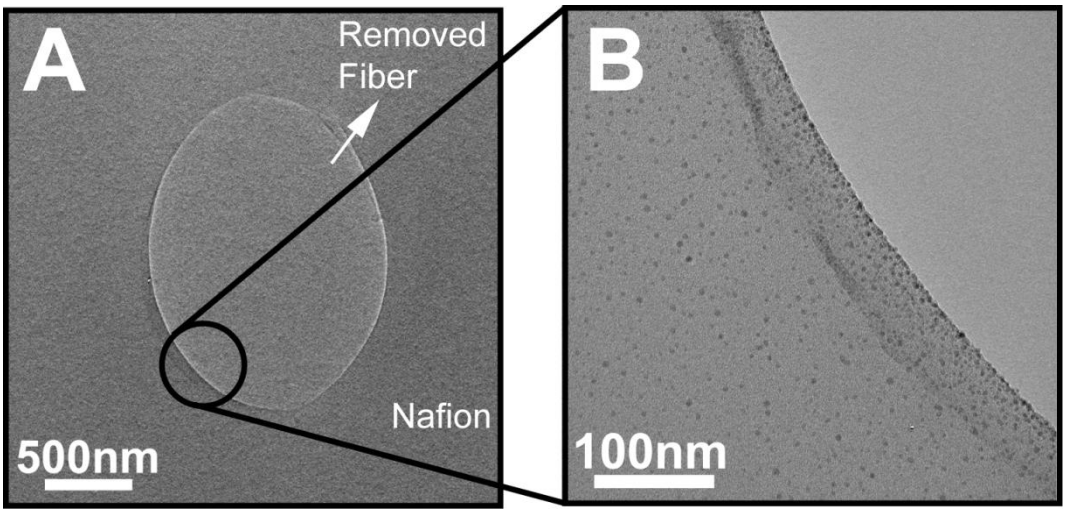

Figure 6.4. TEM images of (A) the cross-sectional view of a hybrid membrane (D = 369 nm), and (B) that with higher magnification, in which the inorganic fibers have been removed by HF. The membrane was stained by sodium ions for clear observation of ionic clusters.

The improved proton conductivity of hybrid membranes can be explained by the

aggregation of protogenic groups on the interfaces of S-ZrO_2 fibers and polymer matrix. During the formation of hybrid membranes, phase separation between the stiff and hydrophobic backbones and the soft and hydrophilic side chains of Nafion causes the formation of ionic clusters, [11, 13, 14, 432, 364, 373] which can been seen in the TEM images in figure 6.4. In order to clearly observe the ionic clusters in the membranes, the inorganic fibers were removed during the sample preparation and the membrane was stained with sodium ions. In the resultant TEM images, the dark dots in the Nafion region represent the hydrophilic domains, i.e., ionic clusters. From figure 6.4A and B, it is obvious that a higher number density of ionic clusters can be observed at the interface than in the bulk Nafion region, indicating the aggregation of protogenic groups on the inorganic/organic interface. This is related to the hydrophilic nature of S-ZrO_2 fibers. During the formation of hybrid membranes, hydrophilic attractions between the sulfate groups on S-ZrO_2 fibers and sulfonic acid groups in Nafion lead to the aggregation of ionic clusters of Nafion onto the interfaces. Consequently, the large amount of ionic clusters at the interface region forms long-distance ionic pathways along the S-ZrO_2 nanofibers that ensure effective proton transport through the entire membranes, as shown schematically in figure 6.5. As a result, the incorporation of S-ZrO_2 nanofibers into Nafion can effectively improve the proton conductivity without significantly changes of IEC and water uptake values.

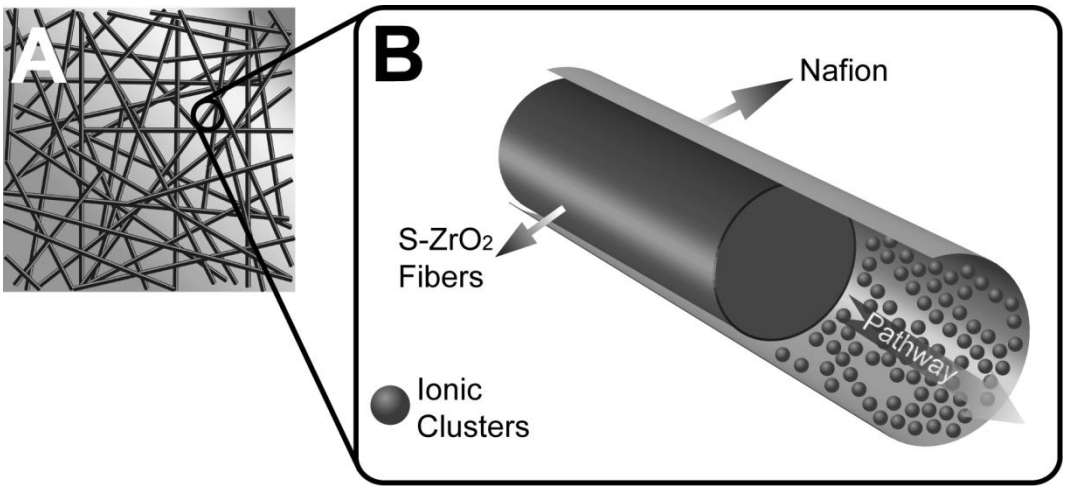

Figure 6.5. Schematic diagrams of (A) a S-ZrO_2 nanofiber/Nafion hybrid membrane, and (B) the interface between a S-ZrO_2 fiber and the Nafion matrix with ionic clusters aggregating on the S-ZrO_2 nanofiber/Nafion interface.

6.2.4 Effect of fiber diameter on the Performance of Hybrid Membranes

The effect of fiber diameter on the proton conductivity of hybrid membranes was also examined, and the results are shown in figure 6.6. The fiber volume fraction in these membranes was fixed at approximately 20%. It is seen that the proton conductivity of hybrid membranes increases with decrease in fiber diameter over the entire temperature range. For instance, hybrid membranes with fiber diameter of 85, 155, and 369 nm have a proton conductivity of 3.0×10^{-1}, 2.1×10^{-1}, and 1.3×10^{-1} S/cm, respectively, at 100 ^{o}C and 80% RH. It is then concluded that thinner fibers can acquire more interfacial area with a larger number of aggregated sulfonic acid groups, which result in easier proton transport on the interfaces and consequently lead to the increased proton conductivity.

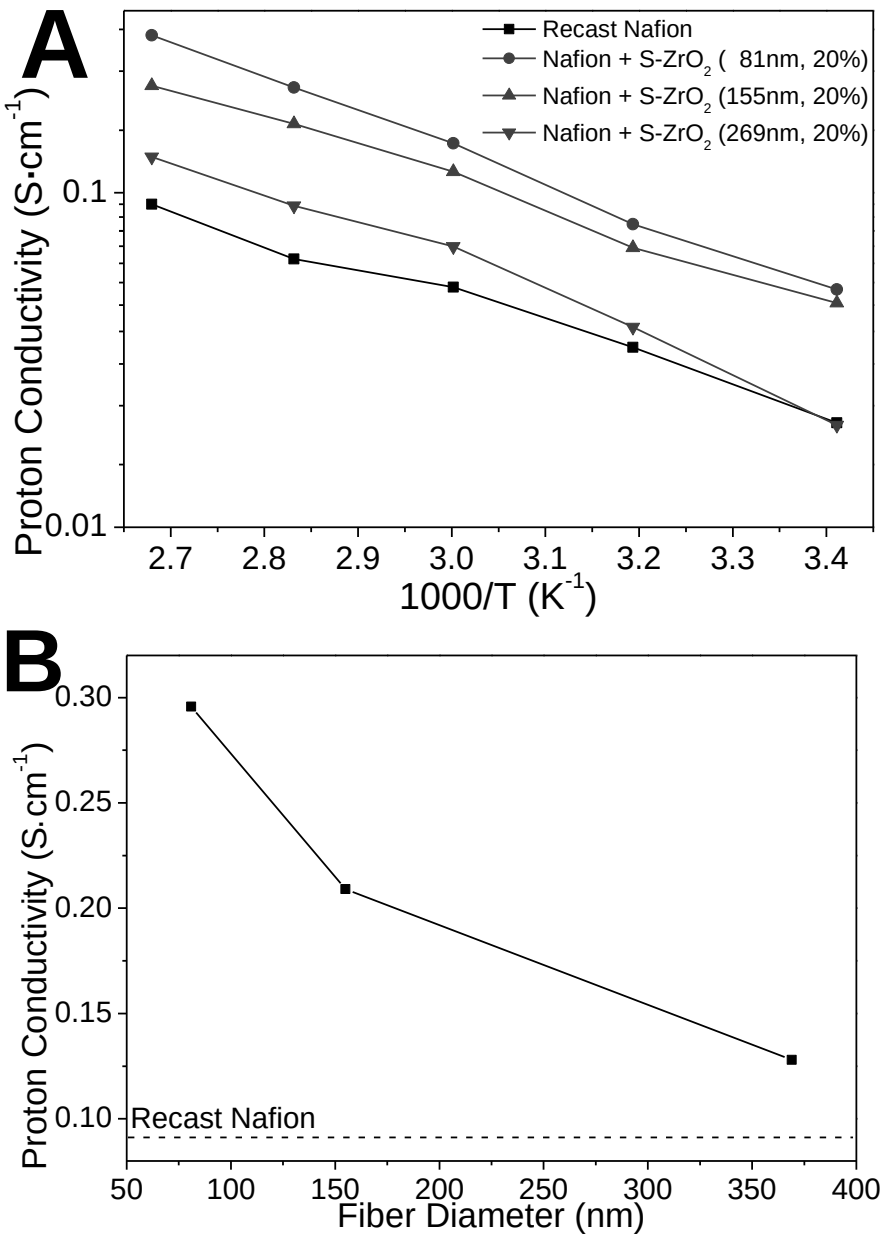

Figure 6.6 (A) Proton conductivities of recast Nafion and S-ZrO_2 nanofiber/Nafion hybrid membranes (fiber volume fraction = 20%) with different fiber diameters at 80% RH. (B) Proton conductivity vs. fiber diameter at 100 ℃ and 80% RH.

6.2.5 Effect of relative humidity on the Performance of Hybrid Membranes

The proton conductivities of recast Nafion and S-ZrO_2 nanofiber/Nafion hybrid membrane (fiber diameter = 85 nm, fiber volume fraction = 20%) were also measured at 80 ^{o}C and different relative humidities, as illustrated in figure 6.7. It is seen that the hybrid membrane possesses much higher proton conductivity than the recast Nafion film over the entire RH range. For example, at 100% RH, the ionic conductivity of the hybrid membrane and recast Nafion are 3.1×10^{-1} and 9.1×10^{-2} S/cm, respectively.

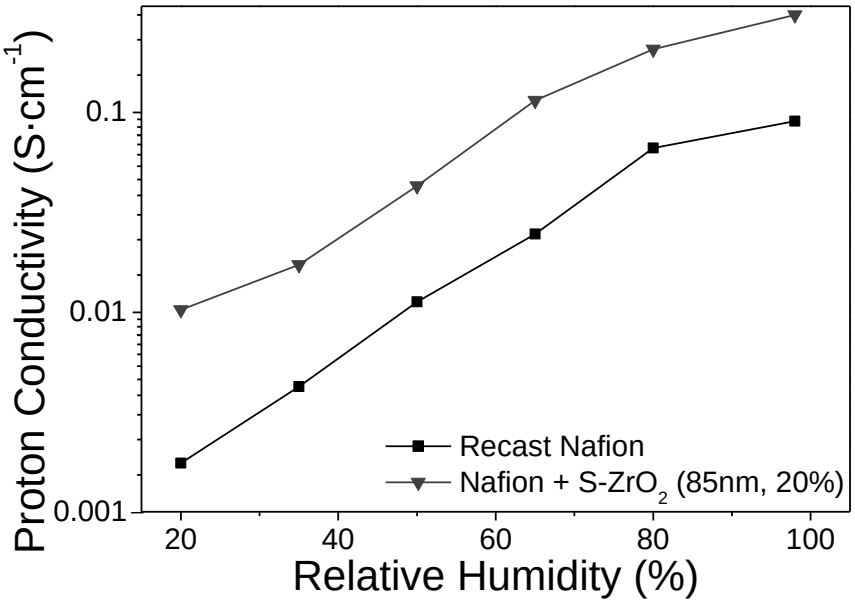

Figure 6.7. Humidity-dependent proton conductivities of recast Nafion and S-ZrO_2 nanofiber/Nafion hybrid membranes (D = 81 nm, fiber volume fraction = 20%) at 80 ℃.

6.3 Summary

In summary, novel superacidic S-ZrO_2 nanofiber/Nafion hybrid membranes have been prepared, in which long-range superacidic inorganic S-ZrO_2 nanofibers were incorporated. With the assistance of S-ZrO_2 nanofibers, a large amount of protogenic groups in Nafion aggregate onto the organic/inorganic interfaces and play a primary role in the improvement of proton conductivity. A high proton conductivity of ~3.1×10^{-1} S/cm is observed at 80 ^{o}C and 100% RH with the fiber diameter of 85 nm and fiber volume fraction of 20%. The superacidic nanofiber/Nafion hybrid membranes are easy to fabricate, highly controllable, and can be used in practical fuel cell systems. Besides, the potential applications of these membranes in biosensors, nanofluidics, and chemical/biological protections are also highly anticipated.

CHAPTER 7. SULFONATED POLYSTYRENE FIBER/NAFION HYBRID PROTON EXCHANGE MEMBRNAES

Abstract

A novel type of hybrid membrane was fabricated by incorporating S-PS electrospun fibers into recast Nafion for the application in PEMFCs. With the introduction of S-PS fiber mats, large amount of sulfonic acid groups in recast Nafion aggregated onto the interfaces between S-PS fibers and the ionomer matrix, forming continuous pathways for fast proton transport. The resultant hybrid membranes had higher proton conductivities than that of recast Nafion, which were controlled by selectively adjusting the fiber diameters. Consequently, Hybrid membranes fabricated by ionomers, such as Nafion, incorporated with sulfonated polystyrene electrospun nanofibers established a potential strategy for rational design of high-performance proton exchange membranes.

7.1 Introduction

A large number of synthesis and fabrication methods have been demonstrated for generating one-dimensional nanostructures such as fibers, rods, wires, tubes, and so forth. [436, 437] Among various methods, electrospinning is one of the most promising technologies to produce continuous nanofibers with diameters ranging from tens of microns down to several nanometers at relatively large scale and low cost. [3-14] The advantages of electrospun nanofibers, including uniform diameters, high surface-to-volume ratio and porosity, good mechanical properties, and diversified architecture, structure, and compositions, make them potential candidates for applications in areas like catalysis, sensors, hydrogen storage, tissue engineering, drug delivery, bioengineering, functional textiles, etc.

In a typical electrospinning process, a high electric field is applied to the droplet of a viscous polymer solution or melt coming out from the tip of a nozzle. The interactions of the electrical charges in the polymer fluid with the external electric field cause the pendant droplet to deform into a conical structure called Taylor cone. When electric charges in the fluid surpass the critical value at which repulsive electrostatic forces overcome the surface tension, a fine charged jet is ejected from the tip of Taylor cone. The charged jet undergoes a whipping motion and is elongated continuously by the electrostatic repulsion until is deposited onto a grounded collector, resulting in the formation of fine fibers. The formation of fibers is a function of operating parameters,

namely voltage, solution feeding rate, and solution properties, such as viscosity, conductivity, surface tension, etc. Consequently, the diameters, architecture, structure and composition of electrospun fibers can be well controlled by selectively adjusting the processing parameters of electrospinning.

So far, electrospun fibers have been extensively studied for use as the supporting materials in electrodes of PEMFCs and DMFCs. [438-441] Several advantages have been demonstrated, such as uniform dispersion, high accessible area for surface interactions and electron transport. However, only a few reports could be found on the application of electrospun fibers in polymer electrolytes, and most of which focused on the polyelectrolyte fibers. [405, 417, 433, 442] It was reported that with the assistance of the long-range electrospun fibers, a proton channel structure due to the aggregated ionic groups was formed and could lead to a rapid proton transport. [433] Herein we report a novel style of PEMs, in which surface-sulfonated polystyrene electrospun fiber mats as three dimensional interconnected networks were imbedded into Nafion, a perfluorosulfonic acid ionomer invented by Dupont. The embedded fibers with inert cores restrict the swelling of fibers as well as membranes in water and provide good membrane integrity and strength. In addition, the sulfonic acid groups on the surfaces of interconnected fibers ensure optimum utilization of percolation pathways for proton transport at the interfaces of embedded fibers and Nafion matrix. The newly-developed S-PS fiber/Nafion hybrid PEMs are easy to fabricate, highly controllable, and can be used in practical fuel cell systems, which offers a potential strategy on the rational

design of PEMs.

7.2 Results and Discussion

7.2.1 Preparation and Structural Characterization of S-PS fiber/Nafion Hybrid PEMs

S-PS fiber/Nafion hybrid PEMs were then fabricated by using the casting method with S-PS fiber mats immersed in Nafion solution. The detailed fabrication procedure is shown in Section 3.3.3.3. Figure 7.1 shows both the top and cross sectional views of S-PS fiber/Nafion hybrid PEMs, in which the S-PS fiber diameter is 0.98 μm. No obvious holes can be found on the surface of the PEM (figure 7.1A). The fibers are clearly seen from the cross-sectional view of the PEM, with uniformly dense polymeric Nafion filling the interfiber voids (figure 7.1B and C), verifying the formation of S-PS fiber/Nafion hybrid PEMs.

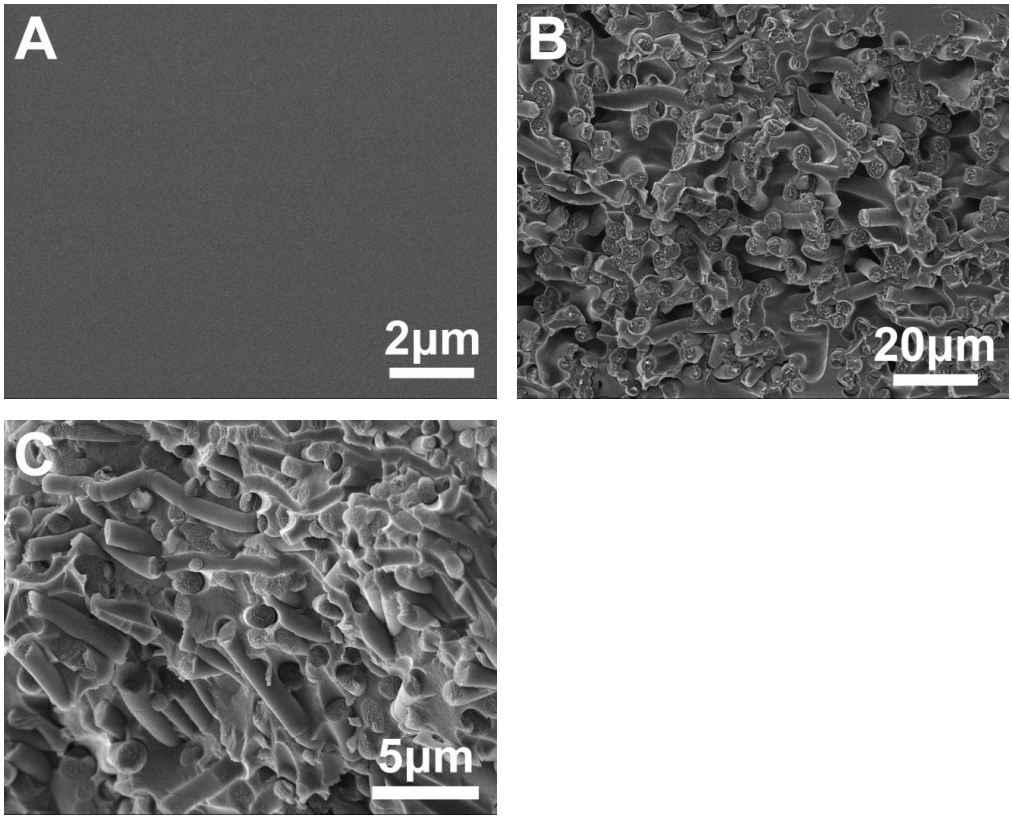

Figure 7.1. SEM images of A) top view, and B, C) cross sectional view on a typical S-PS fiber/Nafion hybrid PEM.

7.2.2 Proton Conductivities of S-PS Fiber/Nafion Hybrid PEMs

Proton conductivity measurement was performed on S-PS fiber/Nafion hybrid PEMs with different diameters of S-PS fibers, and the results are shown in figure 7.2. For comparison, the conductivities of recast Nafion are also shown. It is seen that S-PS fiber/Nafion membranes have higher conductivities than recase nafion over the entire temperature range. In addition, with decrease in fiber diameter, the conductivities of S-PS fiber/Nafion hybrid PEMs increase. For example, at 100 ℃, the proton conductivity of recast Nafion and S-PS fiber/Nafion hybrid PEMs with fiber diameter

of 0.98, 2.21, and 3.60 μm are 9.2×10^{-2}, 1.3×10^{-1}, 1.4×10^{-1}, and 1.6×10^{-1} S/cm, respectively.

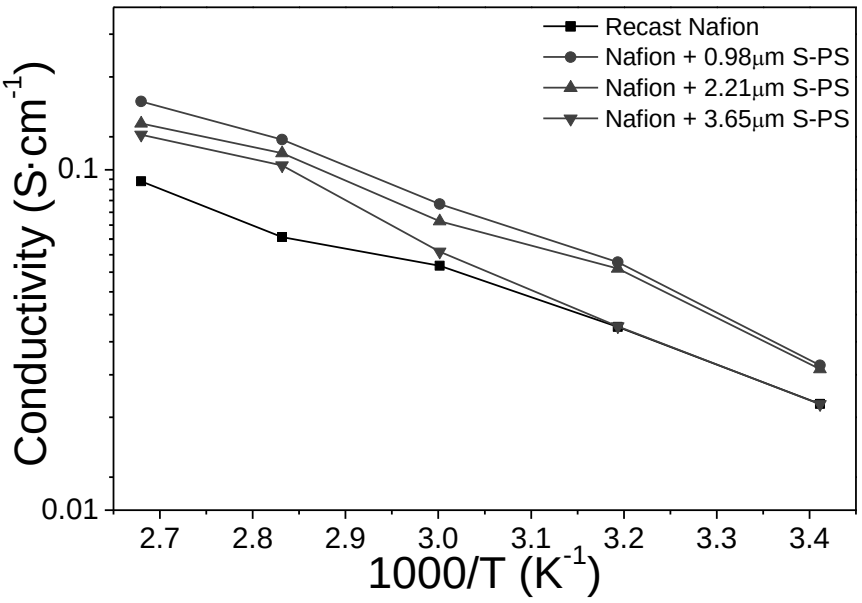

Figure 7.2. Temperature-dependent proton conductivities of recast Nafion and S-PS fiber/Nafion hybrid PEMs with different fiber diameters at 80% RH.

In most reported proton exchange membranes, the proton conductivity of PEMs is strongly related to the amount of sulfonic acid groups or the water content, and PEMs absorbing a large amount of water typically have high proton conductivity. [405, 417] As a result, it seems true that there is a positive correlation between the IEC or water uptake value and proton conductivity. However, as shown in table 7.1, when the proton conductivity increases with the incorporation of fibers and with the reduction of fiber diameters from 3.60, 2.21, to 0.98 μm, the water uptake only increases slightly from 14.4%, 16.9% to 19.7%; while the IEC values of hybrid PEMs increase

slightly from 0.67, 0.71 to 0.73 mequiv/g, which even drop dramatically compared with the IEC value of 0.84 mequiv/g of recast Nafion, probably caused by the small IEC value of S-PS fibers. This indicates that it is unlikely to attribute the improvement in membrane conductivity to the increase of IEC or water uptake values of the membranes. A probable explanation is that a significantly amount of protogenic groups of Nafion has been distributed along the S-PS fiber length, forming long-range ionic pathways which in turn improve the proton conductivity without enhancing the IEC.

Table 7.1. IEC and water uptake values of S-PS, recast Nafion, and S-PS fiber/Nafion hybrid PEMs.

Samples	**IEC (mequiv/g)**	**Water Uptake (%)**
S-PS (0.98 μm[1], 10%[2])	0.24 ± 0.01	10.9 ± 6.4
Recast Nafion	0.84 ± 0.03	14.2 ± 3.9
S-PS (0.98 μm, 10%) + Nafion	0.73 ± 0.02	19.7 ± 6.4
S-PS (2.21 μm, 10%) + Nafion	0.71 ± 0.02	16.9 ± 2.1
S-PS (3.60 μm, 10%) + Nafion	0.67 ± 0.02	14.4 ± 0.3

[1] S-PS fiber diameter.

[2] S-PS fiber volume fraction.

7.2.3 Effect of Relative Humidity on the Performance of Hybrid Membranes

The proton conductivities of S-PS fiber/Nafion hybrid PEM and recast Nafion were measured at different RH, as illustrated in figure 7.3. It is apparent that hybrid PEMs possess higher proton conductivities than recast Nafion over the entire RH range. For

example, at 100% RH, the proton conductivities of hybrid PEM and recast Nafion are $1.8 \times 10^{-1}$and 9.1×10^{-2} S/cm respectively. This clearly demonstrates the premium performance of PEMs with long-range ionic pathways formed by incorporated S-PS fibers.

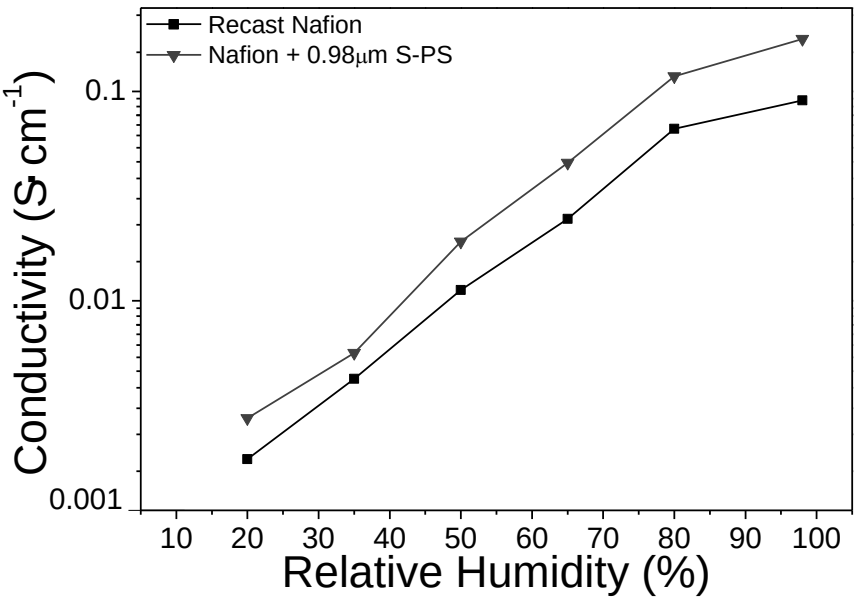

Figure 7.3. Humidity-dependent proton conductivities of recast Nafion, and S-PS fiber (0.98μm)-Nafion hybrid PEM at the temperature of 80 ℃.

7.3 Summary

A novel type of S-PS fiber/Nafion hybrid PEMs has been developed by incorporating a network of interconnected long-range S-PS fibers into commercial Nafion. With the assistance of fibers, a network of long-range ionic pathways is formed and plays a primary role in the improvement of proton conductivity. Highest proton conductivity at ~1.8×10^{-1} S/cm was observed at 100 ℃ and 80% RH with the fiber diameter of

0.98μm. The hybrid membranes comprised with networks of long-range ionic pathways are easy to fabricate, highly controllable, and can be used in practical fuel cell systems. Furthermore, this type of fiber network membranes can also be useful for other purposes, such as electrodialysis separations, sensors, and industrial electrolyses.

CHAPTER 8. CONCLUSIONS

In pursuit of resolving the worldwide critical energy issues and environmental pollution problems, the development of sustainable, clean and renewable energy technologies, such as energy storage and conversion systems, has been widely recognized as an economically and environmentally friendly alternative to conventional energy resourses, such as pertrolium and coals, to settle these urgent global issues facing our society. Among various energy storage and conversion systems, proton exchange membrane fuel cells (PEMFCs) have recently drew a major attention because of their advanges, such as fast startup, high efficiency and power density, and low green-house gas emission. PEMFCs have been widely recognized to be potentially used in electrical vehicles and portable devices.

Recently, particular attention has been given to the design and synthesis of high-performance proton exchange membranes (PEMs), since PEMs with high proton conductivity that can sustain high temperatures have been proved to be vitally important to improve the electrochemical performance of PEMFCs. The disadvantages of present PEMs Nafion, such as high production cost, environmental incompatibility, low operation temperature (<80 ℃), and unsatisfactory proton conductivity (<0.1 S cm^{-1}), hinder the widespread commercialization of PEMFCs.

Until now, various inorganic nanoparticles, including silica, [7, 15-17] zirconia, [18, 19]

titania, etc., have been incorporated into polymer electrolytes to form hybrid membranes. Although several properties of hybrid membranes were improved, such as mechanical strength, thermal stability, selective permeability, and so forth, most filler particles lack protogenic groups, which restrict the fast proton transport and thus the conductivity of the membranes. So far, there are only a handful of reports on the filler materials that can offer additional protogenic groups for acid-water clusters, such as sulfonic acid functionalized single-walled carbon nanotubes, solid acids, and so forth. However, the low content of dispersed filler particles makes it difficult to form effective proton-transport pathways in membranes. Hence, the overall performance of these Nafion-based hybrid membranes still does not meet the requirement of practical fuel cell applications. Therefore, new strategies that can introduce both additional ionic groups and effective ionic pathways are highly demanded, and the technological impact of new fillers would be significant and needs further exploration.

In our work, we focused on the prepararion of fibrous materials attached with sulfonic acid groups through electrospinning and other post-electrospinning processes, and explored them as the filler materials in hybrid proton exchange membranes. Both inorganic superacidic and sulfonated polymeric fibers were fabricated, and incorporated into ionomers. Because of the hydrophilic attractions between functional groups of both the fibers and polymer matrix, protogenic groups, such as sulfonic acid groups in the ionomers aggregate on the interfaces of fibers and polymer matrix,

forming effective nanoscaled pathway for fast proton transport, which in turn increases the proton conductivity of the membranes. The hybrid membranes comprised with networks of long-range ionic pathways are easy to fabricate, highly controllable, and can be used in practical fuel cell systems. Furthermore, this type of fiber network membranes can also be useful for other applications, such as electrodialysis separations, sensors, industrial electrolyses, and chemical/biological protections. The research in this dissertation was divided into following four parts:

I) Fabrication of S-ZrO_2 and S-PS fiber mats by electrospinning and other post-electrospinning processes.

S-ZrO_2 nanofibers were fabricated for the first time. Because of the brittleness of ZrO_2 fibers, subsequent sulfation cannot be carried out while keeping the integrity of ZrO_2 fiber mats. As a result, a more intricate process was applied with an approach with five steps: 1) the sol-gel method was adoped to make Zr-containing fiber, 2) a compressing step was applied on the fiber mat to increase the volume density of fibers, 3) a heat treatment at 280 ℃ in air to form a carbon-like brown mat containing ZrO_2, 4) sulfation with H_2SO_4, 5) calcination at 620 ℃ in air to obtain an S-ZrO_2 fiber mat. The fiber diameters were tuned by controlling the concentrations of $Zr(OPr)_4$ and PVP in the pre-electrospinning solution. The fiber volume fractions were also controlled by cold pressing with different pressures. SEM images, XRD and FT-IR spectra were also made, and the results proved the successful fabrication of S-ZrO_2 fibers.

S-PS fiber mats were also fabricated by sulfonation of electrospun PS fibers in H_2SO_4 solution. The fiber diameters were tuned by controlling the concentrations of PS in the pre-electrospinning solution. And compact fiber mats were made by cold pressing. SEM images and FT-IR spectra were also used. All the results proved the successful fabrication of S-PS fibers.

In summary, with electrospinning technology and other post-electrospinning processes, both S-ZrO_2 and S-PS fiber mats were successfully fabricated. Several parameters were controlled, including fiber diameter and fiber volume fraction.

II) Fabrication and Characterization of S-ZrO_2 fiber/C-PAMPS hybrid membranes.

S-ZrO_2 fiber/C-PAMPS hybrid membranes were prepared and the electrochemical performance of the hybrid membranes was measured.

S-ZrO_2 fiber/C-PAMPS hybrid membranes were firstly prepared by in situ polymerization by immersing S-ZrO_2 fiber mats in AMPS solutions followed by polymerization and crosslinking. SEM images on the top and cross-sectional views demonstrated that S-ZrO_2 fiber/C-PAMPS hybrid membranes had well-defined morphology. The proton conductivity, IEC, and water uptake values were obtained and showed the premium performance of hybrid membranes compared with pure

C-PAMPS and commercial Nafion films.

Besides, the proton conductivity of the hybrid membrane was controlled by changing the crosslinking degree of C-PAMPS, the fiber diameter, and fiber volume fraction. The highest proton conductivity of the hybrid membrane at 3.4×10^{-1} S cm^{-1} was obtained with hybrid membrane with fiber diameter of 155 nm and fiber volume fraction of 30% at 100 ℃ and 80% RH.

III) Fabrication and Characterization of S-ZrO_2 fiber/Nafion hybrid membranes.

S-ZrO_2 fiber/Nafion hybrid membranes were prepared and the electrochemical performance of the hybrid membranes was measured.

S-ZrO_2 fiber/Nafion hybrid membranes were firstly prepared by casting method by immersing S-ZrO_2 fiber mats in Nafion solutions. SEM images on the top and cross-sectional views demonstrated that S-ZrO_2 fiber/Nafion hybrid membranes have well-defined morphology. TEM images showed that large amount of ionic clusters in Nafion aggregated on the interface of fibers and polymer matrix, which gave a good explanation of the remarkably improve proton conductivity. The proton conductivity, IEC, and water uptake values were obtained and showed the premium performance of hybrid membranes compared with pure recast Nafion films.

Besides, the proton conductivity of the hybrid membrane was controlled by changing the fiber diameter, and fiber volume fraction. The highest proton conductivity of the hybrid membrane at 3.1×10^{-1} S cm^{-1} was obtained with hybrid membrane with fiber diameter of 85 nm and fiber volume fraction of 20% at 80 ℃ and 100% RH.

IV) Fabrication and Characterization of S-PS fiber/Nafion hybrid membranes.

S-PS fiber/Nafion hybrid membranes were prepared and the electrochemical performance of the hybrid membranes was measured.

S-PS fiber/Nafion hybrid membranes were firstly prepared by casting method by immersing S-PS fiber mats in Nafion solutions. SEM images on the top and cross-sectional views demonstrated that S-ZrO_2 fiber/Nafion hybrid membranes had well-defined morphology. The proton conductivity, IEC, and water uptake values were obtained and showed the premium performance of hybrid membranes compared with pure recast Nafion films.

Besides, the proton conductivity of the hybrid membrane was controlled by changing the fiber diameter. The highest proton conductivity of the hybrid membrane at 1.8×10^{-1} S/cm was observed at 100 ℃ and 100% RH with the fiber diameter of 0.98μm.

CHAPTER 9. FUTURE WORK

In order to further the research, the recommended future work is included in the following but not limited to:

I) Fabrication of PEMs incorporated with inorganic fibers with ionic polymer brushes and the measurement of electrochemical performance on the hybrid membranes.

Polymer brushes grafted on non-conductive inorganic fibers can be obtained via surface-initiated atomic transfer radical polymerization. Long chains of the polymer brushes attached with multiple protogenic groups, such as sulfonic acid groups, compared with a single group on each site on the S-ZrO_2 fibers, can not only attract protogenic groups of ionomers on the interface, but also provide wider pathways with more hopping sites for fast proton transport. The soft polymer chain with more free volumes can be another promotional reason for fast proton transport, which can remarkably improve the proton conductivity of the hybrid membranes. From the structural characterization and measurement of electrochemical performance, we can compare the properties of ionic polymer brush grafted nanofiber/ionomer hybrid membranes with commercial PEMs, such as Nafion, and the hybrid membranes with fibrous filler materials with less protogenic groups, such as S-ZrO_2 and S-PS. Results obtained from the detailed exploration can be used to improve the structure and

properties of hybrid membranes, and establish a detailed strategy of hybrid membranes with fibrous filler materials.

II) Hybrid Membranes with S-ZrO_2 nanorod arrays penetrating through the membranes

Although the hybrid membranes with S-ZrO_2 fiber as the filling materials show a premium performance than those with particulate fillers, the fiber mats actually mainly improves the in-plane proton conductivity of the membranes. However, the effect of the fiber material to the through-plane proton conductivity is still unknown, which is the conducting direction in the actual application of PEM in fuel cells. With the use of S-ZrO_2 nanorod arrays that penetrating through the ionomer matrix, the effective pathways for effective proton transport on the direction from the anode to the cathode can be obtained, which in turn improves the through-plane proton conductivity on the working direction of hybrid PEMs.

III) Incorporate the hybrid membranes with fibers as filler materials into membrane electrode assemblies (MEAs) to study their electrochemical performance in practical PEMFCs.

MEA, which consists a polymer electrolyte membrane and catalyst loaded porous electrodes for fuel oxidation at the anode and oxygen reduction at the cathode, is the

key component of PEMFCs. In order to understand the electrochemical properties of fiber incorporated hybrid membranes in the pratical PEMFCs, full cell performance, such as voltage vs.current density or power density vs. current density, should be investigated. From the information of the full cell performance, we can compare the properties of hybrid membranes to those of commercial available PEMs, such as Nafion. Results obtained from the detailed comparisons can be used to improve the structure and properties of the hybrid membranes and the overall electrochemical performance of fuel cells.

REFERENCES

[1] Y. Xia, P. Yang, Y. Sun, Y. Wu, B. Mayers, B. Gates, Y. Yin, F. Kim, H. Yan. "One-dimensional nanostructures: synthesis, characterization, and applications." Adv. Mater. 15 (2003) 353 – 389.

[2] J. Hu, T. W. Odom, C. M. Lieber. "Chemistry and physics in one dimension: synthesis and properties of nanowires and nanotubes." Acc. Chem. Res. 32 (1999) 435 – 445.

[3] Y. Dzenis. "Spinning continuous fibers for nanotechnology." Science 304 (2004) 1917 – 1919.

[4] D. Lin, Y. Xia. "Electrospinning of nanofibers reinventing the wheel." Adv. Mater. 16 (2004) 1151 – 1170.

[5] Z.-M. Huang, Y.-Z. Zhang, M. Kotakic, S. Ramakrishna. "A review on polymer nanofibers by electrospinning and their applications in nanocomposites." Composites Sci. Techn. 63 (2003) 2223 – 2253.

[6] W. E. Teo, S. Ramakrishna. "A review on electrospinning design and nanofibre assemblies." Nanotechnology 17 (2006) R89 – R106.

[7] S. Ramakrishna, K. Fujihara, W.-E. Teo, T. Yong, Z. Ma, R. Ramaseshan. "Electrospun nanofibers solving global issues." Materialstoday 9 (2006) 40 – 50.

[8] A. Greiner, J. H. Wendorff. "Electrospinning: a fascinating method for the preparation of ultrathin fibers." Angew. Chem. Int. Ed. 46 (2007) 5670 – 5703.

[9] V. Thavasi, G. Singh, S. Ramakrishna. "Electrospun nanofibers in energy and environmental applications." Energy Environ. Sci. 1 (2008) 205 – 221.

[10] S. Agarwal, J. H. Wendorff, A. Greiner. "Chemistry on electrospun polymeric nanofibers: merely routine chemistry or a real challenge?" Macromol. Rapid Commun. 31 (2010) 1317 – 1331.

[11] Y. Yao, Z. Z. Gu, J. Zhang, C. Pan, Y. Zhang, H. Wei. "Fiber/oriented liquid crystal-polarizers based on anisotropic electrospinning." Adv. Mater. 19 (2007) 3707 - 3711.

[12] Z. Q. Feng, X. H. Chu, N. P. Huang, M. K. Leach, G. Wang, Y. C. Wang, Y. T. Ding, Z. Z. Gu. "Rat hepatocyte aggregate formation on discrete aligned nanofibers of type-I collagen-coated poly(L-lactic acid)." Biomaterials 31 (2010) 3604 – 3612.

[13] L.W. Ji, X. W. Zhang. "Fabrication of porous carbon/Si composite nanofibers as high-capacity battery electrodes." Electrochem. Commun. 11 (2009) 1146 – 1149.

[14] M. Ma, K. Titievsky, E. L. Thomas, G. C. Rutledge. “Continuous concentric lamellar block copolymer nanofibers with long range order.” Nano Lett. 9 (2009) 1678 – 1683.

[15] J. Larmor. “Note on the complete scheme of electrodynamic equations of a moving material medium, and on electrostriction.” Proc. R. Soc. 63 (1898) 365 – 372.

[16] J. F. Cooley. “Apparatus for electrically dispersing fluids.” (US Patent Specification, 692631. 1902).

[17] W. J. Morton. “Method of dispersing fluids.” (US Patent Specification, 705691. 1902)

[18] A. Formhals. “Method and apparatus for the production of fibers.” (US Patent Specification, 2116942. 1938a).

[19] A. Formhals. “Method and apparatus for the production of fibers.” (US Patent Specification, 2123992. 1938b).

[20] A. Formhals. “Method and apparatus for the production of artificial fibers.” (US Patent Specification, 2158416. 1939).

[21] A. Formhals. “Method and apparatus for spinning.” (US Patent Specification, 2160962. 1939).

[22] V. B. Gupta, V. K. Kothari. “Manufactured Fibre Technology.” (London: Chapman and Hall, 1997).

[23] M. S. Khil, S. R. Bhattarai, H. Y. Kim, S. Z. Kim, K. H. Lee. “Novel fabricated matrix via electrospinning for tissue engineering” J. Biomed. Mater. Res. B 72 (2005) 117 - 124.

[24] P. K. Baumgart. “Electrostatic spinning of acrylic microfibers”. J. Colloid Interface Sci. 36 (1971) 71 – 79.

[25] J. Zeleny. “Instability of electrified liquid surfaces”. Phys. Rev. 10 (1917) 1 – 6.

[26] G. Taylor. “Disintegration of water drops in an electric field”. Proc. R. Soc. Lond. A 280 (1964) 383 – 397.

[27] G. Taylor. “Studies in electrohydrodynamics: I. The circulation produced in a drop by electrical field”. Proc. R. Soc. Lond. A 291 (1966) 159 – 166.

[28] G. Taylor. “Electrically driven jets”. Proc. R. Soc. Lond. A 313 (1969) 453 – 475.

[29] L. Larrondo, R. S. J. Manley. “Electrostatic fiber spinning from polymer melts: I. Experimental observations on fiber formation and properties”. J. Polym. Sci. 19 (1981) 909 – 920.

[30] L. Larrondo, R. S. J. Manley. “Electrostatic fiber spinning from polymer melts: II. Examination of the flow field in an electrically driven jet”. J. Polym. Sci. 19 (1981) 921 – 932.

[31] L. Larrondo, R. S. J. Manley. “Electrostatic fiber spinning from polymer melts: III. Electrostatic deformation of a pendent drop of polymer melt”. J. Polym. Sci. 19 (1981) 933 – 940.

[32] J. Doshi, D. H. Reneker. “Electrospinning Process and Application of Electrospun Fibers”. J. Electrostatics 35 (1995) 151-160.

[33] A. L. Yarin, S. Koombhongse, D. H. Reneker. “Bending Instability in Electrospinning of Nanofibers.” J. Appl. Phys. 89 (2001) 3018 – 3026.

[34] D. H. Reneker, A. L. Yarin, H. Fong, S. Koombhongse. “Bending Instability of Electrically Charged Liquid Jets of Polymer Solutions in Electrospinning”. J. Appl. Phys. 87 (2000) 4531 – 4547.

[35] M. M. Hohman, M. Shin, G. Rutledge, M. P. Brenner. “Electrospinning and Electrically Forced Jets. I. Stability Theory.” Phys. Fluids 13 (2001) 2201 – 2220.

[36] M. M. Hohman, M. Shin, G. Rutledge, M. P. Brenner. “Electrospinning and Electrically Forced Jets. II. Applications.” Phys. Fluids 13 (2001) 2221 – 2236.

[37] Lord Rayleigh. “On the Instability of a Cylinder of Viscous Liquid under Capillary Force.” Philos. Mag. 34 (1892) 145 – 155.

[38] S. Tomotika. “On the Instability of a Cylindrical Thread of a Viscous Liquid Surrounded by Another Viscous Fluid.” Proc. R. Soc. London Ser. A 150 (1935) 322 – 337.

[39] F. D. Rumscheidt, S. G. Mason. “Break-up of stationary liquid threads.” J. Colloid Sci. 17 (1962) 260 – 269.

[40] T. Pakula, J. Grebrowicz, M. Kryszewski. “The Kinetics of Spontaneous Changes in the Phase Structure of Molten Two-component Polymer Systems.” Polym. Bull. 2 (1980) 799 – 804.

[41] D. H. Reneker, W. Kataphinan, A. Theron, E. Zussman, A. L. Yarin. “Nanofiber garlands of polycaprolactone by electrospinning.” Polymer 43 (2002) 6785 – 6794.

[42] A. Ziabicki, H. Kawai. “High-Speed Fiber Spinning: Science and Engineering Aspects.” Wiley, New York, 1985.

[43] M. A. Perez, M. N. Maplewood, W. I. Hudson. “Microfibers and Method of Making.” (US Patent, 6110588 2000).

[44] R. D. Pike. “Superfine microfiber nonwoven web.” (US Patent, 5935883 1999).

[45] D. H. Reneker. “Process and apparatus for the production of nanofibers.” (US Patent, 6382526 2002).

[46] A. A. Tseng, A. Notargiacomo, T. P. Chen. “Nanofabrication by scanning probe microscope lithography: A review.” J. Vac. Sci. Technol. B. 23 (2005) 877 - 894.

[47] D. Wouters, U. S. Schubert. “Nanolithography and nanochemistry: Proberelated patterning techniques and chemical modification for nanometersized devices.” Angew. Chem. Int. Ed. 43 (2004) 2480-2495.

[48] J. C. Huie. “Guided molecular self-assembly: a review of recent efforts.” Smart Mater. Struct. 12 (2003) 264–271.

[49] C. F. J. Faul, M. Antonietti. “Ionic self-assembly: Facile synthesis of supramolecular materials.” Adv. Mater. 15 (2003) 673-683.

[50] G. M. Whitesides, M. Boncheva. “Beyond molecules: Self-assembly of mesoscopic and macroscopic components.” Proc. Natl. Acad. Sci. 99 (2002) 4769 – 4774.

[51] S. Zhang. “Emerging biological materials through molecular self assembly.” Biotechnol. Adv. 20 (2002) 321 – 339.

[52] M. Bognitzki, H. Hou, M. Ishaque, T. Frese, M. Hellwig, C. Schwarte, A. Schaper, J. H. Wedorff, A. Greiner. “Polymer, Metal, and Hybrid Nano- and Mesotubes by Coating Degradable Polymer Template Fibers (TUFT Process).” Adv. Mater. 12 (2000) 637 – 640.

[53] M. Bognitzki, W. Czado, T. Frese, A. Schaper, M. Hellwig, M. Steinhart, A. Greiner, J. H. Wedorff. “Nanostructured Fibers via Electrospinning.” Adv. Mater. 13 (2001) 70 – 72.

[54] F. Ochanda, W. E. Jones. “Sub-Micrometer-Sized Metal Tubes from Electrospun Fiber Templates.” Langmuir 21 (2005) 10791 – 10796.

[55] F. Ochanda, W. E. Jones. “Fabrication and Thermal Analysis of Submicron Silver Tubes Prepared from Electrospun Fiber Templates.” Langmuir 23 (2007) 795 – 801.

[56] Q. F. Wei, H. Ye, D. Y. Hou, H. B. Wang, W. D. Gao. “Surface functionalization of polymer nanofibers by silver sputter coating.” J. Appl. Polym. Sci 99. (2006) 2384 – 2388.

[57] Z. Sun, E. Zussman, A. L. Yarin, J. H. Wendorff, A. Greiner. “Compound Core–Shell Polymer Nanofibers by Co-Electrospinning.” Adv. Mater. 15 (2003) 1929 – 1932.

[58] G. Larsen, R. Velarde-Ortiz, K. Minchow, A. Barrero, I. G. Loscertales. “A Method for Making Inorganic and Hybrid (Organic/Inorganic) Fibers and Vesicles with Diameters in the Submicrometer and Micrometer Range via Sol−Gel Chemistry and Electrically Forced Liquid Jets.” J. Am. Chem. Soc. 125 (2003) 1154 – 1155.

[59] J. H. Yu, S. V. Fridrikh, G. C. Rutledge. “Production of Submicrometer Diameter Fibers by Two-Fluid Electrospinning.” Adv. Mater. 16 (2004) 1562 – 1566.

[60] D. Li, Y. Xia. “Direct Fabrication of Composite and Ceramic Hollow Nanofibers by Electrospinning.” Nano Lett. 4 (2004) 933 – 938.

[61] Y. Zhang, Z. M. Huang, X. Xu, C. T. Lim, S. Ramakrishna. “Preparation of Core−Shell Structured PCL-r-Gelatin Bi-Component Nanofibers by Coaxial Electrospinning.” Chem. Mater. 16 (2004) 3406 – 3409.

[62] D. Li, J. T. McCann, Y. Xia. “Use of Electrospinning to Directly Fabricate Hollow Nanofibers with Functionalized Inner and Outer Surfaces.” Small 1 (2005) 83 – 86.

[63] H. Jiang, Y. Hu, Y. Li, P. Zhao, K. Zhu, W. Chen. “A facile technique to prepare biodegradable coaxial electrospun nanofibers for controlled release of bioactive agents.” J. Controlled Release 108 (2005) 237 – 243.

[64] S. N. Reznik, A. L. Yarin, E. Zussman, L. Bercovici. “Evolution of a compound droplet attached to a core-shell nozzle under the action of a strong electric field.” Phys. Fluids 18 (2006) 062101.

[65] M. Wang, J. H. Yu, D. L. Kaplan, G. C. Rutledge. “Production of Submicron Diameter Silk Fibers under Benign Processing Conditions by Two-Fluid Electrospinning.” Macromolecules 39 (2006) 1102 – 1107.

[66] X.-J. Han, Z.-M. Huang, C.-L. He, L. Liu, X.-J. Han, Q.-S. Wu. “Coaxial electrospinning of PC(shell)/PU(core) composite nanofibers for textile application.” Polym. Compos. 27 (2006) 381 – 387.

[67] Y. Z. Zhang, X.Wang, Y. Feng, J. Li, C. T. Lim, S. Ramakrishna. “Coaxial Electrospinning of (Fluorescein Isothiocyanate-Conjugated Bovine Serum Albumin)-Encapsulated Poly(ε-caprolactone) Nanofibers for Sustained Release.” Biomacromolecules 7 (2006) 1049 – 1057.

[68] A. L. Yarin, E. Zussman, J. H. Wendorff, A. Greiner. “Material encapsulation and transport in core–shell micro/nanofibers, polymer and carbon nanotubes and micro/nanochannels.” J. Mater. Chem. 17 (2007) 2585 – 2599.

[69] L. C. Cheryl, J. S. Stephens. “Controlling Surface Morphology of Electrospun Polystyrene Fibers:

Effect of Humidity and Molecular Weight in the Electrospinning Process.” Macromolecules 37 (2004) 573 – 578.

[70] T. E. McKnight, A. V. Melechko, G. D. Griffin, M. A. Guillorn, V. I. Merkulov, F. Serna1 D. K. Hensley, M. J. Doktycz, D. H. Lowndes. M. L. Simpson. “Intracellular integration of synthetic nanostructures with viable cells for controlled biochemical manipulation.” Nanotechnology 14 (2003) 551 – 556.

[71] L. Ji, C. Saquing, S. A Khan, X. Zhang. “Preparation and characterization of silica nanoparticulate-polyacrylonitrile composite and porous nanofibers.” Nanotechnology 19 (2008) 085605.

[72] L. Ji, X. Zhang. “Fabrication of porous carbon nanofibers and their application as anode materials for rechargeable lithium-ion batteries.” Nanotechnology 20 (2009) 155705.

[73] E. D. Boland, G. E. Wnek, D. G. Simpson, K. J. Pawlowski, G. L. Bowlin. “Tayloring tissue engineering scaffolds using electrostatic processing techniques: a study of poly(glycolic acid) electrospinning.” J. Macromol. Sci. A 38 (2001) 1231 – 1243.

[74] C. Y. Xu, R. Inai, M. Kotaki, S. Ramakrishna. “Aligned biodegradable nanofibrous structure: A potential scaffold for blood vessel engineering.” Biomaterials 25 (2004) 877 – 886.

[75] P. Katta, M. R. D. Alessandro, Ramsier, G. G. Chase. “Continuous electrospinning of aligned polymer nanofibers onto a wire drum collector.” Nano Lett. 4 (2004) 2215 – 2218.

[76] R. Dersch, T. Liu, A. K. Schaper, A. Greiner, J. H. Wendorff. “Electrospun nanofibers: internal structure and intrinsic orientation.” J. Polym. Sci. A 41 (2003) 545-553.

[77] D. Li, Y. L. Wang, Y. N. Xia. “Elelctrospinning nanofibers as Uniaxially Aligned Arrays and Layer-by-layer Stacked Films.” Adv. Mater. 16 (2004) 361-366.

[78] B. Sundaray, V. Subramanian, T. S. Natarajan, R.-Z. Xiang, C.-C. Chang, W.-S. Fann. “Electrospinning of continuous aligned polymer fibers.” Appl. Phys. Lett. 84 (2004) 1222-1224.

[79] W. E. Teo, M. Kotaki, X. M. Mo, S. Ramakrishna. “Porous tubular structures with controlled fibre orientation using a modified electrospinning method.” Nanotechnology 16 (2005) 918-924.

[80] W. E. Teo, S. Ramakrishna. “Electrospun fibre bundle made of aligned nanofibres over two fixed points.” Nanotechnology 16 (2005) 1878.

[81] T. B. Bini, S. J. Gao, T. C. Tan, S. Wang, A. Lim, L. B. Hai, S. Ramakrishna. “Electrospun poly(L-lactide-co-glycolide) biodegradable polymer nanofibre tubes for peripheral nerve regeneration.” Nanotechnology 15 (2004) 1459-1464.

[82] T. A. Telemeco, C. Ayres, G. L. Bowlin, G. E. Wnek, E. D. Boland, N. Cohen, C. M. Baumgarten, J. Mathews, D. G. Simpson. “Regulation of cellular infiltration into tissue engineering scaffolds composed of submicron diameter fibrils produced by electrospinning.” Acta. Biomater. 1 (2005) 377 – 385.

[83] S. Kidoaki, K. Kwon, T. Matsuda. “Mesoscopic spatial designs of nano- and microfiber meshes for tissue- engineering matrix and scaffold based on newly devised multilayering and mix electrospinning techniques.” Biomaterials 26 (2005) 37.

[84] P. Katta, M. R. D. Alessandro, Ramsier, G. G. Chase. “Continuous electrospinning of aligned polymer nanofibers onto a wire drumcollector.” Nano Lett 4 (2004) 2215-2218

[85] N. Bhattarai, D. Edmondson, O. Veiseh, F. A. Matsen, M. Zhang. “Electrospun chitosan-based nanofibers and their cellular compatibility.” Biomaterials 26 (2005) 6176 – 6184.

[86] W. E. Teo, M. Kotaki, X. M. Mo, S Ramakrishna. “Porous tubular structures with controlled fibre orientation using a modified electrospinning method.” Nanotechnology 16 (2005) 918 – 924.

[87] W. E. Teo, S. Ramakrishna. “Electrospun fibre bundle made of aligned nanofibres over two fixed points.” Nanotechnology 16 (2005) 1878 – 1884.

[88] A. Theron, E. Zussman, A. L. Yarin. “Electrostatic field-assisted alignment of electrospun nanofibres.” Nanotechnology 12 (2001) 384 – 390.

[89] R. Inai, M. Kotaki, S. Ramakrishna. “Structure and properties of electrospun PLLA single nanofibres.” Nanotechnology 16 (2005) 208 – 213.

[90] C. Y. Xu, R. Inai, M. Kotaki, S. Ramakrishna. “Aligned biodegradable nanofibrous structure, a potential scaffold for blood vessel engineering.” Biomaterials 25 (2004) 877 – 886.

[91] B. Sundaray, V. Subramanian, T. S. Natarajan, R.-Z. Xiang, C.-C. Chang, W.-S. Fann. “Electrospinning of continuous aligned polymer fibers.” Appl. Phys. Lett. 84 (2004) 1222 – 1224.

[92] P. D. Dalton, D. Klee, M. Moller. “Electrospinning with dual rings.” Polym. Commun. 46 (2005) 611 – 614.

[93] E. D. Boland, J. A. Matthews, K. J. Pawlowski, D. G. Simpson, G. E. Wnek, G. L. Bowlin. “Electrospinning collagen and elastin: Preliminary vascular tissue engineering.” Front. Biosci. 9 (2004) 1422 - 1432.

[94] D. H. Reneker, A. L. Yarin, H. Fong, S. Koombhongse. “Bending instability of electrically charged liquid jets of polymer solutions in electrospinning.” J. Appl. Phys. 87 (2000) 4531 – 4547.

[95] H. Fong, I. Chun,D. H. Reneker. “Beaded nanofibers formed during electrospinning.” Polymer 40 (1999) 4585 – 4592.

[96] J. M. Deitzel, J. Kleinmeyer, D. Harris, N. C. Beck Tan. “The effect of processing variables on the morphology of electrospun nanofibers and textiles.” Polymer 42 (2001) 261 – 272.

[97] Y. M. Shin, M. M. Hohman, M. P. Brenner, G. C. Rutledge. “Experimental characterization of electrospinning: the electrically forced jet and instabilities.” Polymer 42 (2001) 9955 – 9967.

[98] S. A. Theron, E. Zussman, A. L. Yarin. “Experimental investigation of the governing parameters in the electrospinning of polymer solutions.” Polymer 45 (2004) 2017 – 2030.

[99] W. K. Son, J. H. Youk, T. Seung Lee, W. H. Park. “The effects of solution properties and polyelectrolyte on electrospinning of ultrafine poly(ethylene oxide) fibers.” Polymer 45 (2004) 2959 – 2966.

[100] R. Kessick, J. Fenn, G. Tepper. “The use of AC potentials in electrospraying and electrospinning processes.” Polymer 45 (2004) 2981 – 2984.

[101] P. Tsai, H. L. Schreuder-Gibson. “The Role of Fiber Charging on Co-electrospinning and Resilient Life of the Residual Charge from the Electrospinning Process.” Adv. Filtr. Sep. Technol. 16 (2003) 340 – 353.

[102] V. K. Daga, M. E. Helgeson, E. Matthew, N. J. Wagner. “Electrospinning of neat and laponite-filled aqueous poly(ethylene oxide) solutions.” J. Polym. Sci. B 44 (2006) 1608 – 1617.

[103] J. Doshi, D. H. Reneker. “Electrospinning Process And Applications of Electrospun Fibers.” J. Electrost. 35 (1995) 151 – 160.

[104] V. N. Morozov, T. Y. Morozova, N. R. Kallenbach. “Atomic force microscopy of structures produced by electrospraying polymer solutions.” Int. J. Mass Spectrom. 178 (1998) 143 – 159.

[105] J. M. Deitzel, J. Kleinmeyer, J. K. Hirvonen, N. C. Beck Tan. “Controlled deposition of electrospun poly(ethylene oxide) fibers.” Polymer 42 (2001) 8163 – 8170.

[106] A. Theron, E. Zussman, A. L. Yarin. “Electrostatic field-assisted alignment of electrospun nanofibres.” Nanotechnology 12 (2001) 384 – 390.

[107] S. Megelski, J. S. Stephans, C. D. Bruce, J. F. Rabolt. "Micro- and nanostructured surface morphology on electrospun polymer fibers." Macromolecules 35 (2002) 8456 – 8466.

[108] P. P. Tsai, H. Schreuder-Gibson, P. Gibson. “Different electrostatic methods for making electret filters.” J. Electrost. 54 (2002) 333 – 341.

[109] S.-H. Lee, J.-W. Yoon, M. H. Suh. “Continuous nanofibers manufactured by electrospinning technique.” Macromol. Res. 10 (2002) 282 – 285.

[110] A. Pedicini, R. J. Farris. “Thermally induced color change in electrospun fiber mats.” J. Polym. Sci. B 42 (2004) 752 – 757.

[111] N. Tomczak, N. F. van Hulst, G. J. Vancso. “Beaded electrospun fibers for photonic applications.” Macromolecules 38 (2005) 7863 – 7866.

[112] M. L. Bellan, J. Kameoka, H. G. Craighead. “Measurement of the Young's moduli of individual polyethylene oxide and glass nanofibers.” Nanotechnology 16 (2005) 1095 – 1099.

[113] S. A. Theron, E. Zussman, A. L. Yarin. “Experimental investigation of the governing parameters in the electrospinning of polymer solutions.” Polymer 45 (2004) 2017 – 2030.

[114] W. K. Son, J. H. Youk, T. S. Lee, W. H. Park. “Effect of pH on electrospinning of poly(vinyl alcohol).” Mater. Lett. 59 (2005) 1571 – 1575.

[115] A. Koski, K. Yim, S. Shivkumar. “Effect of molecular weight on fibrous PVA produced by electrospinning.” Mater. Lett. 58 (2004) 493 – 497.

[116] B. Ding, H.-Y. Kim, S.-C. Lee, D.-R. Lee, K.-J. Choi. “Preparation and characterization of nanoscaled poly(vinyl alcohol) fibers via electrospinning.” Fibers Polym. 3 (2002) 73 – 79.

[117] J. S. Lee, K. H. Choi, H. D. Ghim, S. S. Kim, D. H. Chun, H. Y. Kim, W. S. Lyoo. “Role of molecular weight of atactic poly(vinyl alcohol) (PVA) in the structure and properties of PVA nanofabric prepared by electrospinning.” J. Appl. Polym. Sci. 93 (2004) 1638 – 1646.

[118] C. Zhang, X. Yuan, L. Wu, Y. Han, J. Sheng. “Study on morphology of electrospun poly(vinyl alcohol) mats.” Eur. Polym. J. 41 (2005) 423 – 432.

[119] L. Yao, T. W. Haas, A. Guiseppi-Elie, G.W. L. Bowlin, D. G. Simpson, G. E. Wnek. “Electrospinning and stabilization of fully hydrolyzed poly(vinyl alcohol) fibers.” Chem. Mater. 15 (2003) 1860 – 1864.

[120] Y. H. Jung, H. Y. Kim, D. R. Lee, S.-Y. Park, M. S. Khil. “Characterization of PVOH nonwoven mats prepared from surfactant-polymer system via electrospinning.” Macromol. Res. 13 (2005) 385 – 390.

[121] J. Zeng, A. Aigner, F. Czubayko, T. Kissel, J. H. Wendorff, A. Greiner. “Poly(vinyl alcohol) nanofibers by electrospinning as a protein delivery system and the retardation of enzyme release by additional polymer coatings.” Biomacromolecules 6 (2005) 1484 – 1488.

[122] B. Ding, H.-Y. Kim, S.-C. Lee, C.-L. Shao, D.-R. Lee, S.-J. Park, G.-B. Kwag, K.-J. Choi. "Preparation and characterization of a nanoscale poly(vinyl alcohol) fiber aggregate produced by an electrospinning method." J. Polym. Sci. Part B 40 (2002) 1261 – 1268.

[123] N. Ristolainen, P. HeikkilT, A. Harlin, J. Seppala. "Poly(vinyl alcohol) and polyamide-66 nanocomposites prepared by electrospinning." Macromol. Mater. Eng. 291 (2006) 114 – 122.

[124] S. L. Shenoy, W. D. Bates, G. Wnek. "Correlations between electrospinnability and physical gelation." Polymer 46 (2005) 8990 – 9004.

[125] L. Li, Y.-L. Hsieh. "Ultra-fine polyelectrolyte fibers from electrospinning of poly(acrylic acid)." Polymer 46 (2005) 5133 – 5139.

[126] B. Kim, H. Park, S.-H. Lee, S. M. Sigmund. "Poly(acrylic acid) nanofibers by electrospinning." Mater. Lett. 59 (2005) 829 – 832.

[127] B. Ding, M. Yamazaki, S. Shiratori. "Electrospun fibrous polyacrylic acid membrane-based gas sensors." Sens. Actuators B 106 (2005) 477 – 483.

[128] J. Zeng, H. Hou, J. H. Wendorff, A. Greiner. "Electrospun poly(vinyl alcohol)/poly(acrylic acid) fibres with excellent water-stability." e-polymers 2004 No. 78.

[129] X. Jin, Y.-L. Hsieh. "pH-responsive swelling behavior of poly(vinyl alcohol)/poly(acrylic acid) bi-component fibrous hydrogel membranes." Polymer 46 (2005) 5149 – 5160.

[130] L. Li, Y.-L. Hsieh. "Ultra-fine polyelectrolyte hydrogel fibres from poly(acrylic acid)/poly(vinyl alcohol)." Nanotechnology 16 (2005) 2852 – 2860.

[131] X. Jin, Y.-L. Hsieh. "Anisotropic dimensional swelling of membranes of ultrafine hydrogel fibers." Macromol. Chem. Phys. 206 (2005) 1745 – 1751.

[132] B. Ding, J. Kim, K. Fujimoto, S. Shiratori. "Design, characterization, and optimization of waveguides based on chalcogenide classes for biosensors." Chem. Sens. 20 (2004) 264 – 265.

[133] B. Ding, J. Kim, Y. Miyazaki, S. Shiratori. "Electrospun nanofibrous membranes coated quartz crystal microbalance as gas sensor for NH_3 detection." Sens. Actuators B 101 (2004) 373 – 380.

[134] Q. Yang, Z. Li, Y. Hong, Y. Zhao, S. Qiu, C. Wang, Y. Wei. "Influence of solvents on the formation of ultrathin uniform poly(vinyl pyrrolidone) nanofibers with electrospinning." J. Polym. Sci. Part B 42 (2004) 3721 – 3726.

[135] M. Bognitzki, T. Frese, M. Steinhart, A. Greiner, J. H. Wendorff, A. Schaper, M. Hellwig. "Preparation of fibers with nanoscaled morphologies: Electrospinning of polymer blends."

Polym. Eng. Sci. 41 (2001) 982 – 989.

[136] D. Li, G. Ouyang, J. T. McCann, Y. Xia. "Collecting electrospun nanofibers with patterned electrodes." Nano Lett. 5 (2005) 913 – 916.

[137] D. Li, Y. Xia. "Fabrication of titania nanofibers by electrospinning." Nano Lett. 3 (2003) 555 – 560.

[138] D. Li, Y. Wang, Y. Xia. "Electrospinning of polymeric and ceramic nanofibers as uniaxially aligned arrays." Nano Lett. 3 (2003) 1167 – 1171.

[139] S.-W. Lee, A. M. Belcher. "Virus-based fabrication of micro- and nanofibers using electrospinning." Nano Lett. 4 (2004) 387 – 390.

[140] K. Sawicka, P. Gouma, S. Simon. "Electrospun biocomposite nanofibers for urea biosensing" Sens. Actuators B 108 (2005) 585 – 588.

[141] N. Jing, M. Wang, J. Kameoka. "Fabrication of ultrathin ZrO2 nanofibers by electrospinning." J. Photopolym. Sci. Technol. 18 (2005) 503 – 506.

[142] J. Watthanaarun, V. Pavarajarn, P. Supaphol. "Titanium (IV) oxide nanofibers by combined sol-gel and electrospinning techniques: preliminary report on effects of preparation conditions and secondary metal dopant." Sci. Technol. Adv. Mater. 6 (2005) 240 – 245.

[143] X. Lu, Y. Zhao, C. Wang, Y. Wei. "Fabrication of CdS nanorods in PVP fiber matrices by electrospinning." Macromol. Rapid Commun. 26 (2005) 1325 – 1329.

[144] S. Park, D. Y. Lee, M.-H. Lee, S.-J. Lee, B.-Y. Kim, J. Korean Ceram. Soc. 42 (2005) 548 – 553.

[145] J. Yuh, J. C. Nino, W. M. Sigmund. "Synthesis of barium titanate ($BaTiO_3$) nanofibers via electrospinning." Mater. Lett. 59 (2005) 3645 – 3647.

[146] A.-M. Azad, T. Matthews, J. Swary. "Processing and characterization of electrospun Y_2O_3-stabilized ZrO_2 (YSZ) and Gd_2O_3-doped CeO_2 (GDC) nanofibers." Mater. Sci. Eng. B 123 (2005) 252 – 258.

[147] A.-M. Azad. "Fabrication of yttria-stabilized zirconia nanofibers by electrospinning." Mater. Lett. 60 (2006)67 – 72.

[148] X. Lu, Y. Zhao, C. Wang. "Fabrication of PbS nanoparticles in polymer-fiber matrices by electrospinning." Adv. Mater. 17 (2005) 2485 – 2488.

[149] X. Lu, L. Li, W. Zhang, C. Wan. "Preparation and characterization of Ag2S nanoparticles

embedded in polymer fibre matrices by electrospinning." Nanotechnology 16 (2005) 2233 – 2237.

[150] W.-J. Jin, H. K. Lee, E. H. Jeong, W. H. Park, J. H. Youk. "Preparation of polymer nanofibers containing silver nanoparticles by using poly (N-vinylpyrrolidone)." Macromol. Rapid Commun. 26 (2005) 1903 – 1907.

[151] S. Maensiri, W. Nuansing, J. Klinkaewnarong, P. Laokul, J. Khemprasi. "Nanofibers of barium strontium titanate (BST) by sol-gel processing and electrospinning." J. Colloid Interface Sci. 297 (2006) 578 – 583.

[152] X. Lu, X. Liu, W. Zhang, C. Wang, Y. Wei. "Large-scale synthesis of tungsten oxide nanofibers by electrospinning." J. Colloid Interface Sci. 298(2006) 996 – 999.

[153] R. Ostermann, D. Li, Y. Yin, J. T. McCann, Y. Xia. "V_2O_5 nanorods on TiO_2 nanofibers: A new class of hierarchical nanostructures enabled by electrospinning and calcinations." Nano Lett. 6 (2006) 1297 – 1302.

[154] J. T. McCann, J. I. L. Chen, D. Li, Z.-G. Ye, Y. Xia. "Electrospinning of polycrystalline barium titanate nanofibers with controllable morphology and alignment." Chem. Phys. Lett. 424 (2006) 162 – 166.

[155] W. Nuansing, S. Ninmuang, W. Jarernboon, S. Maensiri, S. Seraphin. "Structural characterization and morphology of electrospun TiO_2 nanofibers." Mater. Sci. Eng. B 131 (2006) 147 – 155.

[156] H. Pan, L. Li, L. Hu, X. Cui. "Continuous aligned polymer fibers produced by a modified electrospinning method." Polymer 47 (2006) 4901 – 4904.

[157] D. Y. Lee, B.-Y. Kim, S.-J. Lee, M.-H. Lee, Y.-S. Song, J.-Y. Lee. "Titania nanofibers prepared by electrospinning." J. Korean Phys. Soc. 48 (2006) 1686 – 1690.

[158] E. Yan, Z. Huang, Y. Xin,Q. Zhao,W. Zhang. "Polyvinylpyrrolidone/tris(8-quinolinolato) aluminum hybrid polymer fibers by electrospinning." Mater. Lett. 60 (2006) 2969 – 2973.

[159] Y. Wang, Y. Li, S. Yang, G. Zhang, D. An, C. Wang, Q. Yang, X. Chen, X. Jing, Y. Wei. "A convenient route to polyvinyl pyrrolidone/silver nanocomposite by electrospinning." Nanotechnology 17 (2006) 3304 – 3307.

[160] Z.-G.Wang, J.-Q.Wang, Z.-K Xu. "Immobilization of lipase from Candida rugosa on electrospun polysulfone nanofibrous membranes by adsorption." J. Mol. Catal. B 42 (2006) 45 – 51.

[161] D. Li, Y. Xia. "Direct fabrication of composite and ceramic hollow nanofibers by electrospinning." Nano Lett. 4 (2004) 933 – 938.

[162] D. Li, A. Babel, S. A. Jehekhe, Y. Xia. “Nanofibers of conjugated polymers prepared by electrospinning with a two-capillary spinneret.” Adv. Mater. 16 (2004) 2062 – 2066.

[163] B. Sun, B. Duan, X. Yuan. “Preparation of core/shell PVP/PLA ultrafine fibers by coaxial electrospinning.” J. Appl. Polym. Sci. 102 (2006) 39 – 45.

[164] S. Koombhongse, W. Liu, D. H. Reneker. “Flat polymer ribbons and other shapes by electrospinning.” J. Polym. Sci. B 39 (2001) 2598 – 2606.

[165] T. Jarusuwannapoom, W. Hongrojjanawiwat, S. Jitjaicham, L. Wannatong, M. Nithitanakul, C. Pattamaprom, P. Koombhongse, R. Rankupan, P. Supaphol. “Effect of solvents on electro-spinnability of polystyrene solutions and morphological appearance of resulting electrospun polystyrene fibers.” Eur. Polym. J. 41 (2005) 409 – 421.

[166] H. Jia, G. Zhu, B. Vugrinovich,W. Kataphinan, D. H. Reneker, P. Wang. “Enzyme-carrying polymeric nanofibers prepared via electrospinning for use as unique biocatalysts.” Biotechnol. Prog. 18 (2002) 1027 – 1032.

[167] S. Megelski, J. S. Stephans, C. D. Bruce, J. F. Rabolt. "Micro- and nanostructured surface morphology on electrospun polymer fibers." Macromolecules 35 (2002) 8456 – 8466.

[168] J. S. Stephens, S. Frisk, S. Megelski, J. F. Rabolt, D. B. Chase. “ ‘Real time’ Raman studies of electrospun fibers” Appl. Spectrosc. 55 (2001) 1287 – 1290.

[169] T. Lin, H. Wang, H. Wang, X. Wang. “The charge effect of cationic surfactants on the elimination of fibre beads in the electrospinning of polystyrene.” Nanotechnology 15 (2004) 1375 – 1381.

[170] G.-T. Kim, Y.-J. Hwang, Y.-C. Ahn, H.-S. Shin, J.-K. Lee, C.-M. Sung. “The morphology of electrospun polystyrene fibers.” Korean J. Chem. Eng. 22 (2005) 147 – 153.

[171] C. Shin, G. G. Chase, D. H. Reneker. “Recycled expanded polystyrene nanofibers applied in filter media.” Coll. Surf. A Physicochem. Eng. Aspects 262 (2005) 211 – 215.

[172] K. Kim, M. Kang, I.-J. Chin, H.-J. Jin. “Unique surface morphology of electrospun polystyrene fibers from a N,N-dimethylformamide solution.” Macromol. Res. 13 (2005) 533 – 537.

[173] S. C. Baker, N. Atkin, P. A. Gunning, N. Granville, K. Wilson, D. Wilson, J. Southgate. “Characterization of electrospun polystyrene scaffolds for three-dimensional in vitro biological studies.” Biomaterials 27 (2006) 3136 – 3146.

[174] S. Y. Gu, J. Ren, G. J. Vancso. “Process optimization and empirical modeling for electrospun polyacrylonitrile (PAN) nanofiber precursor of carbon nanofibers.” Eur. Polym. J. 41 (2005) 2559 – 2568.

[175] Q.-B. Yang, C. Wang, Y.-L. Hong, Z.-Y. Li, Y.-Y. Zhao, S.-L. Qiu, Y. Wei. "Refining of Polyacrylonitrile Nanofiber." Gaodeng Xuexiao Huaxue Xuebao 25 (2004) 589 – 591.

[176] T. Wang, S. Kumar. "Electrospinning of polyacrylonitrile nanofibers." J. Appl. Polym. Sci. 102 (2006) 1023 – 1029.

[177] P. K. Baumgarten. "Electrostatic spinning of acrylic microfibers." J. Colloid Interface Sci. 36 (1971) 71 – 79.

[178] I. Chun, D. H. Reneker, X. Fang, H. Fong, J. Deitzel, N. Beck, K. Kearns. "Carbon Nanofibers From Polyacrylonitrile And Mesophase Pitch." Int. SAMPE Symp. Exhib. 43 (1998) 718 – 729.

[179] A. G. MacDiarmid, W. E. Jones, I. D. Norris, J. Gao, A. T. Johnson, N. J. Pinto, J. Hone, B. Han, F. K. Ko, H. Okuzaki, M. Llaguno. "Electrostatically-generated nanofibers of electronic polymers." Synth. Met. 119 (2001) 27 – 30.

[180] H. L. Schreuder-Gibson, P. Gibson, P. Tsai, P. Gupta, G.Wilkes. "Cooperative Charging Effects of Fibers from Electrospinning of Electrically Dissimilar Polymers." Int. Nonwovens J. 13 (2004) 39 – 45.

[181] C. Kim, K.-S. Yang, W.-J. Lee. "The Use of Carbon Nanofiber Electrodes Prepared by Electrospinning for Electrochemical Supercapacitors." Electrochem. Solid-State Lett. 7 (2004) A397 – A399.

[182] S.-Y. Gu, Q.-L. Wu, J. Ren, G. J. Vancso. "Mechanical properties of a single electrospun fiber and its structures." Macromol. Rapid Commun. 26 (2005) 716 – 720.

[183] Q. B. Yang, D. M. Li, Y. L. Hong, Z. Y. Li, C. Wang, S. L. Qiu, Y. Wei. "Preparation and characterization of a pan nanofibre containing Ag nanoparticles via electrospinning." Synth. Met. 137 (2003) 973 – 974.

[184] P. P. Tsai, W. Chen, J. R. Roth. "Investigation of the Fiber, Bulk, and Surface Properties of Meltblown and Electrospun Polymeric Fabrics." Int. Nonwovens J. 13 (2004) 17 – 23.

[185] S.-Y. Gu, J. Ren, Q. L. Wu. "Preparation and structures of electrospun PAN nanofibers as a precursor of carbon nanofibers." Synth. Met. 155 (2005) 157 – 161.

[186] J. McCann, M. Marquez, Y. Xia. "Highly porous fibers by electrospinning into a cryogenic liquid" J. Am. Chem. Soc. 128 (2006) 1436 – 1437.

[187] H. Liu, Y.-L. Hsieh. "Preparation of water-absorbing poly acrylonitrile nanofibrous membrane." Macromol. Rapid Commun. 27 (2006) 142 – 145.

[188] P. P. Tsai, H. Schreuder-Gibson, P. Gibson. “Different electrostatic methods for making electret filters.” J. Electrost. 54 (2002) 333 – 341.

[189] R. V. N. Krishnappa, K. Desai, C. Sung. “Morphological study of electrospun polycarbonates as a function of the solvent and processing voltage.” J. Mater. Sci. 38 (2003) 2357 – 2365.

[190] S. Koombhongse, W. Liu, D. H. Reneker. “Flat polymer ribbons and other shapes by electrospinning.” J. Polym. Sci. B 39 (2001) 2598 – 2606.

[191] C. Nah, S. H. Han, M.-H. Lee, J. S. Kim, D. S. Lee, Polym. Int. 52 (2003) 429 – 432.

[192] C. Huang, S. Wang, H. Zhang, T. Li, S. Chen, C. Lai, H. Hou, Eur. Polym. J. 42 (2006) 1099 – 1104.

[193] J.-S. Kim, D. H. Reneker. “Mechanical properties of composites using ultrafine electrospun fibers.” Polym. Compos. 20 (1999) 124 – 131.

[194] H. L. Schreuder-Gibson, P. Gibson, K. Senecal, M. Sennett, J. Walker, W. Yeomans, D. Ziegler, P. P. Tsai. “Protective textile materials based on electrospun nanofibers.” J. Adv. Mater. 34 (2002) 44 – 55.

[195] D. H. Reneker, I. Chun. “Nanometre diameter fibres of polymer, produced by electrospinning.” Nanotechnology 7 (1996) 216 – 223.

[196] K. H. Hong, T. J. Kang. “Hydraulic permeabilities of PET and nylon 6 electrospun fiber webs.” J. Appl. Polym. Sci. 100 (2006) 167 – 177.

[197] K.W. Kim, K. H. Lee, B. S. Lee, Y. S. Ho, S. J. Oh, H. Y. Kim. “Effects of blend ratio and heat treatment on the properties of the electrospun poly(ethylene terephthlate) nonwovens.” Fibers Polym. 6 (2005) 121 – 126.

[198] Z. Ma, M. Kotaki, T. Yong, W. He, S. Ramakrishna. “Surface engineering of electrospun polyethylene terephthalate (PET) nanofibers towards development of a new material for blood vessel engineering.” Biomaterials 26 (2005) 2527 – 2536.

[199] M. S. Khil, H. Y. Kim, M. S. Kim, S. Y. Park, D.-R. Lee. “Nanofibrous mats of poly(trimethylene terephthalate) via electrospinning.” Polymer 45 (2004) 295 – 301.

[200] S. Kidoaki, I. K. Kwon, T. Matsuda. “Structural features and mechanical properties of in situ-bonded meshes of segmented polyurethane electrospun from mixed solvents.” J. Biomed. Mater. Res. B 76 (2006) 219 – 229.

[201] P. P. Tsai, H. Schreuder-Gibson, P. Gibson. “Different electrostatic methods for making electret

filters.” J. Electrost. 54 (2002) 333 – 341.

[202] S. A. Riboldi, M. Sampaolesi, P. Neuenschwander, G. Cossu, S. Mantero. “Electrospun degradable polyesterurethane membranes: potential scaffolds for skeletal muscle tissue engineering.” Biomaterials 26 (2005) 4606 – 4615.

[203] J. J. Stankus, J. Guan, K. Fujimoto, W. R. Wagner. “Microintegrating smooth muscle cells into a biodegradable, elastomeric fiber matrix.” Biomaterials 27 (2006) 735 – 744.

[204] H. L. Schreuder-Gibson, P. Gibson, K. Senecal, M. Sennett, J. Walker, W. Yeomans, D. Ziegler, P. P. Tsai. “Protective textile materials based on electrospun nanofibers.” J. Adv. Mater. 34 (2002) 44 – 55.

[205] M. M. Demir, I. Yilgor, B. Erman. “Electrospinning of polyurethane fibers.” Polymer 43 (2002) 3303 – 3309.

[206] M.-S. Khil, D.-I. Cha, H.-Y. Kim, I.-S. Kim, N. Bhattarai. “Electrospun nanofibrous polyurethane membrane as wound dressing.” J. Biomed. Mater. Res. B 67 (2003) 675 – 679.

[207] G. M. McKee, T. Park, S. Unal, I. Yilgor, T. E. Long. “Electrospinning of linear and highly branched segmented poly(urethane urea)s.” Polymer 46 (2005) 2011 – 2015.

[208] D. I. Cha, H. Y. Kim, K. H. Lee, Y. C. Jung, J. W. Cho, B. C. Byung. “Electrospun nonwovens of shape-memory polyurethane block copolymers.” J. Appl. Polym. Sci. 96 (2005) 460 – 465.

[209] T. Matsuda, M. Ihara, H. Inoguchi, I. K. Kwon, K. Takamizawa, K. Keiichi, S. Kidoaki. “Mechano-active scaffold design of small-diameter artificial graft made of electrospun segmented polyurethane fabrics.” J. Biomed. Mater. Res. A 73 (2005) 125 – 131.

[210] K. Lee, B. Lee, C. Kim, H. Kim, K. Kim, C. Nah. “Stress-strain behavior of the electrospun thermoplastic polyurethane elastomer fiber mats.” Macromol. Res. 13 (2005) 441 – 445.

[211] S. B. Mitchell, S. B. Sanders. “A unique device for controlled electrospinning.” J. Biomed. Mater. Res. A 78 (2006) 110 – 120.

[212] S. Thandavamoorthy, N. Gopinath, S. S. Ramakumar. “Self-assembled honeycomb polyurethane nanofibers.” J. Appl. Polym. Sci. 101 (2006) 3121 – 3124.

[213] K. H. Lee, H. Y. Kim, Y. M. La, D. R. Lee, N. H. Sung. “Influence of a mixing solvent with tetrahydrofuran and N,N-dimethylformamide on electrospun poly(vinyl chloride) nonwoven mats.” J. Polym. Sci. B 40 (2002) 2259 – 2268.

[214] R. Ramaseshan, S. Sundarrajan, Y. Liu, R. S. Barhate, N. L. Lala, S. Ramakrishna.

"Functionalized polymer nanofibre membranes for protection from chemical warfare stimulants." Nanotechnology 17 (2006) 2947 – 2953.

[215] S. Megelski, J. S. Stephans, C. D. Bruce, J. F. Rabolt. "Micro- and nanostructured surface morphology on electrospun polymer fibers." Macromolecules 35 (2002) 8456 – 8466.

[216] J. M. Deitzel, W. Kosik, S. H. McKnight, N. C. Beck Tan, J. M. Desimone, S. Crette. "Electrospinning of polymer nanofibers with specific surface chemistry." Polymer 43 (2002) 1025 – 1029.

[217] E. Zussman, A. L. Yarin, A. V. Bazilevsky, R. Avrahami, M. Feldman. "Electrospun polyacrylonitrile/poly (methyl methacrylate)-derived turbostratic carbon micro-/nanotubes." Adv. Mater. 18 (2006) 348 – 353.

[218] M. Bognitzki, M. Becker, M. Graeser, W. Massa, J. H. Wendorff, A. Schaper, D. Weber, A. Beyer, A. GSlzhTuser, A. Greiner. "Preparation of sub-micrometer copper fibers via electrospinning." Adv. Mater. 18 (2006) 2384 – 2386.

[219] S. Koombhongse, W. Liu, D. H. Reneker. "Flat polymer ribbons and other shapes by electrospinning." J. Polym. Sci. B 39 (2001) 2598 – 2606.

[220] P. D. Dalton, K. Klinkhammer, J. Salber, D. Klee, M. MSller. "Direct in vitro electrospinning with polymer melts." Biomacromolecules 7 (2006) 686 – 690.

[221] L. Larrondo, R. St. John Manley. "Electrostatic Fiber Spinning From Polymer Melts. 1. Experimental-Observations on Fiber Formation and Properties." J. Polym. Sci. Polym. Phys. Ed. 19 (1981) 909 – 920.

[222] L. Larrondo, R. St. John Manley. "Electrostatic Fiber Spinning From Polymer Melts. 3. Electrostatic Deformation of a Pendent Drop of Polymer Melt." J. Polym. Sci. Polym. Phys. Ed. 19 (1981) 933 – 940.

[223] J. Lyons, C. Li, F. Ko. "Melt-electrospinning part I: processing parameters and geometric properties." Polymer 45 (2004) 7597 – 7603.

[224] R. Rangkupan, D. H. Reneker. "Electrospinning process of molten polypropylene in vacuum." J. Met. Mater. Miner. 12 (2003) 81 – 87.

[225] S. Lee, S. K. Obendorf. "Developing protective textile materials as barriers to liquid penetration using melt-electrospinning." J. Appl. Polym. Sci. 102 (2006) 3430 – 3437.

[226] L. Larrondo, R. St. John Manley. "Electrostatic Fiber Spinning from Polymer Melts. 2. Examination of the Flow Field in an Electrically Dirven Jet." J. Polym. Sci. Polym. Phys. Ed. 19

(1981) 921 – 932.

[227] J.-S. Kim, D.-S. Lee. “Thermal properties of electrospun polyesters” Polym. J. 32 (2000) 616 – 618.

[228] D. Li, Y. N. Xia, “Fabrication of Titania Nanofibers by Electrospinning.” Nano lett. 3 (2003) 555 – 560.

[229] S.-S. Choi, S. G. Lee, S. S. Im, S. H. Kim, Y. L. Joo. “Silica nanofibers from electrospinning/sol-gel process.” J. Mater. Sci. Lett. 22 (2003) 891 – 893.

[230] J.-B. Ko, S.W. Lee, D. E. Kim, Y. U. Kim, G. Li, S. G. Lee, T.-S. Chang, D. Kim, Y. L. Joo. “Fabrication of SiO_2-ZrO_2 composite fiber mats via electrospinning” J. Porous Mater. 13 (2006) 325 – 330.

[231] G. Larsen, R. Velarde-Ortiz, K. Minchow, A. Barrero, I. G. Loscertales. “A method for making inorganic and hybrid (organic/inorganic) fibers and vesicles with diameters in the submicrometer and micrometer range via sol-gel chemistry and electrically forced liquid jets.” J. Am. Chem. Soc. 125 (2003) 1154 – 1155.

[232] M. Bognitzki, M. Becker, M. Graeser, Werner Massa, Joachim H. Wendorff, Andreas Schaper, Dirk Weber, Andre Beyer, Armin Gölzhäuser, and Andreas Greiner. “Preparation of Sub-micrometer Copper Fibers via Electrospinning.” Adv. Mater. 18 (2006) 2384 – 2386.

[233] W. R. Grove. "On a new voltaic combination". Philosophical Magazine and Journal of Science 13 (1838) 430.

[234] L. Mond, C. Langer. “Proceedings of the Royal Society of London.” 46 (1889) 296 - 304.

[235] F. T. Bacon. “The High Pressure Hydrogen-Oxygen Fuel Cell.” Ind. Eng. Chem. 52 (1960) 301-303.

[236] F. T. Bacon. “Fuel-Cell - Some Thoughts and Recollections.” J. Electrochem. Soc. 126 (1979) C7-C16.

[237] S. Banerjee. “Nafion perfluorinated membranes in fuel cells.” Abstracts of Papers of the American Chemical Society 226 (2003) U524-U524.

[238] S. Banerjee, D. E. Curtin. “Nafion perfluorinated membranes in fuel cells.” J. Fluorine Chem. 125 (2004) 1211-1216.

[239] L. Carrette, K. A. Friedrich, U. Stimming. “Fuel Cells-Fundamentals and Applications.” Fuel Cells 1 (2001) 5-39.

[240] DaimlerChryler at http://www.chrysler.com
Toyota at http://www.toyota.com
General Motors at http://www.gm.com/environment/products/technologies.html.

[241] B. C. H. Steele, A. Heinzel. "Materials for fuel-cell technologies." Nature 414 (2001) 345 – 352;

[242] S. M. Haile, D. A. Boysen, C.R. I. Chisholm, R. B. Merle. "Solid acids as fuel cell electrolytes." Nature 410 (2001) 910 – 913;

[243] D. W. Keith, A. E. Farrell. "Rethinking hydrogen cars." Science 301 (2003) 315 – 316;

[244] M. Z. Jacobson, W. G. Colella, D. M. Golden. "the Air and Improving Health with Hydrogen Fuel-Cell Vehicles." Science 308 (2005) 1901 – 1905;

[245] M. Lefèvre, E. Proietti, F. Jaouen, J.-P. Dodelet. "Iron-Based Catalysts with Improved Oxygen Reduction Activity in Polymer Electrolyte Fuel Cells." Science 324 (2009) 71 - 74.

[246] http://americanhistory.si.edu/fuelcells/pem/pemmain.htm.

[247] S. Gottesfeld and T. Zawodzinski. "Advances in Electrochemical Science and Engineering." (R. C. Alkire, H. Gerischer, D. M. Kolb, C. W. Tobias, Eds. Wiley-VCH: Weinheim, New York, 1997 Vol. 5).

[248] O. Teschke. "Effect of PTFE Coverage on the Performance of Gas Evolving Electrodes." J. Electrochem. Soc. 131 (1983) 1095 – 1097.

[249] Z. Poltarzewski, P. Staiti, V. Alderucci, W. Wieczorek, N. Giordano. "Nafion Distribution in Gas-Diffusion Electrodes for Solid-Polymer-Electrolyte-Fuel-Cell Applications." J. Electrochem. Soc. 139 (1992) 761 – 765.

[250] S. J. Lee, S. Mukerjee, J. McBreen, Y. W. Rho, Y. T. Kho, T. H. Lee. "Effects of Nafion impregnation on performances of PEMFC electrodes." Electrochim. Acta 43 (1998) 3693 – 3701.

[251] http://education.lanl.gov/resourcesh2-gottesfeldeducation.html.

[252] M. Wilson, F. Garzon, K. Sickafus, S. Gottesfeld. "Surface-Area Loss of Supported Platinum in Polymer Electrolyte Fuel-Cells." J. Electrochem. Soc. 140 (1993) 2872 – 2877.

[253] S. Gottesfeld, J. Pafford. "A New Approach to the Problem of Carbon-Monoxide Poisoning in Fuel-Cells Operating at Low-Temperatures." J. Electrochem. Soc. 135 (1988) 2651 – 2652.

[254] K. Kolbrecka, J. Przyluski. "Sub-Stoichiometric Titanium-Oxides as Ceramic Electrodes for

Oxygen Evolution-Structural Aspects of the Voltammetric Behavior of Ti_nO_{2n-1}." Electrochim. Acta 39 (1994) 1591 – 1595.

[255] H.-F. Oetjen, V. M. Schmidt, U. Stimming, F. Trila. "Performance data of a proton exchange membrane fuel cell using H_2/CO as fuel gas." J. Electrochem. Soc. 143 (1996) 3838 – 3842.

[256] J. , H.-F. Oetjen, V. Peinecke, V. M. Schmidt, U. Stimming. "Components for PEM fuel cell systems using hydrogen and CO containing fuels" Electrochim. Acta 43 (1998) 3811 – 3815.

[257] R. J. Bellows, E. Marucchi-Soos, R. P. Reynolds. "The mechanism of CO mitigation in proton exchange membrane fuel cells using dilute H_2O_2 in the anode humidifier" Electrochem. Solid-State Lett. 1 (1998) 69 – 70.

[258] L. Carrette, K. A. Friedrich, M. Huber, U. Stimming. "Improvement of CO tolerance of proton exchange membrane (PEM) fuel cells by a pulsing technique." Phys. Chem. Chem. Phys. 3 (2001) 320 – 324.

[259] W. Chrzanowski, A. Wieckowski. "Surface structure effects in platinum/ruthenium methanol oxidation electrocatalysis." Langmuir 14 (1998) 1967 – 1970.

[260] H. A. Gasteiger, N. Markovic, P. N. J. Ross, E. J. Cairns. "CO Electrooxidation on Well-Characterized Pt-Ru Alloys." J. Phys. Chem. 98 (1994) 617 – 625.

[261] H. A. Gasteiger, N. Markovic, P. N. J. Ross, E. J. Cairns. "Electrooxidation of Small Organic-Molecules on Well-Characterized Pt-Ru Alloys." Electrochim. Acta 39 (1994) 1825 – 1832.

[262] A. V. Petukhov, W. Akemann, K. A. Friedrich, U. Stimming. "Kinetics of electrooxidation of a CO monolayer at the platinum/electrolyte interface." Surf. Sci. 402 (1998) 182 – 186.

[263] K. A. Friedrich, K.-G. Geyzers, U. Linke, U. Stimming, J. Stumper. "CO adsorption and oxidation on a Pt(111) electrode modified by ruthenium deposition: An IR spectroscopic study." J. Electroanal. Chem. 402 (1996) 123 – 128.

[264] G. Holleck, D. Pasquariello, S. Clauson. "Carbon monoxide tolerant anodes for proton exchange membrane (PEM) fuel cells. II. Alloy catalyst development." Second International Symposium on Proton Conducting Membrane Fuel Cells II (1999) 150 – 155.

[265] M. Wakizoe, O. A. Velev, S. Srinivasan. "Analysis of Proton-Exchange Membrane Fuel-Cell Performance with Alternate Membranes." Electrochim. Acta 40 (1995) 335 – 344.

[266] H. L. Yeager, A. Steck. "Cation and Water Diffusion in Nafion Ion-Exchange Membranes - Influence of Polymer Structure." J. Electrochem. Soc. 128 (1981) 1880 – 1884.

[267] K. Kordesch, G. Simader. (“Fuel Cells and Their Applications.” 1 ed. VCH Verlagsgesellschaft mbH: Weinheim, Germany, 1996).

[268] M. Cappadonia, J. W. Erning, S. M. Saberi Niaki, U. Stimming. “Conductance of Nafion-117 Membranes as a Function of Temperature and Water-Content.” Solid State Ionics 77 (1995) 65 – 69.

[269] T. D. Gierke, G. E. Munn, F. C. Wilson. “The Morphology in Nafion Perfluorinated Membranes Products, as Determined by Wide-angle and Small-angle X-ray Studies.” J. Polym. Sci. Polym. Phys. 19 (1981) 1687 – 1704.

[270] M. S. Wilson, C. Zawodzinski, S. Gottesfeld. “Direct Liquid Water Hydration of Fuel Cell Membranes.” Second International Symposium on Proton Conducting Membrane Fuel Cells II (1998) 424 – 434.

[271] M. Watanabe, H. Uchida, Y. Seki, M. Emori. “Self-humidifying polymer electrolyte membranes for fuel cells.” J. Electrochem. Soc. 143 (1996) 3847 – 3852.

[272] M. Watanabe, Y. Satoh and C. Shimura, 183rd Meeting of the Electrochemical Society, Symposium on Batteries and Fuel Cells for Stationary and Electric Vehicle Applications, Honolulu, Hawaii, US, 1993; 302.

[273] M. Rikukawa, K. Sanui. “Proton-conducting polymer electrolyte membranes based on hydrocarbon polymers.” Prog. Polym. Sci. 25 (2000) 1463 – 1502;

[274] L. J. M. J. Blomen, M. N. Mugerwa. (“Fuel cell systems.” New York: Plenum Press, 1993) 493.

[275] M. Higuchi, N. Minoura, T. Kinoshita. “Photocontrol of Micellar Structure of an Azobenzene Containing Amphiphilic Sequential Polypeptide.” Chem. Lett. 23 (1994) 227 - 230.

[276] B. Gupta, F. N. Buchi, G. G. Scherer. “Materials research aspects of organic solid proton conductors.” Solid State Ionics 61 (1993) 213 - 218.

[277] S. D. Flint, R. C. T. Slade. “Investigation of radiation-grafted PVDF-g-polystyrene-sulfonic-acid ion exchange membranes for use in hydrogen oxygen fuel cells.” Solid State Ionics 97 (1997) 299 - 307.

[278] J. L. Bredas, R. R. Chance, R. Silbey. “Comparative theoretical study of the doping of conjugated polymers: Polarons in polyacetylene and polyparaphenylene.” Phys. Rev. B 26 (1982) 5843 - 5854.

[279] H. Kobayashi, H. Tomita, H. Moriyama. “New Metallic C60 Compound: $Na_xC_{60}(THF)_y$.” J. Am. Chem. Soc. 116 (1994) 3153- 3154.

[280] F. Wang, J. Roovers. “Functionalization of poly(aryl ether ether ketone) (PEEK): synthesis and properties of aldehyde and carboxylic acid substituted PEEK.” Macromolecules 26 (1993) 5295 - 5302.

[281] C. Bailly, D. J. Williams, F. E. Karasz, W. J. Macknight. “The sodium salts of sulphonated poly(aryl-ether-ether-ketone) (PEEK): Preparation and characterization.” Polymer 28 (1987) 1009 - 1016.

[282] Z. Qi, P. G. Pickup. “Novel supported catalysts: platinum and platinum oxide nanoparticles dispersed on polypyrrole/polystyrenesulfonate particles.” Chem. Commun. 1 (1998) 15 - 16.

[283] T. I. Wallow, B. M. Novak. “In aqua synthesis of water-soluble poly(p-phenylene) derivatives.” J. Am. Chem. Soc. 113 (1991) 7411 - 7412.

[284] A. D. Child, J. R. Reynolds. “Water-Soluble Rigid-Rod Polyelectrolytes: A New Self-Doped, Electroactive Sulfonatoalkoxy-Substituted Poly(p-phenylene).” Macromolecules 27 (1994) 1975 - 1977.

[285] T. Kobayashi, M. Rikukawa, K. Sanui, N. Ogata. “Proton-conducting polymers derived from poly(ether-etherketone) and poly(4-phenoxybenzoyl-1 4-phenylene).” Solid State Ionics 106 (1998) 219 - 225.

[286] A. J. Chalk, A. S. Hay. “Direct metalation of poly(2 6-dimethyl-1 4-phenylene ether).” J. Polym. Sci. A 7 (1969) 691 - 705.

[287] Z. Qi, M. C. Lefebvre, P. G. Pickup. “Electron and proton transport in gas diffusion electrodes containing electronically conductive proton-exchange polymers.” J. Electroanal. Chem. 459 (1998) 9 - 14.

[288] X. Glipa, M. E Haddad, D. J. Jones, J. Rozière. “Synthesis and characterisation of sulfonated polybenzimidazole: a highly conducting proton exchange polymer.” Solid State Ionics 97 (1997) 323 - 331.

[289] J. Fang, X. Guo, S. Harada, T. Watari, K. Tanaka, H Kita, K. I. Okamoto. “Novel Sulfonated Polyimides as Polyelectrolytes for Fuel Cell Application. 1. Synthesis, Proton Conductivity, and Water Stability of Polyimides from 4 4‘-Diaminodiphenyl Ether-2 2‘-disulfonic Acid.” Macromolecules 35 (2002) 9022 - 9028.

[290] X. L. Wei, Y. Z. Wang, S. M. Long, C. Bobeczko, A. J. Epstein. “Synthesis and Physical Properties of Highly Sulfonated Polyaniline.” J. Am Chem. Soc. 118 (1996) 2545 - 2555.

[291] K. Miyatake, E. Shouji, K. Yamamoto, E. Tsuchida. “Synthesis and Proton Conductivity of Highly Sulfonated Poly(thiophenylene).” Macromolecules 30 (1997) 2941 - 2946.

[292] K. Miyatake, H. Iyotani, K. Yamamoto, E. Tsuchida. “Synthesis of Poly(phenylene sulfide sulfonic acid) via Poly(sulfonium cation) as a Thermostable Proton-Conducting Polymer.” Macromolecules 29 (1996) 6969 - 6971.

[293] X Jin, M. T. Bishop, T. S. Ellis, F. E. Karasz. “A sulphonated poly(aryl ether ketone).” Br. Polym. J. 17 (1985) 4 - 10.

[294] J. Lee, C. S. Marvel. “Polyaromatic ether-ketone sulfonamides prepared from polydiphenyl ether-ketones by chlorosulfonation and treatment with secondary amines.” J. Polym. Sci. Polym. Chem. Ed. 22 (1984) 295 - 301.

[295] A. Noshay, L. M. Robeson. “Sulfonated polysulfone.” J. Appl. Polym. Sci. 20 (1976) 1885 - 1903.

[296] M. I. Litter, C. S. Marvel. “Polyaromatic ether-ketones and polyaromatic ether-ketone sulfonamides from 4-phenoxybenzoyl chloride and from 4 4’-dichloroformyldiphenyl ether.” J. Polym. Sci. Polym. Chem. Ed. 23 (1985) 2205 - 2223.

[297] H. Makowsky, R. D. Lundberg, G. H. Singahl. “Flexible polymeric compositions comprising a normally plastic polymer sulfonated to about 0.2 to about 10 mole % sulfonate.” US Patent. US3870841 1975.

[298] J. S. Wainright, J. –T. Wang, R. F. Savinell, M. Litt, H. Moaddel, C. Rogers. “Electrode Materials and Processes for Energy Conversion and Storage.” Proc. Electrochem. Soc. (1994) 255 – 264.

[299] J. S. Wainright, M. H. Litt, R. F. Savinell, (W. Vielstich, A. Lamm, H. Gasteiger. (eds) “Handbook of fuel cells: fundamentals, technology and applications.” 2003 vol 3. Wiley, Chichester). 436.

[300] X. Glipa, B. Mula, D. J. Jones, J. Rozière, (C. A. C. Sequeira, J. Moffat (eds) “Chemistry, energy and the environment. Royal Society of Chemistry.” 1998 Cambridge, UK). 249.

[301] X. Glipa, B. Bonnet, B. Mula, D. J. Jones, J. Rozière. “Investigation of the conduction properties of phosphoric and sulfuric acid doped polybenzimidazole.” J. Mater .Chem. 9 (1999) 3045 – 3049.

[302] L. Xiao, H. Zhang, T. Jana, E. Scanlon, R. Chen, E. –W. Choe, L. S. Ramanathan, S. Yu, B. C. Benicewicz. “Synthesis and characterization of pyridine-based polybenzimidazoles for high temperature polymer electrolyte membrane fuel cell applications.” Fuel Cells 5 (2005) 287 – 295.

[303] T.D. Gierke, W.Y. Hsu. (A. Eisenberg, H. L. Yeager. (Eds.) “Perfluorinated Ionomer Membranes.” ACS Symposium Series No. 180 American Chemical Society, Washington, DC, 1982). 283.

[304] M. Eikerling, A. A. Kornyshev, U. Stimming. “Electrophysical properties of polymer electrolyte membranes: A random network model.” J. Phys. Chem. B 101 (1997) 10807 – 10820.

[305] H.G. Haubold, T. Vad, H. Jungbluth, P. Hiller. "Nano structure of Nafion: a SAXS study." Electrochim. Acta 46 (2001) 1559 – 1563.

[306] P.J. James, T.J. McMaster, J.M. Newton, M.J. Miles. "In situ rehydration of perfluorosulfonate ion-exchange membrane studied by AFM." Polymer 41 (2000) 4223 – 4231.

[307] Y. Lu, Y. Yang, A. Sellinger, M. Lu, J. Huang, H. Fan, R. Haddad, G. Lopez, A. R. Burns, D. Y. Sasaki, J. Shelnutt, C. J. Brinker. "Self-assembly of mesoscopically ordered chromatic polydiacetylene/silica nanocomposites." Nature 410 (2001) 913 – 917.

[308] O. Savadogo. "Emerging membranes for electrochemical systems - Part II. High temperature composite membranes for polymer electrolyte fuel cell (PEFC) applications." J. Power Sources 127 (2004) 135 – 161.

[309] R. K. Nagarale, W. Shina, P. K. Singh. "Progress in ionic organic-inorganic composite membranes for fuel cell applications." Polym. Chem. 1 (2010) 388–408.

[310] L. L. Hench, J. K. West. "The Sol-gel Process." Chem. Rev. 90 (1990) 33 - 72.

[311] R. V. Gummaraju, R. B. Moore, K. A. Mauritz. "Asymmetric [Nafion®]/[silicon oxide] hybrid membranes via the in situ sol-gel reaction for tetraethoxysilane." J. Polym. Sci. B 34 (1996) 2383 - 2392.

[312] W. Apichatachutapan, R. B. Moore, K. A. Mauritz. "Asymmetric nafion/(zirconium oxide) hybrid membranes via in situ sol-gel chemistry." J. Appl. Polym. Sci. 62 (1996) 417 - 426.

[313] K. A. Mauritz. "Organic-inorganic hybrid materials: perfluorinated ionomers as sol-gel polymerization templates for inorganic alkoxides." Mater. Sci. Eng. C 6 (1998) 121 - 133.

[314] L. C. Klein, Y. Daiko, M. Aparicio, F. Damay. "Methods for modifying proton exchange membranes using the sol-gel process." Polymer 46 (2005) 4504 - 4509.

[315] W. F. Chen, P. L. Kuo. "Covalently cross-linked perfluorosulfonated membranes with polysiloxane framework." Macromolecules 40 (2007) 1987 - 1994.

[316] H. Wang, B. A. Holmberg, L. Huang, Z. Wang, A. Mitra, J. M. Norbeck, Y. Yan. "Nafion-bifunctional silica composite proton conductive membranes." J. Mater. Chem. 12 (2002) 834 - 837.

[317] C. Li, G. Sun, S. Ren, J. Liu, Q. Wang, Z. Wu, H. Sun, W. Jin. "Casting Nafion-sulfonated organosilica nano-composite membranes used in direct methanol fuel cells." J. Membr. Sci. 272 (2006) 50 – 57.

[318] Y. F. Lin, C. Y. Yen, C. C. M. Ma, S. H. Liao, C. H. Lee, Y. H. Hsiao, H. P. Lin. "High proton-conducting Nafion®/-SO_3H functionalized mesoporous silica composite membranes." J. Power Sources 171 (2007) 388 – 395.

[319] M. Lavorgna, L. Mascia, G. Mensitieri, M. Gilbert, G. Scherillo, B. Palomba. "Hybridization of Nafion membranes by the infusion of functionalized siloxane precursors." J. Membr. Sci. 294 (2007) 159 – 168.

[320] B. P. Ladewig, R. B. Knott, D. J. Martin, J. C. D. Costa da, G. Q. Lu. "Nafion-MPMDMS nanocomposite membranes with low methanol permeability." Electrochem. Commun. 9 (2007) 781 – 786.

[321] N. H. Jalani, K. Dunn, R. Datta. "Synthesis and characterization of Nafion®-MO_2 (M = Zr, Si, Ti) nanocomposite membranes for higher temperature PEM fuel cells." Electrochim. Acta 51 (2005) 553 – 560.

[322] S. Hara, M. Miyayama. "Proton conductivity of superacidic sulfated zirconia." Solid State Ionics 168 (2004) 111 – 116.

[323] T. M. Thampan, N. H. Jalani, P. Choi, R. Datta. "Systematic approach to design higher temperature composite PEMs." J. Electrochem. Soc. 152 (2005) A316 – A325.

[324] P. Costamagna, C. Yang, A. B. Bocarsly, S. Srinivasan. "Nafion® 115/zirconium phosphate composite membranes for operation of PEMFCs above 100 degrees C." Electrochim. Acta 47 (2002) 1023 – 1033.

[325] V. Ramani, H. R. Kunz, J. M. Fenton. "Stabilized heteropolyacid/Nafion® composite membranes for elevated temperature/low relative humidity PEFC operation." Electrochim. Acta 50 (2005) 1181 – 1187.

[326] V. Ramani, H. R. Kunz, J. M. Fenton. "Metal dioxide supported heteropolyacid/Nafion® composite membranes for elevated temperature/low relative humidity PEFC operation." J. Membr. Sci. 279 (2006) 506 – 512.

[327] H. J. Kim, Y. G. Shul, H. Hana. "Sulfonic-functionalized heteropolyacid-silica nanoparticles for high temperature operation of a direct methanol fuel cell." J. Power Sources 158 (2006) 137 – 142.

[328] Y. F. Lin, C. Y. Yen, C. C. M. Ma, S. H. Liao, C. H. Hung, Y. H. Hsiao. "Preparation and properties of high performance nanocomposite proton exchange membrane for fuel cell." J. Power Sources 165 (2007) 692 – 700.

[329] P. Bebin, M. Caravanier, H. Galiano. "Nafion®/clay-SO_3H membrane for proton exchange

membrane fuel cell application." J. Membr. Sci. 278 (2006) 35 – 42.

[330] T. Duvdevani, M. Philosoph, M. Rakhman, D. Golodnitsky, E. Peled. "Novel composite proton-exchange membrane based on silica-anchored sulfonic acid (SASA)." J. Power Sources 161 (2006) 1069 – 1075.

[331] J. L. Malers, M. A. Sweikart, J. L. Horan, J. A. Turner, A. H. Herring. "Studies of heteropoly acid/polyvinylidenedifluoride-hexafluoroproylene composite membranes and implication for the use of heteropoly acids as the proton conducting component in a fuel cell membrane." J. Power Sources 172 (2007) 83 – 88.

[332] J. Roziere, D. J. Jones, T. L. Bouckary, B. Bauer. "Hybrid material, use of said hybrid material and method for making same." (European Patent, EP01/07774 2002).

[333] I. Colicchio, H. Keul, D. Sanders, U. Simon, T. E. Weirich, M. Moeller. "Development of hybrid polymer electrolyte membranes based on the semi-interpenetrating network concept." Fuel Cells 6 (2006) 225 – 236.

[334] S. P. Nunes, B. Ruffmann, E. Rikowski, S. Vetter, K. Richau. "Inorganic modification of proton conductive polymer membranes for direct methanol fuel cells." J. Membr. Sci. 203 (2002) 215 – 225.

[335] G. Zhang, Z. Zhou. "Organic/inorganic composite membranes for application in DMFC." J. Membr. Sci. 261 (2005) 107 – 113.

[336] J. H. Chang, J. H. Park, G. G. Park, C. S. Kim, O. O. Park. "Proton-conducting composite membranes derived from sulfonated hydrocarbon and inorganic materials." J. Power Sources 124 (2003) 18 – 25.

[337] S. M. J. Zaidi, S. D. Mikhailenko, G. P. Robertson, M. D. Guiver, S. Kaliaguine. "Proton conducting composite membranes from polyether ether ketone and heteropolyacids for fuel cell applications." J. Membr. Sci. 173 (2000) 17 – 34.

[338] X. Li, D. Xu, G. Zhang, Z. Wang, C. Zhao, H. Na. "Influence of casting conditions on the properties of sulfonated poly(ether ether ketone ketone)/phosphotungstic acid composite proton exchange membranes." J. Appl. Polym. Sci. 103 (2007) 4020 – 4026.

[339] H. Zhang, J. H. Pang, D. Wang, A. Li, X. Li, Z. Jiang. "Sulfonated poly(arylene ether nitrile ketone) and its composite with phosphotungstic acid as materials for proton exchange membranes." J. Membr. Sci. 264 (2005) 56 – 64.

[340] D. E. Katsoulis. "A survey of applications of polyoxometalates." Chem. Rev. 98 (1998) 359 – 387.

[341] P. Kalappa, J. H. Lee. “Proton conducting membranes based on sulfonated poly(ether ether ketone)/TiO_2 nanocomposites for a direct methanol fuel cell.” Polym. Int. 56 (2007) 371 – 375.

[342] P. Krishnan, J. S. Park, C. S. Kim. “Preparation of proton-conducting sulfonated poly(ether ether ketone)/boron phosphate composite membranes by an in situ sol-gel process.” J. Membr. Sci. 279 (2006) 220 – 229.

[343] D. S. Kim, B. Liu, M. D. Guiver. “Influence of silica content in sulfonated poly(arylene ether ether ketone ketone) (SPAEEKK) hybrid membranes on properties for fuel cell application.” Polymer 47 (2006) 7871 – 7780.

[344] Y. H. Su, Y. L. Liu, Y. M. Sun, J. Y. Lai, D. M. Wang, Y. Gao, B. Liu, M. D. Guiver. “Proton exchange membranes modified with sulfonated silica nanoparticles for direct methanol fuel cells.” J. Membr. Sci. 296 (2007) 21 – 28.

[345] S. P. Nunes, B. Ruffmann, E. Rikowski, S. Vetter, K. Richau. “Inorganic modification of proton conductive polymer membranes for direct methanol fuel cells.” J. Membr. Sci. 203 (2002) 215 – 225.

[346] K. Miyatake, T. Tombe, Y. Chikashige, H. Uchida, M. Watanabe. “Enhanced proton conduction in polymer electrolyte membranes with acid-functionalized polysilsesquioxane.” Angew. Chem. Int. Ed. 46 (2007) 6646 – 6649.

[347] V. K. Shahi. “Highly charged proton-exchange membrane: Sulfonated poly(ether sulfone)-silica polyelectrolyte composite membranes for fuel cells.” Solid State Ionics (2007) 177 3395 – 3404.

[348] G. M. Anilkumar, S. Nakazawa, T. Okubo, T. Yamaguchi. “Proton conducting phosphated zirconia-sulfonated polyether sulfone nanohybrid electrolyte for low humidity, wide-temperature PEMFC operation.” Electrochem. Commun. 8 (2006) 133 – 136.

[349] D. Xing, H. Zhang, L. Wang, Y. Zhai, B. Yi. “Investigation of the Ag-SiO2/sulfonated poly(biphenyl ether sulfone) composite membranes for fuel cell.” J. Membr. Sci. 296 (2007) 9 – 14.

[350] D. S. Kim, H. B. Park, J. W. Rhim, Y. M. Lee. “Preparation and characterization of crosslinked PVA/SiO_2 hybrid membranes containing sulfonic acid groups for direct methanol fuel cell applications.” J. Membr. Sci. 240 (2004) 37 – 48.

[351] R. Q. Fu, L. Hong, J. Y. Lee. “Membrane design for direct ethanol fuel cells: A hybrid proton-conducting interpenetrating polymer network.” Fuel Cells 8 (2008) 52 – 61.

[352] R. K. Nagarale, G. S. Gohil, V. K. Shahi, R. Rangarajan. “Organic-inorganic hybrid membrane: Thermally stable cation-exchange membrane prepared by the sol-gel method.” Macromolecules

(2004) 37 10023 – 10030.

[353] V. V. Binsu, R. K. Nagarale, V. K. Shahi. “Phosphonic acid functionalized aminopropyl triethoxysilane-PVA composite material: organic-inorganic hybrid proton-exchange membranes in aqueous media.” J. Mater. Chem. 15 (2005) 4823 - 4831.

[354] I. Honma, S. Hirakawa, K. Yamada, J. M. Bae. “Synthesis of organic/inorganic nanocomposites protonic conducting membrane through sol-gel processes.” Solid State Ionics 118 (1999) 29 - 36.

[355] I. Honma, H. Nakajima, O. Nishikawa, T. Sugimoto, S. Nomura. “Organic/inorganic nano-composites for high temperature proton conducting polymer electrolytes.” Solid State Ionics 162 (2003) 237 – 245.

[356] S. Li, Z. Zhou, H. Abernathy, M. Liu, W. Li, J. Ukai, K. Hase, M. Nakanishi. “Synthesis and properties of phosphonic acid-grafted hybrid inorganic-organic polymer membranes.” J. Mater. Chem. 16 (2006) 858 - 864.

[357] J. D. Kim, T. Mori, I. Honma. “Proton exchange membrane with chemically tolerant organically modified zirconia.” J. Membr. Sci. 281 (2006) 735 – 740.

[358] J. D. Kim, I. Honma. “Proton conducting polydimethylsiloxane/metal oxide hybrid membranes added with phosphotungstic acid(II).” Electrochim. Acta 49 (2004) 3429 – 3433.

[359] R. Kannan, B. A. Kakade, V. K. Pillai. “Polymer Electrolyte Fuel Cells Using Nafion-Based Composite Membranes with Functionalized Carbon Nanotubes.” Angew. Chem. Int. Ed. 47 (2008) 2653 –2656.

[360] B. Yameen, A. Kaltbeitzel, A. Langner, F. Müller, U. Gösele, W. Knoll, O. Azzaroni. “Highly Proton-Conducting Self-Humidifying Microchannels Generated by Copolymer Brushes on a Scaffold.” Angew. Chem. Int. Ed. 48 (2009) 3124 –3128.

[361] B. Yameen, A. Kaltbeitzel, G. Glasser, A. Langner, F. Müller, U. Gösele, W. Knoll, O. Azzaroni. “Hybrid Polymer-Silicon Proton Conducting Membranes via a Pore-Filling Surface-Initiated Polymerization Approach, Hybrid Polymer−Silicon Proton Conducting Membranes via a Pore-Filling Surface-Initiated Polymerization Approach.” ACS Appl. Mater. Interfaces 2 (2010) 279 – 287.

[362] B. Yameen, A. Kaltbeitzel, A. Langner, H. Duran, F. Müller, U. Gösele, O. Azzaroni, W. Knoll. “Facile Large-Scale Fabrication of Proton Conducting Channels.” J. Am. Chem. Soc. 130 (2008) 13140–13144.

[363] S. Moghaddam, E. Pengwang, Y.-B. Jiang, A. R. Garcia, D. J. Burnett, C. J. Brinker, R. I. Masel, M. A. Shannon. “An inorganic–organic proton exchange membrane for fuel cells with a

controlled nanoscale pore structure." Nat. Nanotechn. 5 (2010) 230 - 236.

[364] M. Tagliazucchi, O. Azzaroni, I. Szleifer. "Responsive Polymers End-Tethered in Solid-State Nanochannels: When Nanoconfinement Really Matters." J. Am. Chem. Soc. 132 (2010) 12404–12411.

[365] B. Yameen, A. Kaltbeitzel, A. Langner, F. Müller, U. Gösele, W. Knoll, O. Azzaroni. "Highly Proton-Conducting Self-Humidifying Microchannels Generated by Copolymer Brushes on a Scaffold." Angew. Chem. Int. Ed. 48 (2009) 3124 –3128.

[366] K. Schmidt-rohr, Q. Chen. "Parallel cylindrical water nanochannels in Nafion fuel-cell membranes." Nat. Mater. 7 (2008) 75 – 83.

[367] S. Cukierman. "Et tu, Grotthuss! and other unfinished stories." Biochim. Biophys. Acta-Bioenerg. 1757 (2006) 876 – 885.

[368] G. Larsen, R. Velarde-Ortiz, K. Minchow, A. Barrero, I. G. Loscertales. "A method for making inorganic and hybrid (organic/inorganic) fibers and vesicles with diameters in the submicrometer and micrometer range via sol-gel chemistry and electrically forced liquid jets." J. Am. Chem. Soc. 125 (2003) 1154 – 1155.

[369] Y. Wang, R. Furlan, I Ramos, J. I. Santiago-Aviles. "Synthesis and characterization of micro/nanoscopic $Pb(Zr_{0.52}Ti_{0.48})O_3$ fibers by electrospinning." Appl. Phys. A 78 (2004) 1043 – 1047.

[370] Y. Wang, J. J. Santiago-Aviles. "Synthesis of lead zirconate titanate nanofibres and the Fourier-transform infrared characterization of their metallo-organic decomposition process." Nanotechnology 15 (2004) 32 – 36.

[371] S. S. Choi, S. G. Lee, S. S. Im, S. H. Kim. "Silica nanofibers from electrospinning/sol-gel process." J. Mater Sci. Lett. 22 (2003) 891 – 893.

[372] W. Kataphinan, R. Teye-Mensah, E. A. Evans, R. D. Ramsier, D. H. Reneker, D. J. Smith. "High-temperature fiber matrices: Electrospinning and rare-earth modification." J. Vac. Sci. Technol. A 21 (2003) 1574 – 1578.

[373] D. Li, Y. Xia. "Fabrication of titania nanofibers by electrospinning." Nano Lett. 3 (2003) 555 – 560.

[374] D. Li, Y. Wang, Y. Xia. "Electrospinning of polymeric and ceramic nanofibers as uniaxially aligned arrays." Nano Lett. 3 (2003) 1167 – 1171.

[375] D. Li, T. Herricks, Y. Xia. "Magnetic nanofibers of nickel ferrite prepared by electrospinning."

Appl. Phys. Lett. 83 (2003) 4586 – 4588.

[376] H. Dai, J. Gong, H. Kim, D. Lee. “A novel method for preparing ultra-fine alumina-borate oxide fibres via an electrospinning technique.” Nanotechnology 13 (2002) 674 – 677.

[377] P. Viswanathamurthi, N. Bhattarai, H. Y. Kim, D. R. Lee, S. R. Kim, M. A. Morris. “Preparation and morphology of niobium oxide fibres by electrospinning.” Chem. Phys. Lett. 374 (2003) 79 – 84.

[378] C. Shao, H.-Y. Kim, J. Gong, B. Ding, D.-R. Lee, S.-J. Park. “Fiber mats of poly(vinyl alcohol)/silica composite via electrospinning.” Mater. Lett. 57 (2003) 1579 – 1584.

[379] H. Guan, C. Shao, B. Chen, J. Gong, X. Yang. “A novel method for making CuO superfine fibres via an electrospinning technique.” Inorg. Chem. Commun. 6 (2003) 1409 – 1411.

[380] H. Guan, C. Shao, B. Chen, J. Gong, X. Yang. “Preparation and characterization of NiO nanofibres via an electrospinning technique.” Inorg. Chem. Commun. 6 (2003) 1302 – 1303.

[381] X. Yang, C. Shao, H. Guan, X. Li, J. Gong. “Preparation and characterization of ZnO nanofibers by using electrlospun PVA/zinc acetate composite fiber as precursor.” Inorg. Chem. Chommun. 7 (2004) 176 – 178.

[382] B. Ding, H. Kim, C. Kim, M. Khil, S. Park. “Morphology and crystalline phase study of electrospun TiO_2-SiO_2 nanofibres.” Nanotechnology 14 (2003) 532 – 537.

[383] P. Viswanathamurthi, N. Bhattarai, H. Y. Kim, D. R. Lee. “Vanadium pentoxide nanofibers by electrospinning.” Scr. Mater. 49 (2003) 577 – 581.

[384] H. Guan, C. Shao, S. Wen, B. Chen, J. Gong, X. Yang. “A novel method for preparing Co_3O_4 nanofibers by using electrospun PVA/cobalt acetate composite fibers as precursor.” Mater. Chem. Phys. 3 (2003) 1002 – 1006.

[385] P.I. Gouma. “Nanostructured polymorphic oxides for advanced chemosensors.” Rev. Adv. Mater. Sci. 5 (2003) 147 – 154.

[386] N. Dharmaraj, H. C. Park. B. M. Lee, P. Viswanathamurthi, H. Y. Kim, D. R. Lee. “Preparation and morphology of magnesium titanate nanofibres via electrospinning.” Inorg. Chem. Commun. 7 (2004) 431 – 433.

[387] V. C. F. Holm, G. C. Bailey. “Sulfate-treated zirconia-gel catalyst.” (US. Patent 3032599 1962).

[388] M. Hino, S. Kobayashi, K. Arata. “Solid Catalyst Treated wigh Anion. 2. Reactions of Butane and Isobutane Catalyzed by Zriconium-oxide Treated with Sulfate Ion - Solid Superacid Catalyst.” J.

Am. Chem. Soc. 101 (1979) 6439 – 6441.

[389] M. Hino, K. Arata. “Solid Catalysts Treated with Anions - Synthesis of Solid Superacid Catalyst with Acid Strength of H_0 Less-than-or-equal-to 16.04.” J. Chem. Soc. Chem. Commun. 18 (1980) 851 - 852.

[390] X. Song, A. Sayari. “Sulfated zirconia-based strong solid-acid catalysts: Recent progress.” Catal. Rev. Sci. Eng. 38 (1996) 329 – 412;

[391] G. D. Yadav, J. J. Nair. “Sulfated zirconia and its modified versions as promising catalysts for industrial processes.” Microporous Mesoporous Mater. 33 (1999) 1 – 48.

[392] S. Hara, M. Miyayama. “Proton conductivity of superacidic sulfated zirconia.” Solid State Ionics 168 (2004) 111 – 116.

[393] M.A. Navarra, C. Abbati, B. Scrosati. “Properties and fuel cell performance of a Nafion-based, sulfated zirconia-added, composite membrane.” J. Power Sources 183 (2008) 109–113.

[394] M. S. Scurrel. “Conversion of methane-ethylene mixtures over sulphate-treated zirconia catalysts.” Appl. Catal. 34 (1987) 109 – 117.

[395] M. S. Scurrell, M. Cooks. “Coupling of Methane and Ethylene Over Sulphate-Treated Zirconia.” Stud. Surf. Sci. Catal. 36 (1988) 433 – 438.

[396] R. Srinivasan, D. Taulbee, B. H. Davis. “The Effect of Sulfate on the crystal-structuer of Zirconia.” Catal. Lett. 9 (1991) 1 – 8.

[397] R. Srinivasan, B. H. Davis. “Influence of Zirconium Salt precursors on the Crystal-structures of Zirconia.” Catal. Lett. 14 (1992) 165 – 170.

[398] M. Bensitel, O. Saur, J. C. Lavalley, G. Mabilon. “Acidity of Zirconium-oxide and Sulfated ZrO_2 Samples.” Mater. Chem. Phys. 17 (1987) 249 – 258.

[399] M. Bensitel, O. Saur, J.-C. Lavalley, B. A. Morrow. “An Infrared Study of Sulfated Zirconia.” Mater. Chem. Phys. 19 (1988) 147 – 156.

[400] C. Morterra, G. Cerrato, C. Emanuel, V. Bolis. “On the Surface-acidity of Some Sulfate-doped ZrO_2 Catalysts.” J. Catal. 142 (1993) 349 – 367.

[401] J. R. Sohn, H. W. Kim, Catalytic and Surface-properties of ZrO2 modified with Sulfur-compounds, J. Mol. Catal. 52 (1989) 361 – 374.

[402] S. Baba, Y. Shibata, T. Kawamura, H. Takaoka, T. Kimura, K. Kousaka, Y. Minato, N. Yokoyama,

K. Lida, T. Imai. “Solid strong acid catalyst.” European Patent 174836 1985.

[403] C. Morterra, G. Cerrato, F. Pinna, M. Signoretto, G. Strukul. “On The Acid-catalyzed Ionmerization of Light Paraffins Over A ZrO_2/SO_4 System - the Effect of Hydration.” J. Catal. 149 (1994) 181 – 188.

[404] D. A. Ward, E. I. Ko. “One-step Synthesis and Characterization of Zirconia-sulfate Aerogels and Solid Superacids.” J. Catal. 150 (1994) 18 – 33.

[405] J. Choi, K. M. Lee, R. Wycisk, P. N. Pintauro, P. T. Mather. “Nanofiber network ion-exchange membranes.” Macromolecules 41 (2008) 4569 – 4572.

[406] X. Song, A. Sayari Choi Sulfated Zirconia-based strong solid-aicd catalysts: recent progress.” Catal. Rev. Sci. Eng. 38 (1996) 329 – 412.

[407] I. Bekri-Abbesa, S. Bayoudhb, M. Baklouti. “The removal of hardness of water using sulfonated waste plastic.” Desalination 222 (2008) 81 – 86.

[408] M. Lefèvre, E. Proietti, F. Jaouen, J.-P. Dodelet. “Iron-Based Catalysts with Improved Oxygen Reduction Activity in Polymer Electrolyte Fuel Cells.” Science, 324 (2009) 71 – 74.

[409] K. A. Mauritz, R. B. Moore. “State of understanding of Nafion.” Chem. Rev. 104 (2004) 4535 – 4585.

[410] J. Roziè re, D. J. Jones. “Non-fluorinated polymer materials for proton exchange membrane fuel cells.” Annu. Rev. Mater. Res. 33 (2003) 503 – 555.

[411] G. Alberti, M. Casciola. “Composite membranes for medium-temperature PEM fuel cells.” Annu. Rev. Mater. Res. 33 (2003) 129 – 154.

[412] R. K. Nagarale, W. Shin, P. K. Singh. “Progress in ionic organic-inorganic composite membranes for fuel cell applications.” Polym. Chem. 1 (2010) 388 – 408.

[413] B. Yameen, A. Kaltbeitzel, A. Langner, F. Müller, U. Gösele, W. Knoll, O. Azzaroni. “Highly Proton-Conducting Self-Humidifying Microchannels Generated by Copolymer Brushes on a Scaffold.” Angew. Chem. Int. Ed. 48 (2009) 3124 – 3128.

[414] K. A. Mauritz, R. B. Moore. “State of understanding of Nafion.” Chem. Rev. 104 (2004) 4535 – 4585.

[415] H. Diao, F. Yan, L. Qiu, J. Lu, X. Lu, B. Lin, Q. Li, S. Shang, W. Liu, J. Liu Choi High Performance Cross-Linked Poly(2-acrylamido-2-methylpropanesulfonic acid)-Based Proton Exchange Membranes for Fuel Cells.” Macromolecules 43 (2010) 6398 – 6405.

[416] Z. Chai, C. Wang, H. Zhang, C. M. Doherty, B. P. Ladewig, A. J. Hill, H. Wang. “Nafion-Carbon Nanocomposite Membranes Prepared Using Hydrothermal Carbonization for Proton-Exchange-Membrane Fuel Cells.” Adv. Func. Mater. 20 (2010) 4394–4399.

[417] B. Dong, L. Gwee, D. S. Cruz, K. I. Winey, Y. A. Elabd. “Super Proton Conductive High-Purity Nafion Nanofibers.” Nano Lett. 10 (2010) 3785 – 3790.

[418] V. A. Sethuraman, J.W. Weidner, A. T. Haug, L. V. Protsailo. “Durability of perfluorosulfonic acid and hydrocarbon membranes: Effect of humidity and temperature.” J. Electrochem. Soc. 155 (2008) B119 – B124.

[419] B. Bae, T. Yoda, K. Miyatake, H. Uchida, M. Watanabe. “Proton-Conductive Aromatic Ionomers Containing Highly Sulfonated Blocks for High-Temperature-Operable Fuel Cells.” Angew. Chem. Int. Ed. 49 (2010) 317 –320.

[420] J. Y. Kim, W. C. Choi, S. I. Woo, W. H. Hong. “Proton conductivity and methanol permeation in Nafion((TM))/ORMOSIL prepared with various organic silanes.” J. Membr. Sci. 238 (2004) 213 – 222.

[421] W. Y. Hsu, T. D. Gierke. “Ion-transport and Clustering in Nafion Perfluorinated Membranes.” J. Membr. Sci. 13 (1983) 307 – 326.

[422] K. A. Mauritz, C. E. Rogers. “A Water Sorption Isotherm Model for Ionomer Membranes with Cluster Morphologies.” Macromolecules 18 (1985) 483 - 491.

[423] F. P. Orfino, S. Holdcroft. “The morphology of Nafion: are ion clusters bridged by channels or single ionic sites?” J. New Mater. Electrochem. Syst. 3 (2000) 287 - 290.

[424] G. Gebel. “Structural evolution of water swollen perfluorosulfonated ionomers from dry membrane to solution.” Polymer 41 (2000) 5829 - 5838.

[425] A. Greiner, J, H. Wendorff. “Electrospinning: A fascinating method for the preparation of ultrathin fibres.” Angew. Chem. Int. Ed. 46 (2007) 5670 – 5703.

[426] H. Chen, J. D. Snyder, Y. A. ELabd. “Electrospinning and solution properties of Nafion and poly(acrylic acid).” Macromolecules 41 (2008) 128 – 135.

[427] V. D. Noto, R. Gliubizzi, E. Negro, G. Pace. “Effect of SiO_2 on relaxation phenomena and mechanism of ion conductivity of [Nafion/$(SiO_2)_{(x)}$] composite membranes.” J. Phys. Chem. B 110 (2006) 24972-24986.

[428] A. K. Sahu, G. Selvarani, S. Pitchumani, P. Sridhar, A. K. Shukla. “A sol-gel modified alternative nafion-silica composite membrane for polymer electrolyte fuel cells.” J. Electrochem. Soc. 154

(2007) B123 – B132.

[429] M. Watanabe, H. Uchida, M. Emori. “Polymer electrolyte membranes incorporated with nanometer-size particles of Pt and/or metal-oxides: Experimental analysis of the self-humidification and suppression of gas-crossover in fuel cells.” J. Phys. Chem. B 102 (1998) 3129 – 3137.

[430] Z.-G. Shao, H. Xu, M. Li, I-M. Hsing. “Hybrid Nafion-inorganic oxides membrane doped with heteropolyacids for high temperature operation of proton exchange membrane fuel cell.” Solid State Ionics 177 (2006) 779 – 785.

[431] S. M. Haile, D. A. Boysen, C. R. I. Chisholm, R. B. Merle. “Solid acids as fuel cell electrolytes.” Nature 410 (2001) 910 - 913.

[432] T. Yamaguchi, H. Zhou, S. Nakazawa, N. Hara. “An extremely low methanol crossover and highly durable aromatic pore-filling electrolyte membrane for direct methanol fuel cells.” Adv. Mater. 19 (2007) 592 – 596.

[433] T. Tamura, H. Kawakami. “Aligned Electrospun Nanofiber Composite Membranes for Fuel Cell Electrolytes.” Nano Lett. 10 (2010) 1324 – 1328.

[434] F. Wang, M. Hickner, Y. S. Kim, T. A. Zawodzinski, J. E. McGrath. “Direct polymerization of sulfonated poly(arylene ether sulfone) random (statistical) copolymers: candidates for new proton exchange membranes.” J. Membr. Sci. 197 (2002) 231 – 242.

[435] O. Savard, T. J. Peckham, Y. Yang, S. Holdcroft. “Structure-property relationships for a series of polyimide copolymers with sulfonated pendant groups.” Polymer 49 (2008) 4949 – 4959.

[436] Y. Xia, P. Yang, Y. Sun, Y. Wu, B. Mayers, B. Gates, Y. Yin, F. Kim, H. Yan. “One-dimensional nanostructures: Synthesis, characterization, and applications.” Adv. Mater. 15 (2003) 353 – 389.

[437] J. Hu, T. W. Odom, C. M. Lieber. “Chemistry and physics in one dimension: Synthesis and properties of nanowires and nanotubes.” Acc. Chem. Res. 32 (1999) 435 – 445.

[438] E. S. Steigerwalt, G. A. Deluga, D. E. Cliffel, C. M. Lukehart. “A Pt-Ru/graphitic carbon nanofiber nanocomposite exhibiting high relative performance as a direct-methanol fuel cell anode catalyst.” J. Phys. Chem. B 105 (2001) 8097 – 8101.

[439] F.-J. Liu, L.-M. Huang, T.-C. Wen, A. Gopalan. “Large-area network of polyaniline nanowires supported platinum nanocatalysts for methanol oxidation.” Synth. Met. 157 (2007) 651 – 658.

[440] H. Gharibi, M. Zhiani, A. A. Entezami, R. A. Mirzaie, M. Kheirmand, K. Kakaei. “Study of polyaniline doped with trifluoromethane sulfonic acid in gas-diffusion electrodes for

proton-exchange membrane fuel cells.” J. Power Sources 155 (2006) 138 – 144.

[441] F. Yuan, H. Ryu. “The synthesis, characterization, and performance of carbon nanotnbes and carbon nanofibres with controlled size and morphology as a catalyst support material for a polymer electrolyte membrane fuel cell.” Nanotechnology 15 (2004) S596–S602.

[442] H. Chen, J. D. Snyder, Y. A. Elabd. “Electrospinning and solution properties of Nafion and poly(acrylic acid).” Macromolecules 41 (2008) 128 – 135.